

REPORT ON GEOLOGICAL SURVEY  
OF  
CENTRAL SULAWESI, INDONESIA

Vol. V

GEOLOGICAL SURVEY  
GEOCHEMICAL SURVEY  
GEOPHYSICAL SURVEY  
DRILLING EXPLORATION

JUNE 1973

METALLIC MINERALS EXPLORATION AGENCY

OVERSEAS TECHNICAL COOPERATION AGENCY

GOVERNMENT OF JAPAN

REPORT ON GEOLOGICAL SURVEY  
OF  
CENTRAL SULAWESI, INDONESIA

Vol. V

GEOLOGICAL SURVEY  
GEOCHEMICAL SURVEY  
GEOPHYSICAL SURVEY  
DRILLING EXPLORATION

JICA LIBRARY



1055325[3]

JUNE 1973

METALLIC MINERALS EXPLORATION AGENCY

OVERSEAS TECHNICAL COOPERATION AGENCY

GOVERNMENT OF JAPAN

国際協力事業団	
受入 月日 '84. 5. 19	108
登録No. 05909	66
	SD

## PREFACE

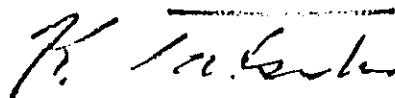
The Government of Japan, intending to perform geological and other related surveys, in response to the request by the Republic of Indonesia, for the purpose of confirming the potentialities of occurrence of mineral resources in Block No. 4 Area located in the central region of Sulawesi Island, delegated the implementation of such surveys to the Overseas Technical Cooperation Agency. This Agency, in turn, requested Metallic Minerals Exploration Agency of Japan to carry out the said surveys in view of the project touching, in particular, specialized fields such as geology and mineral resources surveys.

This year was the last to complete a series of surveys extending over three years, and for this, a survey team was formed consisting of 17 members headed by Mr. Toshio Wakiyama, Chief of Planning Section, Overseas Dept., Metallic Minerals Exploration Agency, and was dispatched to Indonesia for a period from September 12, 1972 to February 3, 1973. The surveys at site were completed as planned with cooperation extended by agencies concerned of the Government of the Republic of Indonesia.

The Report comprises the results of the third year surveys and the generalization of those obtained through the period of three years.

In conclusion, I wish to express my heartfelt appreciation for all that has been dedicated to the completion of the surveys by agencies concerned of the Government of the Republic of Indonesia, the Ministry of International Trade and Industry, the Ministry of Foreign Affairs, Metallic Minerals Exploration Agency and each corporation concerned.

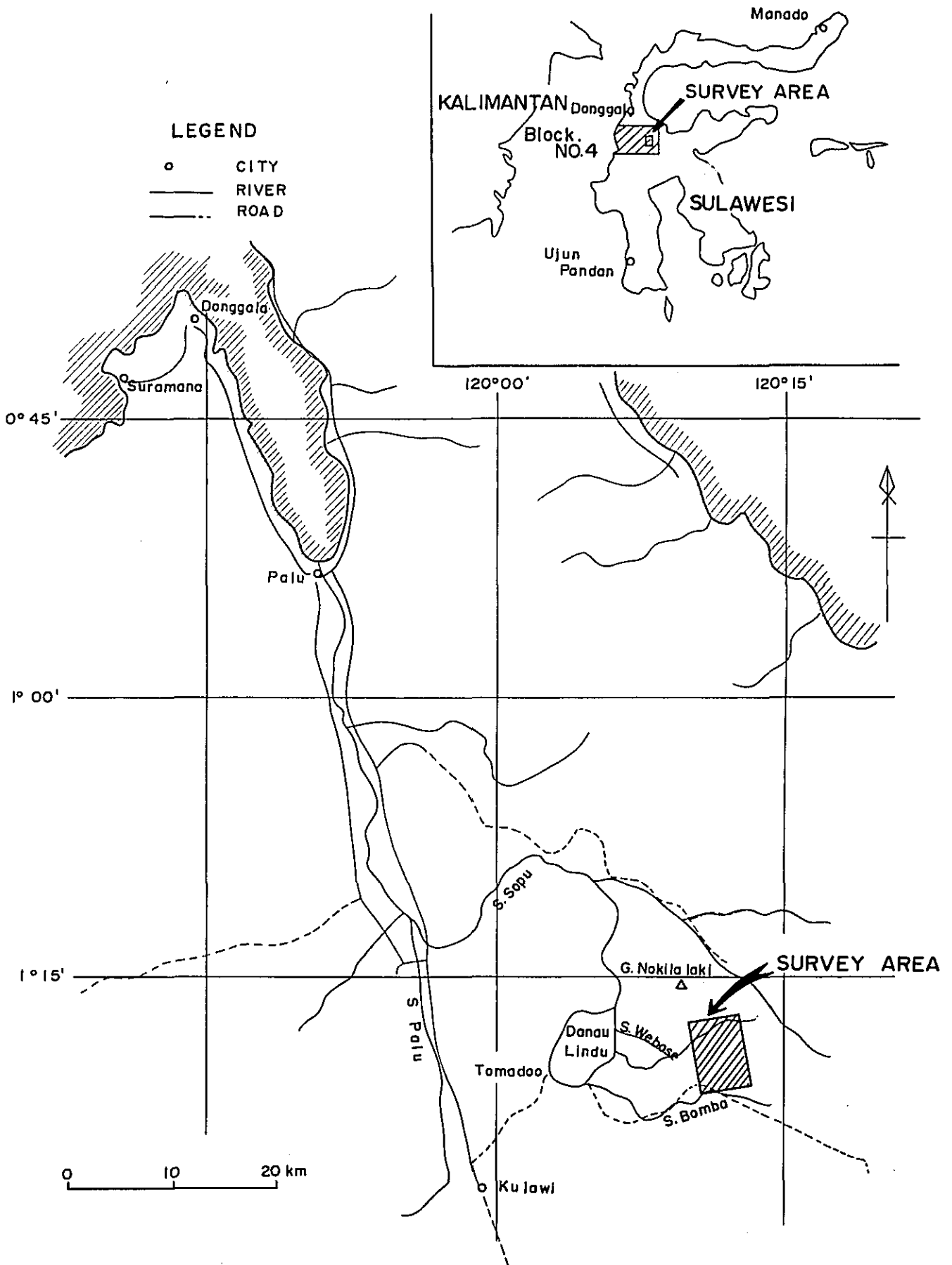
June, 1973



Keiichi Tatsuke  
Director General  
Overseas Technical Cooperation Agency

海外技術協力事業団	
受入 月日	E210 5.1
BRN03052	0-5

# KEY MAP AND LOCATION MAP



## CONTENTS

	Page
PREFACE .....	ii
KEY MAP AND LOCATION MAP .....	iii
SUMMARY .....	xiii
INTRODUCTION .....	1
1. Purpose of Survey .....	2
2. Duration of Survey .....	2
3. Members .....	2
4. Content of Project .....	5
5. Location .....	5
6. Access .....	6
7. Topography and Climate .....	7
8. Transportation of Equipments and Materials .....	7
 PART I    GEOLOGICAL SURVEY .....	 9
Chapter 1. Outline of Survey .....	10
Chapter 2. Geology .....	11
2-1       Stratigraphy .....	12
2-2       Metamorphism .....	22
2-3       Geologic Structure .....	32
Chapter 3. Ore Deposits .....	37
3-1       The Distribution and Scale of the Mineralized Areas .....	37
3-2       Alteration .....	37
3-3       Ore Minerals .....	40
3-4       Mineralization .....	43

	Page
PART II. GEOCHEMICAL SURVEY .....	45
Chapter 1. Outline of Survey .....	46
Chapter 2. Sampling .....	47
Chapter 3. Chemical Analyses .....	48
3-1 Preparation of Samples .....	48
3-2 Method of Analysis .....	48
Chapter 4. Interpretation .....	50
4-1 Data Processing .....	50
4-2 Selection of Anomalous Areas and Interpretation .....	53
 PART III. GEOPHYSICAL SURVEY .....	 56
Chapter 1. Outline of Surveys .....	57
Chapter 2. Electromagnetic Survey .....	59
2-1 Traverse Lines .....	59
2-2 Survey Method .....	60
2-3 Instrumentation .....	62
2-4 Survey Results .....	64
Chapter 3. Induced Polarization Survey .....	67
3-1 Traverse Lines .....	67
3-2 Survey Method .....	68
3-3 Instrumentation .....	69
3-4 Survey Results .....	70

	Page
Chapter 4.      Remarks on Geophysical Survey.....	80
4-1          Measurement of Properties of Rocks and Ores .....	80
4-2          Remarks on Electromagnetic Survey .. .. .	84
4-3          Remarks on Induced Polarization Survey .....	90
 PART IV.      DRILLING EXPLORATION .....	 96
Chapter 1.    Outline of Drilling .....	97
Chapter 2.    Drilling Method and Equipment .....	98
Chapter 3.    Selection of Drilling Sites .....	101
Chapter 4.    Result of Drilling .....	103
4-1          Operation .....	103
4-2          Geologic Columns .....	104
4-3          Discussion .....	110
 PART V.      CONCLUDING REMARKS .....	 115
 REFERENCES    .. .. .	 122



## FIGURES

		Page
Fig. 1-1	Geological Column .....	23
Fig. 1-2	Stratigraphy and Geological Events .....	24
Fig. 2	Cumulative Frequency Distributions for Copper Content of Soil Samples in Different Lithology .....	51
Fig. 3-1	Horizontal Coplanar .....	62
Fig. 3-2	Vertical Coplanar .....	62
Fig. 3-3	Vertical Coaxial .....	62
Fig. 3-4	Simplified Circuit Diagram .....	63
Fig. 3-5	Outline of Apparatus .....	81
Fig. 3-6	Examples of F. E. Pattern .....	83
Fig. 3-7	Argand Diagram .....	89
Fig. 3-8	Ratio of Maxima Observed on a Slingram Anomaly Curve over a Thin Sheet as a Function of Dip .....	89
Fig. 3-9	Two-dimensional Model Calculation for Resistivity and Frequency Effect .....	95
Fig. 4-1	Geological Cross Section along DH-1, DH-2 and DH-3 (V ; 1 : 5,000) (H ; 1 : 10,000) .....	113
Fig. 4-2	Cross Section of S. Webose Mineralized Area (1 : 10,000) .....	114

## TABLES

		Page
Table 1-1	Geological Correlation .....	11
Table 1-2	Chemical Compositions of Common Garnets ..	27
Table 1-3	Chemical Analyses of Garnets .....	28
Table 1-4	Endmember Ratios of Garnets .....	29
Table 1-5	Opaque Mineral Assemblages .....	41
Table 2-1	Number of Samples in Different Lithology....	50
Table 2-2	Background Values and Threshold Values of Copper Content in Soil .....	52
Table 2-3	Geochemical Anomalous Areas .....	54
Table 3	Results of Measurements on Rock Samples ..	82
Table 4-1	Drilling Equipments . . . . .	98
Table 4-2	Drilling Condition (DH-1) .....	105
Table 4-3	Drilling Condition (DH-2) .....	106
Table 4-4	Drilling Condition (DH-3) .....	107

## APPENDIXES

Appendix 1-1	Observation of Handspecimens .....	A-2
Appendix 1-2	Microscopic Observation in Thin Sections ..	A-15
Appendix 1-3	Mineral Assemblages of Metamorphic Rocks in Thin Sections .....	A-39
Appendix 1-4	Mineral Assemblages Determined by X-ray Diffraction .....	A-42

	Page
Appendix 1-5	Microscopic Observation of Polished Sections .....A-43
Appendix 1-6	Chemical Analyses of Sulphides-disseminated Rock Samples .....A-49
Appendix 2	Copper Contents of Geochemical Soil Samples, .A-50
Appendix 4	Drill Log ..... A-57

## PLATES

		Scale
PL 1-1	GEOLOGICAL MAP	1 : 10,000
PL 1-2	GEOLOGICAL CROSS SECTIONS	1 : 10,000
PL 1-3	TECTONIC MAP	1 : 10,000
PL 1-4	MAP SHOWING THE RELATION BETWEEN MINERALIZATION AND TECTONICS	1 : 10,000
PL 1-5	ALTERATION MAP	1 : 10,000
PL 1-6	ROUTE MAP	1 : 10,000
PL 2-1	LOCATION OF GEOCHEMICAL SOIL SAMPLES	1 : 10,000
PL 2-2	MAP OF GEOCHEMICAL ANOMALIES	1 : 10,000
PL 3-1	MAP OF TRAVERSE ROUTES	1 : 10,000
PL 3-2-1	CONTOURS OF ELECTROMAGNETIC DIP ANGLE ANOMALY (VERTICAL LOOP METHOD)	1 : 10,000
PL 3-2-2	PROFILE OF ELECTROMAGNETIC ANOMALY (VERTICAL LOOP METHOD)	1 : 5,000
PL 3-2-3	"	1 : 5,000
PL 3-2-4	"	1 : 5,000
PL 3-2-5	"	1 : 5,000
PL 3-2-6	"	1 : 5,000
PL 3-2-7	"	1 : 5,000
PL 3-2-8	PROFILE OF ELECTROMAGNETIC ANOMALY (VERTICAL AND HORIZONTAL LOOP METHODS)	1 : 5,000

PL 3-2-9	PROFILE OF ELECTROMAGNETIC ANOMALY (VERTICAL LOOP METHOD)	1 : 5,000
PL 3-2-10	PROFILE OF ELECTROMAGNETIC ANOMALY (VERTICAL AND HORIZONTAL LOOP METHODS)	1 : 5,000
PL 3-2-11	"	1 : 5,000
PL 3-2-12	PROFILE OF ELECTROMAGNETIC ANOMALY (HORIZONTAL LOOP METHOD)	1 : 5,000
PL 3-2-13	IN PHASE COMPONENT OF ELECTROMAGNETIC ANOMALY	1 : 10,000
PL 3-2-14	OUT OF PHASE COMPONENT OF ELECTROMAGNETIC ANOMALY	1 : 10,000
PL 3-3-1	CROSS SECTIONS OF INDUCED POLARIZATION ACROSS A-LINE	1 : 5,000
PL 3-3-2	CROSS SECTIONS OF INDUCED POLARIZATION ACROSS B-LINE	1 : 5,000
PL 3-3-3	CROSS SECTIONS OF INDUCED POLARIZATION ACROSS C-LINE	1 : 5,000
PL 3-3-4	CROSS SECTIONS OF INDUCED POLARIZATION ACROSS D-LINE	1 : 5,000
PL 3-3-5	CROSS SECTIONS OF INDUCED POLARIZATION ACROSS E-LINE	1 : 5,000
PL 3-3-6	CROSS SECTIONS OF INDUCED POLARIZATION ACROSS F-LINE	1 : 5,000
PL 3-3-7	CROSS SECTIONS OF INDUCED POLARIZATION ACROSS G-LINE	1 : 5,000
PL 3-3-8	CROSS SECTIONS OF INDUCED POLARIZATION ACROSS H-LINE	1 : 5,000

PL 3-3-9	CROSS SECTIONS OF INDUCED POLARIZATION ACROSS I-LINE	1 : 5,000
PL 3-3-10	CROSS SECTIONS OF INDUCED POLARIZATION ACROSS J-LINE	1 : 5,000
PL 3-3-11	CROSS SECTIONS OF INDUCED POLARIZATION ACROSS X-LINE	1 : 5,000
PL 3-3-12	CROSS SECTIONS OF INDUCED POLARIZATION ACROSS Y-LINE	1 : 5,000
PL 3-3-13	CROSS SECTIONS OF INDUCED POLARIZATION ACROSS Z-LINE	1 : 5,000
PL 3-3-14	CONTOURS OF PERCENT FREQUENCY EFFECT (F. E.) FOR $n-1$	1 : 10,000
PL 3-3-15	CONTOURS OF PERCENT FREQUENCY EFFECT (F. E.) FOR $n-2$	1 : 10,000
PL 3-3-16	CONTOURS OF PERCENT FREQUENCY EFFECT (F. E.) FOR $n-3$	1 : 10,000
PL 3-3-17	CONTOURS OF APPARENT RESISTIVITY IN $\Omega$ -m FOR $n-1$	1 : 10,000
PL 3-3-18	CONTOURS OF APPARENT RESISTIVITY IN $\Omega$ -m FOR $n-2$	1 : 10,000
PL 3-3-19	CONTOURS OF APPARENT RESISTIVITY IN $\Omega$ -m FOR $n-3$	1 : 10,000
PL 3-3-20	CONTOURS OF METAL CONDUCTION FACTOR (M. C. F.) FOR $n-1$	1 : 10,000
PL 3-3-21	CONTOURS OF METAL CONDUCTION FACTOR (M. C. F.) FOR $n-2$	1 : 10,000
PL 3-3-22	CONTOURS OF METAL CONDUCTION FACTOR (M. C. F.) FOR $n-3$	1 : 10,000
PL 3-4	INTERPRETATION MAP OF GEOPHYSICAL SURVEY	1 : 10,000

## SUMMARY

The Government of Japan has carried out since 1970, a series of geological surveys and exploration work for various mineral resources in Central Sulawesi of the Republic of Indonesia in compliance with the request from the Government of the Republic of Indonesia. In fiscal 1970, geological reconnaissance, photo-geology, and airborne magnetic survey were conducted for a total area of 14,160 km<sup>2</sup> and a topographical map of the area was drawn. Promising area of 4,600 km<sup>2</sup> was delineated as the result of the above surveys, and detailed geological survey and geochemical prospecting were carried out in fiscal 1971 and S. Bomba area, (35 km<sup>2</sup>) east of the Lindu lake, was concluded to be the most promising.

1972 is the final year of the project and detailed geological survey, geochemical survey, geophysical survey (IP and EM), and drilling exploration were carried out in a total area of 35 km<sup>2</sup> in S. Bomba with the purpose of clarifying mineralized areas.

The details of the mineralized area, the distribution of the granitic intrusive bodies, geological structure of the metamorphic rocks and other important features were clarified by this work.

The major mineralized area is the S. Webose mineralized area which was located at the central part of the estuary of the Webose river. This area is inferred to have been formed by weak hydrothermal solutions derived from granitic intrusive bodies.

Copper was used as the indicator element for geochemical survey, and the distribution of copper correlated well with the host rocks, but mineralized area could not be detected by this

method because of the weak mineralization.

Geophysical methods were applied in order to find the mineralized areas. EM method (vertical loop method) was employed mainly in streams and ridges and located 12 anomalies of low resistivity. Of these anomalies, several which were considered to be promising were investigated by IP and three large anomalies which agree very well with the results of the EM method were found.

Drilling was done at three points which were selected on the basis of the results of detailed geological survey, geochemical survey, and geophysical survey. These drill holes were all vertical and 130 m deep. Weak sulfides mineralization was detected in drill holes.

The result of the above investigation showed the existence of S. Webose mineralized area whose dimensions were 1 km wide and 3 km in NW-SE direction. It was formed by weak hydrothermal activities associated with the intrusion of granitic bodies. The possibility of these areas developing into promising deposits is very small.



# INTRODUCTION

1. Purpose of Survey

The purpose of the survey in this year is to clarify the features of mineralization in the S. Bomba promising area which was selected by the survey carried out during the previous fisical year.

2. Duration of Survey

Duration of the stay including the preparatory period in the Indonesia.

From 12th September, 1972 to 3rd February, 1973.  
145 days.

Duration of the field survey

From 22nd September, 1972 to 29th January, 1973.  
130 days.

3. Members

Project manager :

TOSHIO WAKIYAMA      Metallic Minerals Exploration  
Agency

Management and negociation party :

YASUSHI KAMBE                      - ditto -

MICHIHISA SHIMODA      Overseas Technical  
Cooperation Agency of Japan

TORU OTAGAKI              Nikko Exploration &  
Development Co., Ltd.

TOMIO SAEKI

Nikko Exploration &  
Development Co., Ltd.

HARDJONO

Geological Survey of  
Indonesia

Geological survey party :

TAKASHI ONO

Nikko Exploration &  
Development Co., Ltd.

(Management and negociation)

ERDITA DIPURA

Geological Survey of  
Indonesia

(Field Survey)

AKITSURA SHIBUYA

Nikko Exploration &  
Development Co., Ltd.

(Field Survey)

Geochemical survey party :

TETSUO TAKAGI

Nikko Exploration &  
Development Co., Ltd.

HARIWIDJAJA

Geological Survey of  
Indonesia

(Analyses of geochemical samples)

Geophysical survey party :

KATSUNOSUKE WANI      Nikko Exploration &  
Development Co., Ltd.

(Planning and management)

MARZUKI SANI              Geological Survey of  
Indonesia

(I. P. survey)

WAHJU SUNOTO              - ditto -

(E. M. survey)

TERUO OHASHI              Nikko Exploration &  
Development Co., Ltd.

(E. M. survey)

KIYOSHI KAWASAKI        - ditto -

(E. M. survey)

YUKIO TOMIKAWA          - ditto -

(Control point survey)

KATSURO SATO              - ditto -

(I. P. survey)

TOMOHIRO NARITA         - ditto -

(I. P. survey)

Drilling party :

KOICHI NAMIKI              Nikko Exploration &  
Development Co., Ltd.

(Planning and management)

TAKASHI KAKISHITA        - ditto -

SUNAO UMEMOTO            - ditto -

DUDUNG TARJONO Geological Survey of  
Indonesia

IKIN - ditto

Supply and transportation party :

NANA PRIJATNA Geological Survey of  
Indonesia

4. Contents of the Project

The project carried out during fiscal 1972 consisted of the following surveys.

Geological survey  
Geochemical survey  
Geophysical survey (EM and IP methods)  
Drilling Exploration

5. Location

The area surveyed during the present project is a four-cornered square defined as follows and located east of the Lindu lake in the central part of Sulawesi.

Northern corner:

Intersection of lat.  $1^{\circ}17'00''$ S. and long.  $120^{\circ}12'40''$ E

Southern corner :

Intersection of lat.  $1^{\circ}21'12''$ S. and long.  $120^{\circ}10'44''$ E

Eastern corner :

Intersection of lat.  $1^{\circ}20'47''$ S. and long.  $120^{\circ}13'22''$ E

Western corner :

Intersection of lat.  $1^{\circ}17'28''$ S. and long.  $120^{\circ}10'06''$ E

## 6. Access

Materials and provisions for this survey were procured at Palu city, Central Sulawesi State. This city is located 60 km north of the surveyed area and is one of the large city of Sulawesi with a population of 40 thousand. Kulawi village is located 70 km south (as the crow flies) of Palu city and the materials and provisions were stocked and reloaded at this village.

The main transportation to Palu city is by air on two routes. One is the route from Jakarta via Balikpapan with one flight every week, and the other is also from Jakarta with transfer at Ujun Pandang with two flights per week. The travel time is about six hours from Jakarta for both routes.

About 80 per cent of the road between Palu city and Kulawi village has been paved including the portion presently under construction. The remaining 20 percent is unpaved and it is supposed to be passable by jeep, but there are several locations along the river bed which become temporarily unnegotiable during the rainy season.

The communication between Kulawi village and Lindu lake is by one path along a steep mountainside which is passable only by men and horses. There are no roads from Lindu lake, and in order to reach the surveyed area, it is necessary to cross the lake by boat, proceed about 20 km eastward through swampy areas, and then about 20 km upstream along the Webose river. The base camp was established half way down along the Webose river.

7. Topography and Climate

In the area surveyed, flat terrain continues to the western margin from the Lindu lake, and other parts consisted almost entirely of mountainous terrain constituting the Nokila laki mountains which trend in NW-SE direction. The elevation of the flat area is 1100 - 1200 m and the highest peak is 1800 m above sea level. All the drainage flow into the Lindu lake in the west and can be classified into those parallel to the Nokila laki mountains in NW-SE direction and those normal to that direction.

Meteorological data of the area were not available, but it is inferred from the data of the vicinity that the diurnal range of temperature is 15°-30°C, annual average temperature about 20°C, and the average precipitation in the range of 3000 - 4000mm. The difference in precipitation between the wet and dry seasons is distinct.

Weathered crust is not very well developed and the thickness of the soils is 1 m. Lateritic soil is not found in the area.

8. Transportation of Equipment and Material

Transportation of materials from Palu city to Kulawi village was done by jeep, and from the village to the base camp by horse and human labor. Lindu lake was crossed by native canoes. Heavy equipments such as drilling equipments were transported directly from Palu city to the base camp by helicopters.

9. The Contents of the Report

This report consists of five major parts. They are; 1 Geology, 2 Geochemical Survey, 3 Geophysical Survey, 4 Drilling, Exploration and in Part 5 the results of the present survey has been summarized and discussed and the future prospects of this area is described.



**PART I**

**GEOLOGICAL SURVEY**

## Chapter 1. Outline of Survey

The present geological survey was carried out in the S. Bomba mineralized area which was delineated as being promising by the survey carried out during the previous fiscal year (1971).

The main objectives of the survey were to clarify the followings: The distribution of the mineralized area, the conditions of the ore deposits, and geologic structure.

The topographic map which was used in the survey was prepared by enlarging the map of 1/50,000 to 1/10,000. The surveyed area covers the whole area planned (35 km<sup>2</sup>). Duration of the survey is same as in INTRODUCTION.

## Chapter 2. Geology

The geology of the surveyed area is composed of metamorphic rocks such as gneiss and schist; sedimentary formations consisting of sandstone and conglomerate; and igneous rocks mainly granite. The area surveyed during the present fiscal year was rather small and as the entire area lied within the area worked in fiscal 1971, the stratigraphic nomenclature adopted in the previous year was used with minor changes. The stratigraphic correlation of the names used in fiscal 1971 and 1972 are laid out in Table 1-1.

Table 1-1 Geological Correlation

Survey in 1971	Survey in 1972
Alluvium	Alluvium
S. Tinauka Formation	S. Tinauka Formation
S. Pakawa Formation	(No distribution)
Sidondo Formation	(No distribution)
S. Rompo Schist Formation	S. Rompo Schist
Towulu Schist Formation	(No distribution)
G. Nokila laki Gneiss Formation	G. Nokila laki Gneiss

## 2-1 Stratigraphy

### 2-1-1 G. Nokila laki gneiss

#### (1) Distribution

This area is the type locality of G. Nokila laki gneiss formation which was named during the survey of fiscal 1971. This rock is distributed throughout the area. This unit is classified into melanocratic gneiss zone and leucocratic gneiss zone, this will be mentioned in detail later. Webose river which flows through the area in E - W direction is the division of the lithology, the north of the river is melanocratic and the south leucocratic.

#### (2) Thickness

The unit is cut into blocks by faults and it is not possible to determine the thickness with accuracy, but it is inferred that the leucocratic gneiss is more than 1,200 m thick in apparence and melanocratic type is thicker than 1,000 m.

#### (3) Occurrence

The gneiss occurs as a roofpendant over the granitic basement, and a part of the unit is observed as xenoliths in the biotite granitic mass.

(4) Constituent rocks

The major constituent of this unit is gneiss which is believed to have been derived from argillaceous rocks.

(5) Lithology

In hand specimen, this unit can be classified into garnet-bearing biotite gneiss and biotite gneiss. Also the rock is classified into melanocratic (those with color index higher than 25) and leucocratic (color index less than 25) gneisses as shown in Appendix 1-1.

Leucocratic gneiss is distributed to the north of the faults (NWW-SEE and NNE-SSW series) which occur along the Webose river, and melanocratic type predominates to the south of the divide. Thus this unit in this area is divided into leucocratic and melanocratic zones.

The following is the classification of the rocks by characteristic mineral assemblage (Appendix 1-2).

*Sillimanite-biotite gneiss*

*Biotite-clinopyroxene-amphibole gneiss*

*Biotite-garnet gneiss*

*Garnet-clinopyroxene-biotite gneiss*

Quartz and plagioclase are contained in these gneisses in large amounts and sphene, apatite, and graphite are the common accessory minerals. In some parts, muscovite, sericite, potash feldspar, epidote, allanite, zoisite, chlorite, diallage, and tourmaline occur in these rocks.

Regularity is not observed concerning the distribution of these four types of gneisses. The difference of color index of these gneisses is mostly attributed to the difference in biotite content.

(6) Stratigraphy

This unit is overlain by S. Rompo schist in appearance, and is intruded by biotite granite, and is overlain unconformably by S. Tinauka formation.

The leucocratic and melanocratic gneiss zones are divided, by NWW-SEE and NNE-SSW trending faults and thus there is no direct evidence concerning the relation between the two zones. It is easier, however, to explain the geology of the area with the leucocratic gneiss in higher horizon as seen in the geological cross section (PL 1-2).

2-1-2 S. Rompo schist

(1) Distribution

This unit occurs in an area 2 km east-west and 1 km north-south with the northern margin near the division of the leucocratic and melanocratic gneisses in the central part of the area.

(2) Thickness

The thickness of this unit is inferred to be more than 500 m, although direct evidence is lacking because it is bounded by faults.

(3) Occurrence

This unit occurs in the G. Nokila laki gneiss. It grades into gneiss to the south and is in contact with the gneiss through faults to the north, west, and east.

(4) Constituent rocks

This unit consists mainly of biotite-amphibole schist, and quartz schist is found in some parts.

(5) Lithology

The rocks in this unit are mostly hard, fine-grained, and schistose and melanocratic in hand specimen.

Banded quartz schist containing small amount of amphibole is found in rare cases.

Biotite-amphibole schist, diopside- amphibole -biotite schist, biotite-garnet-amphibole schist, and biotite-diopside quartz schist are distinguished microscopically.

(6) Stratigraphy

This unit apparently overlies the melanocratic zone of the G. Nokila laki gneiss. That is the lithology of this formation grades into gneiss to the south (apparent lower horizon) in some places. This formation, however, is isolated as a block bounded by faults in most areas and is intruded by biotite granite.

This unit has the same original rock and metamorphic facies as the schist formation named S. Rompo schist formation in 1971 which overlies the G. Nokika laki gneiss formation and is intruded by granite at Torro

area (25 km southwest of the present area). Therefore this unit is correlated to the S. Rompo schist formation.

2-1-3 S. Tinauka formation

(1) Distribution

This formation is distributed in the western margin of the area in N - S direction and has a width of 300 m. It extends into the flat areas to the north of the surveyed area.

(2) Thickness

This formation is very thin in the order of 150 m.

(3) Occurrence

This formation has a strike of N15°-50°E and dip of 35°- 40°N, overlies gneiss, schist, and biotite granite unconformably, and has a basal conglomerate layer.

(4) Constituent rocks

This formation consists of alternation of conglomerate, sandstone, and siltstone. There are at least three *sedimentary cycles seen in this formation*, and from the distribution and occurrence, it is considered to be a lacustrine deposit by the survey of 1971.

(5) Lithology

The fresh surface of the sandstone and siltstone is



bluish gray, but it alters readily to pale brown by oxydation. It is soft and not altered. Conglomerate consists mostly of rounded pebbles of 10 - 20 cm, but the basal conglomerate consists of rounded to sub-angular pebbles and boulders of 10 - 30 cm and occasionally 100 cm. The pebbles are mostly gneiss and granite and the matrix is sandy.

(6) Stratigraphy

This formation unconformably overlies all geological units in the area with the exception of alluvium.

2-1-4 Alluvium

(1) Distribution

Alluvium is thinly developed along the estuaries of rivers in this area, and the distribution becomes wider toward Lindu lake to the west and grades into lacustrine sediments.

(2) Thickness

It is about 10 m thick near the river beds, becomes thicker to the west and is estimated to be more than 50 m at the western edge of the area.

(3) Constituent materials

This formation consists of unconsolidated gravel, sand, and silt. The sand and silt component rapidly increases in the flat terrain to the west of Lindu lake.

The gravel is mostly gneiss and biotite granite.

(6) Stratigraphy

This overlies all geological units of the surveyed area unconformably.

2-1-5 Intrusive rocks

Approximately 40 percent of the surveyed area consists of granitic bodies. From regional stand point, the surveyed area corresponds to a roofpendant on biotite granitic batholith, therefore the major part of the intrusive bodies are biotite granite, and remaining small bodies of biotite-hornblende quartz porphyry, epidiorite and peridotite and gabbro.

Description of these rocks is followed in order of intrusion.

2-1-5-1 Epidiorite

(1) Distribution and occurrence

Epidiorite occurs in this area mostly along faults in small bodies with dimensions in the range of 20 - 50 m in width and 100 - 150 m in length.

(2) Lithology

The rock is melanocratic (color index 40), equigranular and somewhat metamorphosed. Weak gneissose structure is observed in some parts. Under the

microscope, remnant texture of diorite consisting of plagioclase and augite with minor amount of quartz is observed. The metamorphic minerals are green hornblende, garnet, biotite with brown to reddish brown pleochroism, allanite, and others. Also minerals which are believed to have been formed by hydrothermal alteration such as chlorite, quartz, and laumontite are found.

(3) Period of intrusion

The epidiorite bodies have been intruded into G. Nokilaki gneiss and is intruded by biotite granite. And these epidiorite bodies have undergone metamorphism of the amphibolite facies which is the same as the gneiss formation (see 2-2-3). From these evidences, it is believed that the epidiorite intrusion occurred after the deposition of the original rocks of the gneiss and before regional metamorphism. The relation of these bodies to the S. Rompo schist is not clear.

2-1-5-2 Biotite granite

(1) Distribution and occurrence

Biotite granite is distributed throughout the surveyed area forming stocks and dykes of various dimensions.

(2) Lithology

Mineral composition and the ratio of constituent minerals are more or less uniform through different intrusive bodies and also within individual bodies. The rock is leucocratic (color index 10 - 15), medium-grained,

and holocrystalline. The major component minerals are potash feldspar, plagioclase, quartz, and biotite, also small amount of green hornblende is contained in rare cases. The common accessory minerals are apatite and sphene. Chlorite, epidote, allanite, and carbonate minerals are observed in some cases.

A small stock near lat.  $1^{\circ}17'50''$  S., long.  $120^{\circ}1'20''$  E., has suffered intense sericitization.

(3) Period of intrusion

Biotite granite bodies have been intruded into G. Nokilaki gneiss and S. Rompo schist, and is intruded by peridotite and gabbro. The isotopic age determination carried out at the time of the survey in 1970 showed the age of the rocks to be Neogene Tertiary to Pleistocene ( $4.80 \times 10^6$  -  $1.62 \times 10^6$  years, K-Ar method).

This intrusive body can be divided into two; the intrusions of earlier and later stages (see 2-3-5), and it is inferred that the mineralization in this area is related to the later stage intrusion of the biotite granite.

2-1-5-3 Biotite-hornblende quartz porphyry

(1) Distribution

This quartz porphyry is not observed on the surface but is found in the drilling core of DH-3. It occurs at depth greater than 100 m and the bottom is not confirmed.

(2) Lithology

The rock is greenish gray, porphyritic, compact, and hard.

Phenocrysts of quartz, plagioclase, biotite, hornblende and other rock-forming minerals with corroded structure occur within the matrix of micrographic to graphic or myrmekitic texture. Biotite shows brown pleochroism and many of the grains have been altered to chlorite. Almost all of the hornblende grains have been altered to chlorite and epidote. Weak pyrite dissemination is generally observed.

(3) Period of intrusion

Acidic porphyritic rocks have been found in the estuary of the Palu river during the survey of 1971, and the intrusion of this rock is inferred to have occurred simultaneously with the activities of the porphyritic rocks, i. e., later than the intrusion of the biotite granite and earlier than the intrusion of the ultrabasic rocks.

2-1-5-4 Peridotite and Gabbro

(1) Distribution

These rocks are distributed throughout the surveyed area as dykes along fault zones. These dykes are small with width of 20 - 40 m and length of 200 - 400 m.

(2) Constituent rocks

The intrusives consist mainly of peridotite. As parts of peridotite body or individual bodies,

gabbro is occurred.

(3) *Lithology*

Peridotite is grayish black and compact. Augite, diallage, and garnet occur as large crystals in the order of 0.5 mm and olivine and some augite and garnet are in smaller crystals in the order of 0.1 mm. The texture is porphyritic. Garnet is different from in gneiss to show brownish color. Olivine is serpentinized along cracks.

Gabbro is grayish black, coarse-grained, holocrystalline, and massive. The major constituent minerals are quartz, plagioclase, biotite, amphibole, and clinopyroxene, and the texture is graphic.

(4) *Period of intrusion*

These bodies have been intruded into G. Nokila laki gneiss and biotite granite. It is concluded from the results of the survey of 1971 that these rocks were formed after the intrusion of the granite, either in late Tertiary or early Quaternary.

2-2 *Metamorphism*

Metamorphic rocks such as gneiss and schist are widely distributed in the surveyed area and these rocks are the major ones which suffered mineralization and alteration. It was necessary, consequently, as the first step to distinguish the minerals formed by regional metamorphism from those by hydrothermal alteration.

Fig. 1 - 1 Geological Column

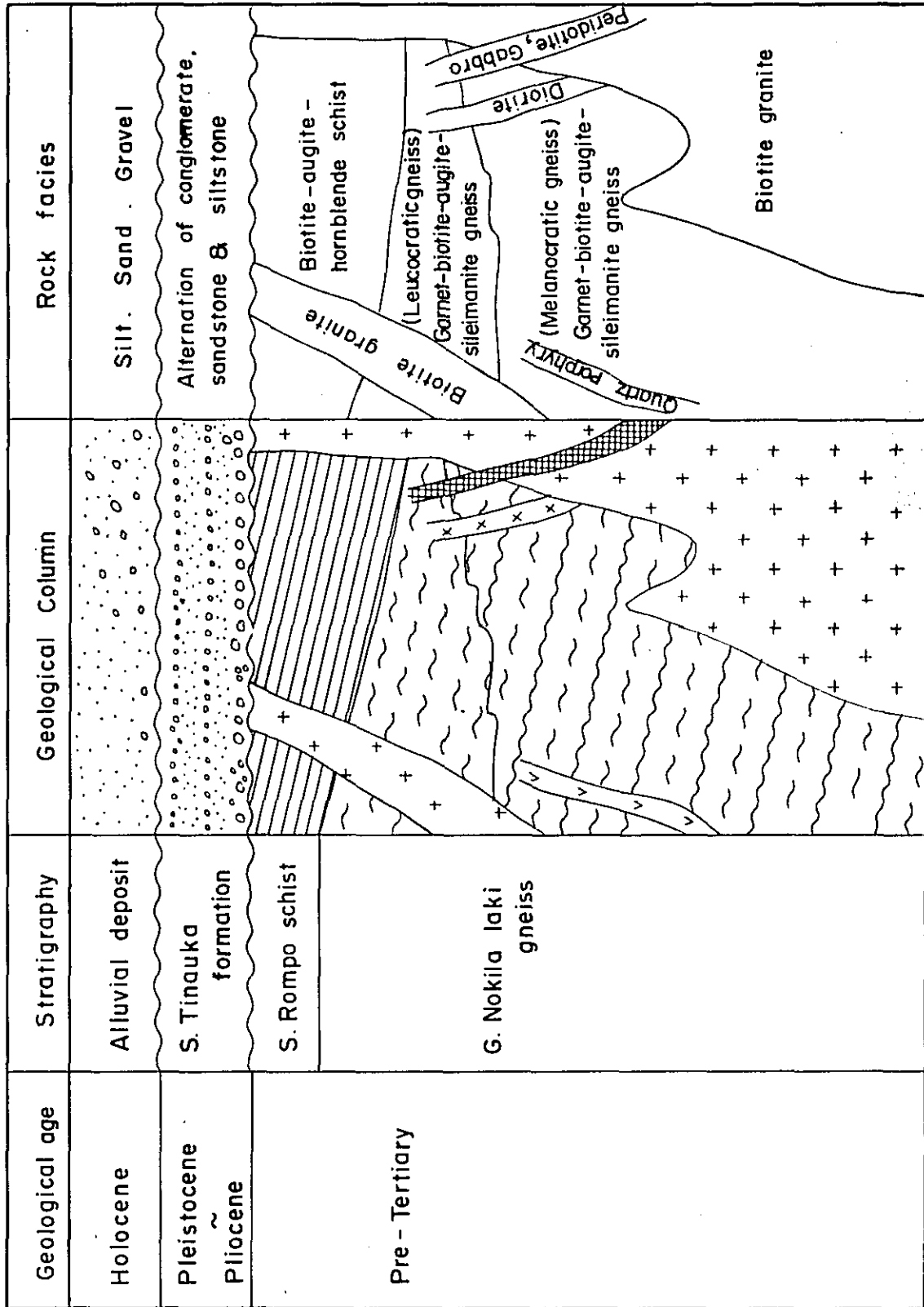


Fig. 1-2 Stratigraphy and Geological Events

Geological age		Stratigraphy	Metamorphism	Crustal movement	Igneous activity	Mineralization
Quaternary	Holocene	Alluvial deposit				
	Pleistocene					
Tertiary	Pliocene	S. Tinauka formation				
	Miocene					
	Oligocene					
	Eocene					
	Palaeocene					
Mesozoic		Metamorphic complex *	Regional metamorphism	NEE-SW · NNW-SSE faults NW-SE · NNE-SSW faults	Diorite	
Paleozoic		{ S. Rompo schist G. Nokila laki gneiss		Uphaving	Biotite granite	
					Biotite-hornblende-quartz porphyry	
					Peridotite, Gabbro	S. Webose mineralized area and other weak mineralizations related to granite intrusion.

\* The age of original rocks is not certified



This work, as a matter of fact, has enabled us to reveal in some detail the features of the alteration areas related with mineralization. This also we believe will serve not only for mineral exploration, but for understanding of the geology of the area. In the following are given the petrographic characters of the metamorphic rocks with some petrogenetic interpretation.

2-2-1. G. Nokila laki gneiss

The mineral assemblages of the G. Nokila laki gneiss can be classified into the following four groups.

- (1) Biotite - (sillimanite) - quartz - plagioclase  
(muscovite, potash feldspar, chlorite, and sericite are sometimes associated)
- (2) Biotite - clinopyroxene - (amphibole) - (sillimanite) - quartz - plagioclase  
(potash feldspar, muscovite, epidote, zoisite, diallage, tourmaline, actinolite, chlorite, and sericite are associated in some cases)
- (3) Garnet - biotite - quartz - plagioclase  
(spinel, sillimanite, chlorite, sericite, and zeolite are sometimes associated)
- (4) Garnet - augite - biotite - (sillimanite) - (spinel) - quartz - plagioclase  
(diopside, allanite, muscovite, potash feldspar, chlorite, sericite, and zeolite are sometimes associated)

The biotite in these rocks are reddish brown. Generally the color of biotite can be an indication of the metamorphic temperature (Miyashiro 1965), greenish brown biotite being often found in the rocks of relatively low temperature formation and reddish brown variety which is rich in titanium in the rocks formed at relatively high metamorphic temperature.

The biotite in the present rocks is also believed to have formed at higher temperature. Most of amphiboles, not being very common in these rocks, are green hornblende. Actinolite is rarely found. Pyroxenes are much more common than amphiboles and most of them are clinopyroxene either Ca-rich augite or diopside.

Garnets occur in gneiss at frequencies of 60 - 70 per cent, and the content of the mineral in the rocks of this area is generally 1 - 5 mode per cent with the maximum of about 20 per cent. The garnets are pinkish red and most of them are 2 - 3 mm in diameter. Optical anomalies which are common in grandites (Table 1-2) do not occur and in some cases inclusions of quartz and feldspars are observed. Garnets and sillimanite in this area have been considered as the products of thermal metamorphism of granite, but the distribution of the minerals is not related to the mode of occurrences of the individual granitic bodies.

Table 1-2. Chemical Composition of Common Garnets

	Mineral	Chemical Formulae	Refractive Index, $n_D$	Specific Gravity, $d$	Lattice Constant, $a_0$ (Å)
Pyrospite	Pyrope	$Mg_3Al_2Si_3O_{12}$	1.714	3.582	11.459
	Almandine	$Fe^{+2}Al_2Si_3O_{12}$	1.830	4.318	11.526
	Spessartine	$Mn^{+2}Al_2Si_3O_{12}$	1.800	4.190	11.621
Grandite	Grossular	$Ca_3Al_2Si_3O_{12}$	1.734	3.598	11.851
	Andradite	$Ca_3Fe_2^{+3}Si_3O_{12}$	1.887	3.859	12.048

By B. J. Skinner (1956).

Table 1-3. Chemical Analyses of Garnets

	103104		DH-1, 18.6 m		122101	
	(1)wt %	(2)wt %	(1)wt %	(2)wt %	(1)wt %	(2)wt %
SiO <sub>2</sub>	38.15	38.73	38.69	38.95	37.52	36.08
TiO <sub>2</sub>	0.10	0.10	0.08	0.07	0.06	0.06
Al <sub>2</sub> O <sub>3</sub>	21.89	22.14	21.45	21.10	21.45	21.46
FeO	24.40	23.64	22.69	24.23	27.19	27.63
MnO	0.42	0.40	0.97	1.03	0.79	0.88
MgO	9.05	9.88	6.41	6.88	6.30	6.16
CaO	4.82	4.05	9.02	7.15	5.35	5.11
Na <sub>2</sub> O	0.03	0.01	0.02	0.03	0.02	0.02
K <sub>2</sub> O	0.02	0.01	0.01	0.02	0.01	0.01
Total	98.87	99.16	99.35	99.46	98.70	97.42

Analytical method : Electron probe micro analyser

Analyst : Prof. H. Kano, Institute of  
Mining Geology, Akita University.

Sample Location :

103104 S. 1°17'30" E. 120°11'40"

DH-1, 18.6m S. 1°18'11" E. 120°11'32"

122101 S. 1°20'30" E. 120°11'00"

Table 1-4. Endmember Ratios of Garnets

103104	(1)	Py35	Alm 51	Sp 1	Gr 10	And 3
	(2)	Py38	Alm 50	Sp 1	Gr 10	And 1
	Average	Py37	Alm 50	Sp 1	Gr 10	And 2
DH-1, 18.6 m	(1)	Py25	Alm 48	Sp 2	Gr 23	And 2
	(2)	Py27	Alm 51	Sp 2	Gr 16	And 4
	Average	Py26	Alm 50	Sp 2	Gr 19	And 3
122101	(1)	Py25	Alm 58	Sp 2	Gr 13	And 2
	(2)	Py25	Alm 58	Sp 2	Gr 14	And 1
	Average	Py25	Alm 58	Sp 2	Gr 13	And 2

Abbreviations

Py : Pyrope, Alm : Almandine,

Sp : Spessartine, Gr : Grossular,

And : Andradite

Sample locations are same as in Table 1-3.

The chemical analyses of the garnets from the surveyed area are listed in Table 1-3. The compositions of the minerals in terms of the five end-members shown in Table 1-2 are calculated and are laid out in Table 1-4. It is seen that pyrope molecule and almandine molecule forms the majority and spessartine molecule is minor at 1 - 2 per cent. Grandite molecule constitutes 12 - 22 per cent of the bulk composition. Generally the composition of pyralspite derived from argillaceous rocks changes in Mn → Fe → Mg order with the rise of temperature. Thus the fact that the garnets of this area are relatively rich in pyrope molecule and poor in spessartine molecule indicates that they were formed at relatively high temperature. Also the fact that the grandite component constitutes 12 - 22 per cent of the mineral is considered to be the indication that the argillaceous rocks from which gneiss was derived were relatively rich in calcium.

The three analysed samples of 103104, DH-1 18.6 m, and 122101 are located from north to south within the surveyed area. The number of these analysed samples are few, but it can be seen that there is a tendency of decrease of spessartine and andradite molecules and increase of pyrope molecule northward in this area. This shows the rise of the metamorphic temperature towards north.

Kyanite and andalusite are not found in the gneiss while sillimanite and spinel are common. Titanium minerals such as rutile ( $\text{TiO}_2$ ), ilmenite ( $\text{FeTiO}_3$ ), and sphene ( $\text{CaTiO}_5$ ) are relatively common in these rocks.

The characteristic features described above show that the gneiss of this area is in the intermediate stage between

amphibolite and granulite facies. In these rocks, low temperature - low pressure minerals such as sericite, chlorite, epidote, and zoisite occur together with the high grade metamorphic minerals. As the distribution of these minerals is controlled by the S. Webose mineralized zone, they are believed to have been formed by later hydrothermal processes.

2-2-2            S. Rompo schist

This schist is generally rich in mafic minerals and the mineral assemblages are as follows.

Amphibole - biotite - (garnet) - quartz - plagioclase

Biotite - amphibole - augite - quartz - plagioclase

The amphiboles in these rocks are hornblende with greenish tint which are common in the rocks of amphibolite facies, and the biotite has reddish tint which is also common in the high temperature metamorphic rocks. Garnets are porphyroblasts with inclusions of quartz and opaque minerals.

2-2-3            Epidiorite

The mineral composition of this rock is green hornblende derived from clinopyroxene, reddish biotite, pinkish garnet, quartz and plagioclase and is of amphibolite facies.

#### 2-2-4 Discussion

The gneiss, schist, and epidiorite mentioned in the previous sections show various mineral assemblages referred to the difference in bulk chemical composition of the original rocks as well as to the heterogeneity of the metamorphic grade. As a whole, however, they are in the intermediate region between amphibolite and granulite facies. Sericite, chlorite, epidote, laumontite, and potash feldspars (aduralia) are believed to be the products of later hydrothermal alteration.

#### 2-3 Geologic Structure (PL. 1-3)

##### 2-3-1 The Geologic Structure of the adjoining areas

The survey carried out in the year 1970 showed that there is a north-south trending central lineation (Tawaëlia graben) to the east of the present area and in the west there is the Fossa Sarasina (Palu fault) with N20°W - S20°E trend.

The present area is composed mainly of gneiss and forms the southwestern part of the G. Nokila laki gneiss body, of the Nokila laki mountains. This gneissose body is 22 km long and 12 km wide and is elongated in NNW-SSE direction. It is surrounded by granite, and forms a roof pendant of these granites.



2-3-2            The structure of metamorphic rocks and sedimentary rocks

The metamorphic rocks are divided into several blocks by faults and are intruded by many intrusive bodies. The planar structure (gneissose and schistose structures) of various metamorphic rocks are summarized as follows.

Melanocratic gneiss zone: The strike of the planar structure is in E-W to NWW-SEE direction.

Leucocratic gneiss zone : The strike of the planes varies with individual zones.

S. Rompo schist : The strike of the planar structure is mainly in NWW-SEE direction and conformable relation with the melanocratic gneiss is observed.

The dip of these gneissose and schistose structures are often 30 to 60 degrees, and steep dip of 70 to 80 degrees are found in some parts of the area.

The results of the survey up to 1971 shows that the metamorphic zones are arranged in N - S direction and the degree of metamorphism increases from west to east. In the present area, however, the strike of the planar structure of the metamorphic rocks is generally in the E - W direction and this does not coincide with the planar structure of the adjoining areas. The tectonic disturbance of the metamorphic rocks by the intrusion of the granitic bodies which followed metamorphism is one of the possible causes for this disturbance. To distinguish a lineation in metamorphic rocks is difficult because of abundant platy minerals in the survey.

S. Tinruka formation has strike of N15 - 50°E and the dip is 35 - 40°NW. This steeper inclination than the formation at the type locality indicates the uplift movement during or after Pleistocene time.

### 2-3-3 Folds

The fold structure of this area is confirmed only at two localities as shown in the geological cross section (PL 1-2) and geologic structure map (PL 1-3). From the minute folds observed in the drill cores (DH-3) and in boulders, it is believed that there are many folds of various scales.

### 2-3-4 Faults

In Plate 1 - 3, the faults which are observed in field, are inferred by distribution of metamorphic rocks, tendency of planner structure, and photo-geologically.

The trends of the faults differ in the northern and southern part of the area. That is, in the southern part of the area, there are two main systems of faults, i. e., NEE-SWW system and NNW-SSE system. The latter faults cut through the former faults in the matamorphic areas. Whereas in the northern part, faults of NWW-SEE system and NNE-SSW system are developed in the metamorphic and granitic rocks, here again the former systems are cut by the latter ones. The faults of the latter systems in NWW-SEE and NNE-SSW directions agree with the lineament in the granitic basement in a wide region including the present area (Report on Geological Survey of Central Sulawesi, 1971, vol. 2, part 2.). And the latter faults in NEE-SWW and NNW-SSE direc-

tion cut the former faults, and thus they were formed later.

2-3-5     The Relation between igneous rocks and geologic structure

There are many biotite granitic intrusive bodies in this area and their elongation is generally in the NW-SE direction. This is in general agreement with the elongation of the G. Nokilaki gneiss (NNW-SSE). The relatively larger granitic bodies (100 m x 400 m or larger) are distributed mainly at the southern side of the Webose river and there is a tendency to follow the trend of the NNW-SSE faults. Also some of these intrusive bodies are cut by the faults of the NWW-SEE and NNE-SSW systems. On the other hand, smaller biotite granitic bodies (100 m x 400 m or smaller) are related to mineralization as will be mentioned later, and these stocks cut through the faults of NWW-SEE and NNE-SSW systems.

Thus, two stages are considered for the biotite granitic - and faults - activities. These are from earlier to later stages as follows.

- (1) Formation of the NEE-SWW and NNW-SSE faults.
- (2) The intrusion of the granitic stocks and dykes.
- (3) The formation of NWW-SEE and NNE-SSW faults.
- (4) The intrusion of small biotite granitic stocks which brought about mineralization.

2-3-6     Geological history

The following is the history of the metamorphic process and igneous activities of the area compiled from the data obtained from the whole our surveys.

- (1) Geosynclinal sediments consisting mainly of argillaceous rocks underwent regional metamorphism and formed G. Nokila laki gneiss and S. Rompo schist of intermediate metamorphic facies between amphibolite and granulite facies. The elongation of the metamorphic zone in this period was N-S.
- (2) At the latest stage or after the regional metamorphism, granitic magma was intruded along the axis of the most intensive metamorphism, uplifted and disturbed the metamorphic rocks, and formed the faults of the NEE-SWW, NNW-SSE systems.
- (3) The granitic intrusion itself has given rise to the formation of batholith. Dykes and stocks were branched out from the batholith into the metamorphic rocks.
- (4) Extensive faulting occurred through the whole granitic area and it is represented by the NWW-SEE and NNE-SSW fault systems in the surveyed area.
- (5) Small scale intrusion of granitic stocks occurred and this was accompanied by mineralization. The mineralized areas of S. Webose and some other ones were formed in this period.
- (6) Small dykes of peridotite and gabbro were intruded along the faults.

## Chapter 3. Ore Deposits

### 3-1 The Distribution and Scale of the Mineralized Areas

Most of the mineralized areas in the surveyed area are characterized by the dissemination of iron sulfide. The distribution is shown in PL 1-4. Specimens from exposures with mineralization were sampled at random and analysed for copper and sulphur content, the grade is shown in PL 1-4 and Appendix 1-6.

The mineralized area of 1 km in width and 3 km in length in the area extending from the western side of the northern edge of the estuary of Webose River southeastward is the largest (S. Webose mineralized area). Other mineralized areas are smaller with the average of extension about 100 m x 300 m, maximum about 500 m x 1,000 m, and occur sporadically. These small mineralized areas are distributed along the smaller (less than 100 m x 400 m) biotite granitic bodies and also near fault zones.

The maximum copper content of the samples from the S. Webose mineralized area is 0.14 per cent and the arithmetic means of the copper content of ten samples is 0.04 per cent, the maximum sulphur content is 6.8 per cent and mean value is 2.4 per cent. The copper content of the samples from other smaller mineralized areas is usually 0.01 per cent or less and rarely reaches 0.02 per cent, and the sulphur content is less than 1 per cent. Majority of the mineralized areas is in gneiss and some in schist and small biotite granitic stocks.

### 3-2 Alteration

Hydrothermal alteration in this area is generally not very

intensive, and clay minerals could be identified in hand specimens only from those sampled along fissures such as faults, and it was difficult to identify the minerals formed by hydrothermal alteration in the field. Through laboratory work including optical and X-ray work, alteration minerals were found to occur fairly widely. The following is the outline of the alteration process in this area constructed on the basis of the data obtained from these laboratory studies. ( Appendix 1-3, 1-4)

Hydrothermal alteration occurred mostly near the S. Webose mineralized area as shown in PL 1-5. The following three alteration zones are recognized in the area.

- (1) Quartz - sericite - potash feldspar zone (silicified zone)
- (2) Sericite - chlorite zone
- (3) Chlorite - (montmorillonite) zone

Laumontite occurs in all of these zones as vein form.

Silicified zones extend in NW - SE direction in three locations and are enveloped in the sericite-chlorite zone. The sericite-chlorite zone is distributed in NW-SE direction and followed by the chlorite - (montmorillonite) zone on the outer sides.

- (1) Quartz - sericite - potash feldspar zone

The features of the alteration varies from completely silicified to felsic gneissose. Under the microscope, the major constituent is quartz, and sericitized plagioclase, minutely fragmented garnets, and potash feldspar are associated. The rock is often cut by veinlets of laumontite and clinozoisite.

Since in this area, this zone is the unique geological unit in which potash feldspar is found in the rocks other than biotite granite, it is believed that this mineral was

formed by hydrothermal alteration. This zone is poor in sulfide minerals.

(2) Sericite - chlorite zone

Sericite - chlorite zone is observed in gneiss and some biotite granite area, and occupies an area of 2.5 km long and 1 km in maximum width elongated in NW - SE direction. At the center of this zone, strongly argillitized zone with sericite and chlorite as the major component is observed in the area of 100 m in width and 500 m long elongated in E - W direction.

In this zone the texture of the original rock is not destroyed by alteration, and weak sericitization of plagioclase, and also weak chloritization of biotite and garnets are observed as replacement and veinlet. The content of pyrrhotite is higher in this zone than in others and minor amount of chalcopyrite is also found. This zone coincides fairly well with the S. Webose mineralized area.

(3) Chlorite - (montmorillonite) zone

This zone is found in both gneiss and biotite granite, and there are strongly argillitized zones along fissures such as faults. There is a general tendency of higher chlorite content in the altered metamorphic rocks and higher montmorillonite content in the altered biotite granite. In some weakly altered rocks, parts of the mafic minerals are slightly altered to chlorite.

These arrangement of the altered zones was confirmed to extend vertically by drill holes. Their concentric arrangement was also clarified. (Fig. 4-2).

### 3-3 Ore Minerals

The rocks of the mineralized zone of this area consists of dissemination, films, or veinlets of small amount of iron sulphides and minor amount of chalcopyrite. The host rocks are mostly gneiss and partly schist and biotite granite. Any difference in the mode of occurrence of the ore minerals do not exist between the S. Webose area and other smaller mineralized areas.

The ore minerals which occur in this area are pyrrhotite, pyrite, marcasite, chalcopyrite, magnetite, rutile, and ilmenite. Pyrrhotite is most abundant and it occurs as anhedral grains of 0.1 to 1.0 mm in size. It is inferred to be the hexagonal type because of weak etching by saturated chromium acid, and very weak magnetism. In some parts pyrrhotite is altered to marcasite.

Pyrite is much less than pyrrhotite and it occurs mostly as euhedral grains of 0.1 to 0.2 mm in diameter. The pyrite in metamorphic rocks are sometimes altered to marcasite. In some cases, magnetite inclusions are found in pyrite from the dissemination in biotite granite.

Many of the chalcopyrite grains are rounded and with sizes in the range of 0.05 - 0.1 mm or smaller. It is mainly associated with pyrrhotite or pyrite. The detailed mineralogical data are laid out in Appendix 1-5.

The mineral paragenesis of the ores and the host rocks of this area are shown in Table 1-5.

In this area, the following relationship exists between the iron minerals and the host rocks.



Table 1-5. Opaque Mineral Assemblages

Host Rocks	Ore Minerals	Gangue Minerals
Gneiss	Pyrrhotite-Chalcopyrite Pyrrhotite-Marcasite-Chalcopyrite Pyrrhotite-Pyrite-Chalcopyrite	Graphite, Rutile, Ilmenite Rutile, Ilmenite
Biotite-amphibole schist	Pyrite-Marcasite-Chalcopyrite	Ilmenite
Biotite granite	Pyrite-Magnetite-Chalcopyrite	
Biotite-amphibole quartz porphyry	Pyrite	

- (1) The iron minerals in biotite granite which is associated with mineralization are pyrite-magnetite.
- (2) Graphite-bearing gneiss which is the major host rock of the S. Webose mineralized area contains pyrrhotite and marcasite after pyrrhotite.
- (3) The iron minerals in gneiss which do not contain graphite are pyrrhotite-pyrite.
- (4) Biotite - amphibole schist contains pyrite and marcasite.

The variation of the paragenesis of the iron minerals with the difference of host rocks can be explained qualitatively by the role of graphite during mineralization.

Not only the stability of iron oxides, but also the stability conditions of pyrite, pyrrhotite and siderite are greatly affected by oxygen fugacity (Holland 1959, 1965, Krauskopf 1964). On the other hand, graphite plays an important role concerning the redox conditions within the crust (Miyashiro 1964a, b). Also the zonal arrangement of the iron minerals is explained very clearly by the stability relations of the iron minerals under low oxygen fugacity caused by the oxydation of graphite during mineralization (Yui 1966).

Now, if graphite is present in excess such as in the case of graphite bearing gneiss, the oxygen fugacity decreases and only pyrrhotite will be precipitated. In cases where graphite is not present in sufficient quantity such as in the cases of schist and gneiss without graphite, oxygen fugacity will not decrease sufficiently and pyrite or pyrite-pyrrhotite will become the stable phase.

### 3-4 Mineralization

The following is the summary of the facts pertinent to the mineralization in this area.

- (1) The mineralization is believed to be related with the intrusion of smaller (100m×400m or smaller) biotite granite stocks. No lithological difference is observed between the smaller granite bodies which are related with the mineralization and those not related to the mineralization; they are both medium-grained and holocrystalline.
- (2) The activities of the granite related to the mineralization process are believed to be of the latest stage of the intrusion. This observation is based on the geologic structure of the area.
- (3) The host rock of the mineralized area are mainly gneiss and partly schist and granite.
- (4) The ore minerals are scattered in the host rocks as dissemination, veinlets or thin films.
- (5) The extension of the S. Webose mineralized area is 1 km in maximum width and 3 km in NW - SE direction. It is located in highly fractured zone.
- (6) The grade of mineralized rocks of the S. Webose mineralized area is copper 0.01 - 0.14 per cent (average 0.04 per cent) and sulphur 0.7 - 6.8 per cent (average 2.4 per cent).
- (7) Quartz - sericite - potash feldspar zone (silicified zone), sericite - chlorite zone, and chlorite - (montmorillonite) zone surround the S. Webose mineralized area outwardly

enumerated order. The mineralized area coincides with this sericite - chlorite zone.

- (8) The primary ore minerals are pyrrhotite, pyrite, chalcopyrite, and magnetite in decreasing order of abundance. The only secondary mineral found is marcasite which is believed to have derived from pyrrhotite and pyrite. Secondary copper minerals were not found.

From the above observation, it is concluded that the formation of the S. Webose mineralized area is related to the intrusion of small granite stocks, occurring mostly in the metamorphic rocks which were intruded by the said granitic bodies. The mineralized mass can be said as a sort of copper bearing disseminated deposit. The facts mentioned in (1), (2), (4), and (7) indicate that this mineralization is similar to porphyry copper type. The difference, however, is that the major ore mineral in this mineralized area is pyrrhotite, and also molybdenite and bornite is not associated.

**PART II**

**GEOCHEMICAL SURVEY**

## Chapter 1. Outline of Survey

Geochemical survey: was carried out in the S. Bomba mineralized area with the total area of 35 km<sup>2</sup>. This area was delineated as being the most promising by the result of the geological and geochemical surveys carried out in fiscal 1971. The basis for the delineation was the relatively wide distribution of disseminated iron sulphides and the occurrence of copper and zinc anomalies in the river sediments.

The objectives of this survey were to obtain informations concerning the scale of the known mineralized areas and to locate new mineralized areas. For this purpose, soils in which the secondary dispersion of the indicator element is easier to follow than in river sediments were used and copper was selected as the indicator.

The topography is relatively steep and the vegetation is completely virgin and is generally dense. The vegetation, however, becomes sparse with the increase of elevation. The soil of this area with the above meteorological and topographic characteristics is about 1 m thick and is very thin compared to those of typical tropical humid flat areas. Field work of this survey started on 22, September 1972 and finished on 3, December 1972. Period of the work is 73 days.

## Chapter 2. Sampling

The soil samples for geochemical survey were collected at 100 m intervals on the geophysical traverse at the time of geophysical work. The location of the samples are shown in PL 2-1. The number of samples are 555 from the EM traverse along rivers, 220 from IP traverse opened through the jungle, with a total of 775. The average density of sampling was 22 per square kilometer.

The soil column in this area showed the A horizon to be about 30 cm, and the geochemical samples were collected from the depth of 30 - 50 cm; the uppermost part of the B horizon. On the traverse along the rivers, river beds were avoided as much as possible and sampled from mountain slopes. Each sample was about 100 g and the grain size and the color were recorded.

## Chapter 3. Chemical Analyses

### 3-1 Preparation of Samples

The collected samples were processed in the laboratory at the base camp as follows.

- (1) The total samples were dried for about two hours on a sand bath in an aluminum container.
- (2) The dried samples were consolidated and it was crushed by gentle crushing in a steel mortar.
- (3) The samples were sieved through 80 mesh stainless steel sieve, and the -80 mesh portions were used for analysis.

### 3-2 Method of Analysis

Rapid bi-quinoline colormetry was used for the rapid analysis of the indicator element, copper. The analytical procedure was as follows.

- (1) 0.200 g of the prepared sample was taken into a silica glass test tube, 1 g of powdered potassium pyrosulphate was added, and stirred by shaking.
- (2) The mixture was fused over a propane gas burner.
- (3) After cooling, 10 ml of hydrochloric acid (1 N) was added and the fused material was dissolved over a water bath.
- (4) After cooling, 1.00 ml of the clear solution was decanted into another test tube.
- (5) Hydroxylamine hydrochloride ( $\text{NH}_2\text{OH} \cdot \text{HCl}$  5% solution) 1 ml, copper buffer solution (pH 7, sodium acetate 400 g, and potassium sodium tartrate 100 g dissolved in 1,000 ml of water) 10 ml,  $\alpha - \alpha'$  bi-quinoline solution (0.02 %, amyl



alcohol) 1.00 ml were added and stirred vigorously for two minutes.

- (6) A series of standard solutions were prepared by the process (2) to (5) and colorimetry of the  $\alpha$ - $\alpha'$ bi-quinoline solution of the sample and the standard solution was done by the unaided eyes.

Standard solutions were newly prepared each day, and a standard reference prepared by mixing about 50 soil samples was included in the analysis each every day for the check. The analysis of this standard was  $31 \pm 0.5$  ppm and thus the accuracy of the analysis was considered to be satisfactory.

The limit of quantitative analysis of copper by this method was 3 ppm and the number of samples analysed was about 35 samples per day.

## Chapter 4. Interpretation

### 4-1 Data Processing

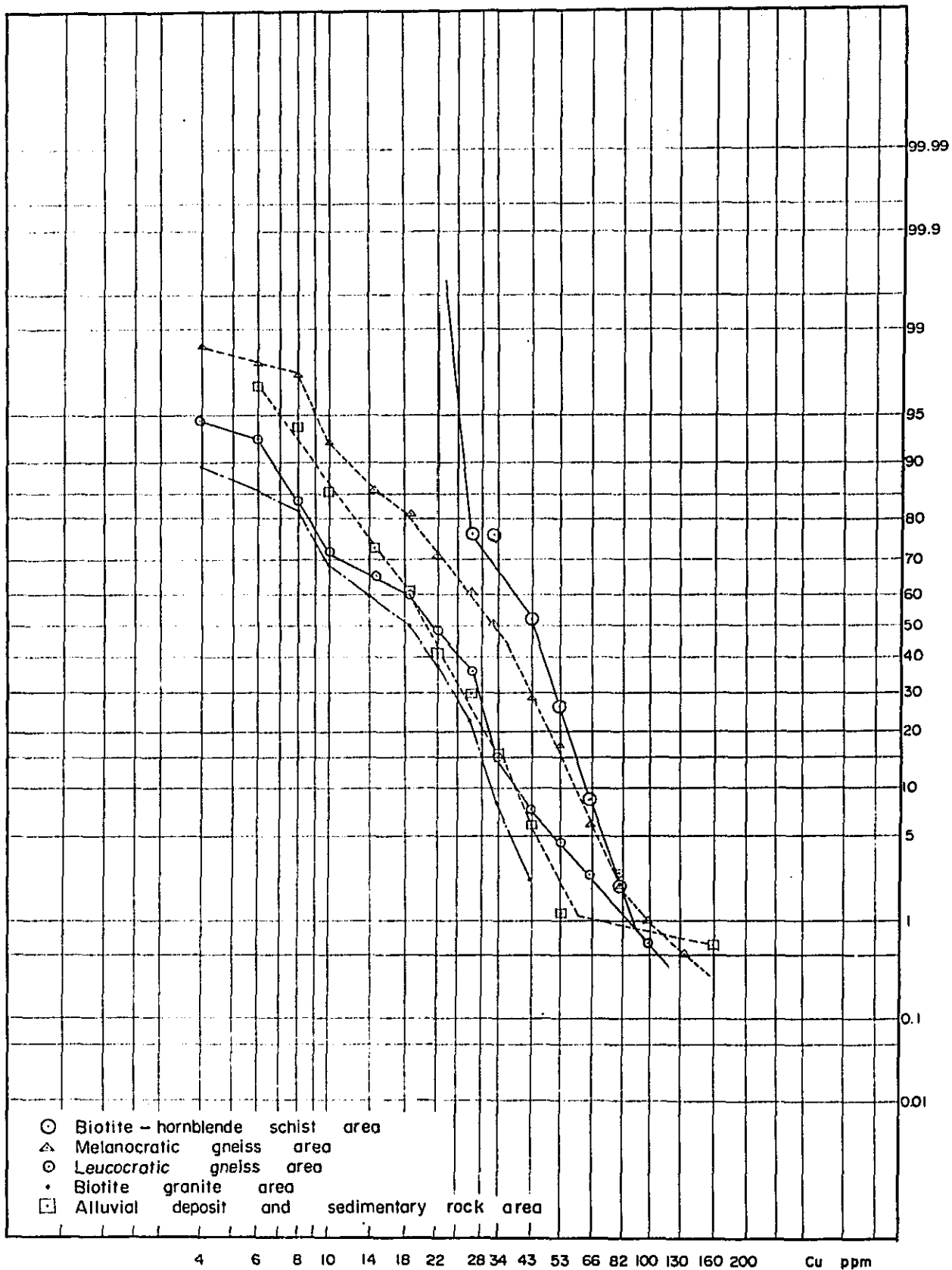
The results of the analysis of the soil samples are listed in Appendix 2. These samples are classified according to their occurrence in Table 2-1.

Table 2-1. Number of Samples in Different Lithology

Lithology	Number of Samples
Biotite-hornblende schist area	46
Melanocratic gneiss area	197
Leucocratic gneiss area	160
Biotite granite area	208
Alluvium and Younger sedimentary rock area	164
Whole area	Total 775

The cumulative frequency distribution in the individual geological units is shown in Fig. 2. It is clear from this figure that the frequency distribution of copper content in soils in a lithology do not show simple log normal distribution as in many geochemical data. It is a complex distribution somewhat like a combination of many log normal distributions. Therefore, it is very difficult to process these complex distributions geologically and geochemically and to extract those geochemical anomalies derived from the mineralization. Therefore, in this survey, we have determined the background and threshold values from a simple

Fig. 2 Cumulative Frequency Distributions for Copper Content of Soil Samples in Different Lithology



numerical process of the mean values and standard deviation.

Background	$\bar{X}$
Second order threshold	$\bar{X} + \sigma$
First order threshold	$\bar{X} + 2\sigma$

$\bar{X}$  is the mean value, and  $\sigma$  the standard deviation. Thus the first and second order threshold values correspond to the first and second order anomalies. The threshold values and the background of the copper content in soils are listed in Table 2-2 by each lithology.

Table 2-2 Background Values and Threshold Values of Copper Content in Soil

Lithology	Background value (ppm)	2nd order threshold value (ppm)	1st order threshold value (ppm)
Biotite-hornblende schist area	45	61	77
Melanocratic gneiss area	36	58	79
Leucocratic gneiss area	24	42	60
Biotite granite area	19	30	42
Alluvium and Younger sedimentary rock area	23	40	57

#### 4-2 Selection of Anomalous Areas and Interpretation

A copper anomaly map (PL. 2-2) was prepared from the threshold values of Table 2-2. In this map, (Q<sub>1</sub>) cases when first order anomalies continue for more than two points, (Q<sub>2</sub>) when first and second order anomalies continue for more than two points, and (Q<sub>3</sub>) when second order anomalies continue for more than three points; were treated as copper anomalous area. As seen in Plate 2-2, 12 areas (A - L) were delineated as anomalous. The outline of these areas are shown in Table 2-3. The following characteristics are seen in these copper anomalous areas.

- (1) Second order anomalies do not continue for more than five points, and cases of anomalous areas extending into adjoining traverses were almost nil. In other words, in this area, there are no anomalous zones of significant size, only small anomalies are occur sporadically.
- (2) The number of anomalies are smaller along the opened IP traverse and larger on the EM traverse along rivers. This shows the possibility that the copper anomalies were formed mainly by topographical factors, i. e., rivers.
- (3) Of the 12 anomalous areas, six occur in the biotite granite area and is most abundant. The copper content in this geological unit, however, is very low, the 2nd order threshold in biotite granite is only 30 ppm while even the background in the melanocratic gneiss area which occurs adjoining the granitic area most often, is 36 ppm. The fact that the copper content of the soils derived from biotite granite which is generally distributed in small areas is very low, is interpreted as the result of contamination of copper from the relatively copper-rich soils in the vicinity by mixing completely independently from mineralization.

Table 2-3. Geochemical Anomalous Area

Anomalous Area	Number of Anomaly		Lithology	Mineralization
	1st order	2nd order		
A	2	0	Leucocratic gneiss	unknown
B	1	1	Leucocratic gneiss	no indication
C	4	0	Biotite granite	partly observed
D	1	2	Biotite granite	no indication
E	1	1	Melanocratic gneiss	no indication
F	1	2	Melanocratic gneiss	no indication
G	1	3	Biotite granite	no indication
H	0	4	Biotite granite and melanocratic gneiss	no indication
I	0	4	Biotite granite	no indication
J	2	2	Biotite granite and melanocratic gneiss	no indication
K	2	1	Melanocratic gneiss	observed
L	0	3	Melanocratic gneiss and biotite granite	unknown

- (4) Copper anomalous areas were not found in the S. Webose mineralized area confirmed by surface geological survey and geophysical survey. This is concluded to be caused by the fact that this mineralized area is characterized by iron sulphide dissemination with low copper content in the order of 0.04 per cent. Other smaller mineralized areas contain

even smaller amount of copper in the range of 0.01 to 0.02 per cent and it is very difficult to extract these geochemical anomalies.

**PART—III**

**GEOPHYSICAL SURVEY**



## Chapter 1 Outline of Surveys

The objectives of this surveys were to obtain informations concerning the already-known mineralized areas and newly expected mineralized area.

At this survey, two methods of geophysical survey, i. e. , electromagnetic method and induced polarization method were carried out.

An electromagnetic survey was carried out in the whole survey district in order to pick up an area promising of ore deposits. The electromagnetic method we adopted here was divided into two parts; vertical loop method for a rough and comprehensive survey and horizontal loop method for a close investigation of an area promising of ore deposits in connection with induced polarization method.

Furthermore, an induced polarization survey was also applied to some of the electromagnetically anomalous areas. It is generally well known that sulphide minerals are readily detectable by means of induced polarization method, so that this method is applicable as one of the most effective tools of finding mineral deposits as well as making clear the corresponding geological structure.

The main part of the survey area is occupied with rugged mountains wholly covered with wild forests. In addition, the topographic maps of this area was small-scale for the present survey so that, in case of vertical loop method, survey stations were planned

to establish along valleys and ridges, where are relatively easily identifiable in the maps.

Induced polarization survey routes were planned to establish around S. Webose mineralized area with simple geodetic measurements. Some parts of these routes were also used for precise electromagnetic survey by means of horizontal loop method.

According to the above working project, sometimes we could not help changing some parts of our project because of the practical difficulties, especially in the case of IP survey, but we extended the survey routes in order to keep the total number of observation stations.

The electromagnetic survey was conducted in an area of 35 km<sup>2</sup>, mentioned in INTRODUCTION. The induced polarization survey was dealt with in the northern part, about 10 km<sup>2</sup>, of this area.

Duration of the surveys both electromagnetic and induced polarization was from 22, September 1972 to 3, December 1972. Period of the work is 73 days.

## Chapter 2 Electromagnetic Survey

### 2-1 Traverse Lines

PL 3-1-1 shows the arrangement of traverse lines. The details are given by the following tables of Vertical and Horizontal Loop Methods.

#### 2-1-1 Vertical loop method

Line	Length (km)	Line	Length(km)	Line	Length(km)
A	2.0	5	1.3	20	4.4
B	2.0	6	1.9	21	1.3
C	2.0	7	0.4	22	0.4
D	2.0	8	1.1	23	1.0
E	2.0	9	1.5	24	0.7
F	1.0	10	2.6	25	1.9
G	2.0	11	1.3	26	0.8
H	1.0	12	0.7	27	0.3
I - I'	1.5	13	1.5	28	0.4
J - J'	1.7	14	1.6	29	4.7
X	3.0	15	0.5	30	1.6
1	2.0	16	2.0	31	5.6
2	0.2	17	0.8	32	7.0
3	1.1	18	1.4	33	2.4
4	1.3	19	2.4		

Total length of lines	:	78.0 km
Spacing of stations	:	50 m
Coil separation	:	100 m
Number of lines	:	44 lines

2-1-2 Horizontal loop method

Line	Length(km)
A	1.0
B	1.0
C	1.0
D	1.0
E	1.0
G	0.7
X	2.0
Y	2.0
Z	2.0
32	3.8
33	0.9

Total length of lines	:	16.4 km
Spacing of stations	:	50 m
Coil separation	:	200 ft
Number of lines	:	11 lines

2-2 Survey Method

2-2-1 Vertical loop method (In-line Tandem Array)

This method is called as "Dip Angle Method". Dip angle of the magnetic field is measured by minimizing a signal from the transmitter coil while rotating the receiver

coil around the horizontal axis. In "Fixed Source Method", the transmitter coil is fixed, while it is shifted with the receiver coil in "Moving Source Method". It is of course important that the transmitter coil should be always kept vertical in both the methods.

From how to arrange traverse lines, we also classify the vertical loop method into two systems: "Broad Side Method (Parallel Line Method)" and "In Line Method". In the former, the transmitter and receiver coils move in parallel along mutually adjoining lines, while in the latter each coil moves along the same line.

The present survey was carried out by means of the in-line tandem array moving source method. The method is generally employed in a reconnaissance survey conducted along roads or mountain paths, but in case that detailed informations are required the fixed source and broad side methods should be used. In the present survey, the transmitter coil was kept vertical while the receiver coil horizontal. The coil separation was usually taken as 100 m, but sometimes the separation shrank to 50 m according to the terrain condition in the end of traverse lines. The frequency we used was set to be 1,600 Hz.

#### 2-2-2 Horizontal loop method

The horizontal loop method was developed by Wenner in 1958, belonging to the Slingram Method or Loop Frame Method. The in-phase and out-of-phase components of the voltage induced in the receiver coil are measured with the same instrument used in the dip angle method. The method is also effective to quantitative analyses of the data

obtained from precise IP surveys.

The following coil configurations are generally used in electromagnetic surveys.

#### Coil Configurations for Two-Loop Sounding

- (1) Horizontal coplanar : Fig. 3-1
- (2) Vertical coplanar : Fig. 3-2
- (3) Vertical coaxial : Fig. 3-3



Fig. 3-1



Fig. 3-2



Fig. 3-3

In the present survey, we took the horizontal coplanar for the coil arrays with an interval of 200 ft. (61 m). The frequency we used was 1,600 Hz.

#### 2-3 Instrumentation

We used here SE-600 Electromagnetic Horizontal Loop System, Geometrics Co., the specifications are as follows:

#### Specifications

Frequency	:	1600 c. p. s.
Coil Spacing	:	200 ft and 300 ft
Cable Lengths	:	206 ft and 306 ft
Reading Range		
In-Phase	:	0 - 200 % in 1 % graduations
Out-of-Phase	:	-50 % to +50 % in 1 % graduations

**Field Weight**

Transmitter Unit	:	17 1/2 pounds
Receiver Unit	:	12 pounds
206 ft Cable	:	9 1/2 pounds
306 ft Cable	:	14 pounds
Shipping Weight	:	Approximately 65 pounds
Batteries	:	
Transmitter	:	2 X #731 - 6 volt Eveready Batteries
Receiver	:	1 X #239 - 13.5 volt Eveready battery (or equivalent)

Simplified circuit diagram of an a. c. potentiometer (or ratiometer) used in measurements of the electromagnetic field is shown in Fig. 3-4.

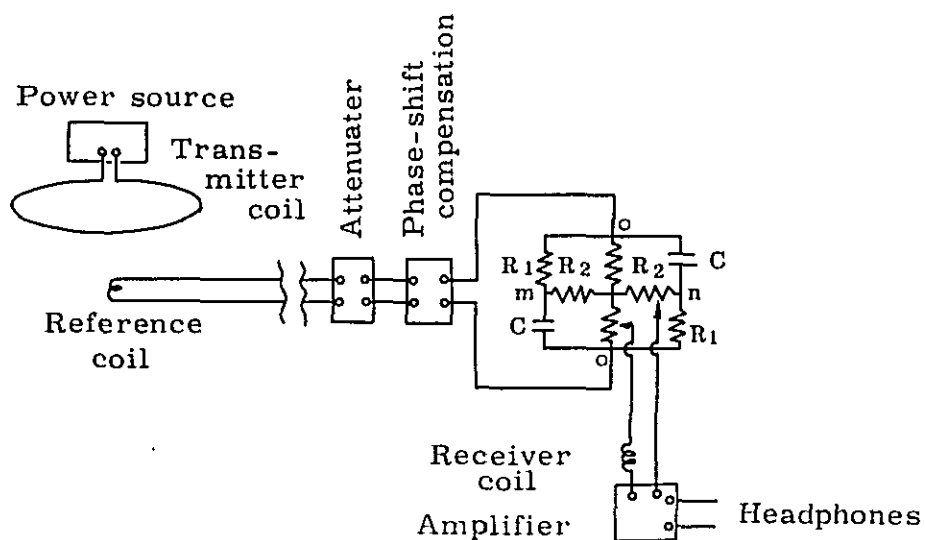


Fig. 3-4 Simplified Circuit Diagram

## 2-4 Survey Results

In the electromagnetic survey, two kinds of methods were usually employed : vertical and horizontal loop methods. The outline of the analyses and the results are presented in the following.

### 2-4-1 Vertical loop method

Dip angle values obtained at observation stations were plotted in the topographic profile for each traverse line. (PLs. 3-2-10 to 3-2-12). Here, dip angles are in unit of degree, which take positive or negative values depending on the inclination of the coil. We call a pair of positive - negative pattern of dip angle, more than  $10^\circ$ , "dip angle anomaly".

Most of the anomalies obtained in the survey are distributed in the northern part of the survey area. We notice a NW trend passing through anomalies A, B, G, H, I, J and K. Anomalies A and B have extensive patterns, the negative zones being dominant.

Meanwhile, no significant anomaly was detected in the central part of the survey area except anomaly C in the south-west part and anomaly L in the south end. Anomaly C, the extension of which is next to that of anomalies A and B, is formed with some pairs of positive-negative pattern showing rather complex feature.

### 2-4-2 Horizontal loop method

Similarly to the vertical loop method, we obtained profiles of in-phase and out-of-phase components together with the topographic sections. (PLs. 3-2-10 to 3-2-12 and PL. 3-2-8)



The use of 'Argand Map' is one of the methods of the horizontal loop analysis. For distinct anomalies we obtained, argand maps were utilized, by which the inclinations, depths, thicknesses and electric conductivities of the corresponding ore deposits were quantitatively estimated.

Contour maps of anomalous in-phase and out-of-phase components are shown in PLs. 3-2-13 and 3-2-14, respectively. The absolute values of 110 % or more and those of 10 % or more are adopted as anomalies against the electromagnetic background response for the in-phase and out-of-phase components respectively.

(1) In-phase component plan map

Relatively significant anomalies  $A_1$  to  $A_4$  have been selected out from the small-scale anomalies distributing over the survey area. (PL. 3-2-13).

The most obvious is anomaly  $A_1$ , which extends widely and has a distinct positive-negative pattern. While, anomalies  $A_2$  to  $A_4$  are formed by dominant negative zones but no significant positive zones are indicated.

(2) Out-of-phase component plan map

Significant anomalies  $A_1$  to  $A_4$  are obtained in the survey as seen in PL. 3-2-14.

Anomaly  $A_1$ , observed around station No. 65 on Line 32, is the most obvious one and has a large-scale consistent pattern. Positive anomalies  $A_2$  and  $A_3$  are also pointed out to be significant.

In the northern part of Line A extensive negative anomaly  $A_4$  has been observed. It is noticed from the

results that positive anomalies dominate in many cases over the survey area.

## Chapter 3 Induced Polarization Survey

### 3-1 Traverse Lines

In PL. 3-1 show the arrangement of traverse lines and observation stations. The details are as follows:

Line	Length (m)
A	2,000
B	2,000
C	2,000
D	2,000
E	2,000
F	1,000
G	2,000
H	1,000
I	1,000
J	1,000
X	2,000
Y	2,000
Z	2,000
Total length	22,000 m
Line spacing	500 m
Station spacing	100 m
Number of lines	13 lines

The actual arrangement of traverse lines are somewhat different from the original project. It was impossible to establish lines in some areas of steep landslide terrain. However, the number of survey stations, as a whole, are

consistent with the original project.

### 3-2 Survey Method

Induced polarization is an electrochemical phenomenon, which is applied to mineral-mining explorations. The induced polarization, which is put to practical use at present, consists of two methods : frequency domain and time domain. As each method has its merits and demerits depending on the volume and depth of object to be detected, we use it properly case by case. Time domain, however, has recently come into the limelight.

Induced polarization method is very effective in directly detecting such a subterranean object as porphyry copper, sulphide copper, lead and zinc ore deposits. Clay, sericite, chlorite, etc. can be readily polarized in laboratory experiments, but in practice the induced polarization method is not so useful for searching these kinds of deposit except special cases.

The detailed account of the present induced polarization survey is as follows :

Configuration of electrodes	:	dipole-dipole
Survey method	:	frequency domain
Spacing of electrodes	:	100 m
Electrode spacing coefficient (n)	:	1, 2 and 3
Spacing of traverse line	:	500 m

### 3-3 Instrumentation

The followings are the instruments used in the present survey. These instruments can be applied to the detection of subterranean objects at depth of 200 m.

#### Specifications

##### (1) Receiver

Manufactory	:	Burr-Brown, U. S. A.
Type	:	IP Receiver Model 9741
Weight	:	9.5 kg
Sensitivity	:	1 $\mu$ V - 100 V
Frequencies	:	0.1, 0.3, 1.0 and 3.0 Hz
Integration time	:	2, 6, 15, 60 and 150 sec.

##### (2) Transmitter

Manufactory	:	Yokogawa Electric Company, Ltd., Japan
Type	:	IP Transmitter Y.N.C. 502
Weight	:	25 kg
Output	:	1,000 V, 0.2 - 2A
Power input	:	95 - 120 V, 400 Hz
Stability	:	less than 0.2 % (for load change of $\pm 10$ %)
Frequencies	:	0.1, 0.3, 1, 3 and 10 Hz

##### Transmitter (spare)

Manufactory	:	Burr-Brown, U. S. A.
Type	:	IP Transmitter Model 9740
Weight	:	18 kg
Output	:	450 V, 0.2 - 2 A
Power input	:	95 - 120 V, 400 Hz

- |             |   |  |
|-------------|---|--|
| Stability   | : | less than 0.1 %<br>(for load change of $\pm 10$ %) |
| Frequencies | : | 0.1, 1, 3 and 10 Hz                                |
- (3) Generator
- |              |   |                            |
|--------------|---|----------------------------|
| Manufactory  | : | McCulloch, U. S. A.        |
| Type         | : | Engine Generator Model 440 |
| Weight       | : | 36 kg                      |
| Power supply | : | 120 V, 400 Hz, 2 kw        |
- (4) Receiver
- |                |   |                            |
|----------------|---|----------------------------|
| Manufactory    | : | Burr-Brown, U. S. A.       |
| Type           | : | IP Calibrator Model 9742   |
| Weight         | : | 6.4 kg                     |
| Frequencies    | : | 0.01 - 110 Hz              |
| Output voltage | : | $\pm 0.01$ mV - $\pm 11$ V |

### 3-4 Survey Results

The induced polarization survey was carried out by means of the frequency domain method. We made profiles of apparent resistivity  $\rho$  ( $\Omega$  - m), frequency effect FE (%) and metal conduction factor MCF, which were calculated from the observed data. Both apparent resistivity  $\rho$  for 3.0 Hz a. c. and FE, i. e. frequency characteristic, for 0.3 and 3.0 Hz a. c. express an IP effect. MCF is equal to a quantity of  $(FE/\rho) \times 10^3$ .

Among these factors, FE is the most effective in reflecting induced polarization characteristics of ore bodies.  $\rho$  is similar to apparent resistivity obtained from a conventional specific-resistivity method. MCF may compensate FE when both  $\rho$  and FE are small in comparison with a quantity of sulphide ore deposit.

Moreover, FE has an advantage that it is substantially free from topographic effects, so that we can easily neglect such an effect in surveying over rugged mountainous areas. In contrast to the above, both  $\rho$  and MCF are affected by the topographic undulation, to which a terrain correction should be made. However, such a correction is quite difficult.

The general conditions for the measurements were so favorable that the reliable data were obtained in the present survey. PLs. 3-3-1 to 3-3-13 show profiles of the IP results together with the topographic sections (scale : 1/5,000 ). MCFs obtained at different depths are represented in the plane topographic maps drawn to a scale of 1/10,000 (PLs. 3-3-14 to 3-3-22).

#### 3-4-1 Interpretation

##### Line A (PL. 3-3-1)

All the FE values observed along Line A are lower than 5 %. The maximum appears between Stations No. 8 and No. 10, centering at around Station No. 9. The anomaly may be speculated as an anomalous frequency-effective body distributing at a depth of 200 - 300 m below the surface.

A zone of resistivity higher than 300 ohm-m was observed at the north end of Line A. It seems likely that this zone extends northwards. The resistivity tends to decrease in the southern part of this line, and a low resistivity zone (lower than 100 ohm-m) is distributed over the south of Station No. 13. MCF is small at the center of the FE anomaly because of high resistivity. The correlation between MCF and FE is not clear.

Line B (PL. 3-3-2)

The FE values observed along Line B are lower than 3 %, almost same order as the background response. A high resistivity zone (higher than 300 ohm-m) extends to the north of Station No. 15. This is essentially the same information as the high resistivity at the north end of Line A. A weekly anomalous MCF zone stretching to the north of Station No. 13 corresponds to the distribution of high resistivity zone. A low resistivity zone (lower than 100 ohm-m) existing between Stations No. 3 and 9 may continue to the low resistivity zone on Line A.

Line C (PL. 3-3-3)

Judging from the FE values as high as 3 - 4 % observed along Line C, we assume an anomalous FE body lying at depths of 150 - 200 m. However, we suppose that this anomaly may be meaningless for lack of the continuity in the FE pattern.

An extension of high resistivity zones detected on Lines A and B is found between Stations No. 14 and 16 on this line. It is recognized that the high resistivity zone becomes narrower than those on Lines A and B. We contrarily see a zone of resistivity lower than 100 ohm-m is adjoining to the north of the above-mentioned high zone. It is also noticed that the low resistivity zone (lower than 100 ohm-m) observed between Stations No. 8 and 14 is an extension of low resistivity zone from Lines A and B.



#### Line D (PL. 3-3-4)

Two FE anomalies were observed on Line D, i. e. Stations No. 3 - 4 and No. 15 - 18. The former, 7 % in the center, can be explained by a computer simulation model, the pattern of which is shown in Fig. 3 - 9. On the other hand, the latter shows a V-shaped pattern, which does not correspond to any of computer simulation models. Resistivity zones, higher than 300 ohm-m, is distributed over Stations No. 5 - 6 and the north of Station No. 14. A low resistivity zone (lower than 100 ohm-m) seen at Stations No. 7 - 9 becomes narrower than those on Line A, B and C.

MCF values exceed 30 at Stations No. 3 - 4, where a FE anomaly is also observed. On the other hand, a low MCF anomaly lying between Stations No. 15 and 18 may be caused by the high resistivity.

#### Line E (PL. 3-3-5)

There are two FE anomalies on Line E : Stations No. 6 - 9 and No. 10 - 16. The former can be explained by a model, the upper part of which has 5 - 6 % FE but the lower 2 - 4 %. The latter indicates 5 - 8 % FE, one of the highest values observed in our present surveys. This accounts for a deep structure with high FE.

On Line E disappears the continuous low-resistivity zone, less than 100 ohm-m, the extension of which is seen in the south of Station No. 13, Line A, at Stations No. 3 - 9, Line B, No. 8 - 14, Line C and No. 7 - 9, Line D. An anomalous resistivity zone higher than 300 ohm-m distributing underneath the FE anomalous area in regard to No. 10 - 16 may possibly connect with the high zone at Station No. 14 on

Line D and extend to the north. Relatively high MCFs detected at Stations No. 2 - 6 and No. 11 - 16 may be less important because no correlation was found out between the MCF and FE values.

#### Line F (PL. 3-3-6)

Although Line F was originally planned to extend up to 2 km long, we were forced to cut down the length of line to 1 km owing to a cliff, where it was practically impossible to make a route for land surveys. A high FE exceeding 5 % observed in the north of Station No. 6 may connect with the FE high on Line E. No anomalous FE, however, was detected in the south of this station.

A high resistivity zone exceeding 300 ohm-m is found at about the same location as FE anomaly on this line.

#### Line G (PL. 3-3-7)

We detected two anomalous FE zones, i. e. Stations No. 11 - 13 and No. 15 - 17. The former is thought to be a response of a V-shaped model pattern with 5 - 7 % FE. Meanwhile, we see 5 - 7 % FE in the central part of the latter anomaly, which is adjoined by low anomaly zones on both the sides. A negative zone is also found beneath them.

A zone of resistivity higher than 300 ohm-m widely distributing over Stations No. 14 - 15 may reflect a high resistivity anomalous body deeply developing. In the south of Station No. 5, high and low resistivity zones alternatively arrange, implying a complex structure.

At Stations No. 15 - 17, where anomalous FE were observed, we detected a high resistivity anomaly which possibly indicates a deep structure. The high anomaly is surrounded with low anomalies.

The distribution of MCF well coincides with that of the high FE anomaly obtained at Stations No. 15 - 17, but can not be explained by any relation with it at the other stations.

#### Line H (PL. 3-3-8)

A FE anomaly, 5 - 6 %, detected on this line extends to the south of Station No. 3. As the anomaly is located at the end of the line, we can not give the entire picture of the anomalous body. It is presumed, however, that the anomaly may extend further to the south.

We notice resistivity values lower than 100 ohm-m at Station No. 3 where we detected the FE anomaly as mentioned above. Contrarily a high resistivity zone of 300 ohm-m is found in the north of Station No. 4. The distribution of MCF can be well explained by the corresponding high FE anomaly and low resistivity zones.

#### Line I (PL. 3-3-9)

A 5 - 6 % FE found at Stations No. 2 - 5, Line I, may be regard as a polarizable body widely extending in shallow layers but decreasing its width with depth. This type of FE anomaly is quite similar to what we obtained at Stations No. 6 - 9, Line E.

The high resistivity (higher than 300 ohm-m) continued from that on Line H stretches to the north of Station No. 5.

There is no MCF anomaly in the north of Station No. 6, since MCF generally converges to zero when resistivity is very large. In the south of Station No. 3, we recognize a low resistivity anomaly independent of the FE anomaly.

Line J (PL. 3-3-10)

We can not make out the whole feature of the FE anomaly extending to the south of Station No. 3 due to the shortness of Line J. It appears, however, that there is no possibility of the further extension of induced-polarized body beyond the south end of Line J, judging from the center of the anomaly located just beneath Station No. 3.

We assume a rock boundary in the low resistivity anomaly of 100 ohm-m around Station No. 3, although a southern extension of this anomaly is quite obscure for lack of sufficient data. Due to the same reason, we could not give the entire picture of the high MCF anomaly seen in the south of Station No. 3.

Line X (PL. 3-3-11)

In order to know the precise location and extension of the anomalous FE observed around Stations No. 10s on Lines A - E, we established Line X perpendicular to the Lines A - E. The anomalous FE observed at Station No. 20, Line X, corresponds to that at Station No. 10, Line E, which is thought to be a response of relatively shallow polarizable body. According to the results, this anomaly obviously connects with an anomalous body deeply stretching down underneath Station No. 15, Line X. But there is no corresponding anomaly at Station No. 10, Line D. It is

accordingly noticed that the anomalous FE body slopes westwards, i. e. the depth increases. We also see a small-scale deep-seated anomalous body in the west of Station No. 10 on this line.

The pattern of resistivity is so closely related to that of FE anomaly, that the resistivity, higher than 300 ohm-m, corresponds to the shallow anomalous FE zone, on the other hand, the zone lower than 100 ohm-m to the anomalous FE deep-seated in the west of Station No. 15.

Anomalous MCF values are observed only in the area of anomalous FE and low resistivity. It is natural that MCF is negligibly small in very high resistivity areas because MCF is in inverse proportion to resistivity.

#### Line Y (PL. 3-3-12)

We established Line Y, a tie line, for the purpose of thoroughly verifying the extension of the anomalous FE area observed at Stations No. 3 - 4, Line D. The results of the measurements proves that the anomalous FE areas continues from Line E to Y, and the center of the area is situated between Station No. 3 and 4.

#### Line Z (PL. 3-3-13)

An end of traverse line is a weak point for a dipole-dipole configuration survey. Line Z, perpendicular to Lines A - E at the south end, was established in order to complement such a deficiency of dipole-dipole configuration by confirming the southwest extension of the FE anomaly observed at Stations No. 4, Line D, and No. 3, Line E. As a result, the 1 - 2 % FE we measured in the southwest

of the above FE anomaly is regarded as a background response. Another small-scale anomalous FE, 3 - 4 %, newly detected at Stations No. 5 - 6 may be less important because of the *disordered shape of the pattern.*

#### 3-4-2 Interpretation on plane maps

PLs. 3-3-14 to 3-3-16 illustrate the FE data for different depths. The isoanomaly contours are drawn for FE values higher than 3 %. It is noticed in these figures that a north-westward trend of anomalous zone is comprehensively distributed over Lines D - G and the center of the anomaly is located at Stations No. 11, Line E, and No. 8, Line F. The other anomaly centered at Stations No. 3 - 4, Line D, seems to be isolated from the above-mentioned anomaly in case of maps ( $n=1$  and  $n=2$ ), but identified with it in case of  $n=3$  (see PL. 3-3-16).

The relatively small-scale anomalous zone extending to the west of Line C may be corresponding to a deep-seated body. The FE anomaly observed on Lines H - J in the east of the survey area is rather high in the shallow but low in the deep. At Station No. 16, Line G, we detected the small-scale FE anomaly, which is isolated from the above-mentioned anomalous zones. This appears to extend further to the east, but we can not make out the whole pattern of it.

In PLs. 3-3-17 to 3-3-19 are shown the results from the resistivity data obtained at different depths with contours of 100, 200, 500 and higher than 700 ohm-m. The resistivity zone, higher than 300 ohm-m, has the same northwestward trend as the FE anomalies. However, the relation between the patterns of FE and resistivity anomalies is not so obvious

especially in case of low resistivity.

The plane maps of MCF are shown in PLs. 3-3-20 to 3-3-22. As seen in these figures, anomalous MCF values are resulted from low resistivity and high FE. We have to bear in mind, however, that the MCF values are not reliable if they are obtained in the area where low resistivity is dominant.

## Chapter 4      Remarks on Geophysical Survey

### 4-1      Measurements of Properties of Rocks and Ores

#### 4-1-1      Apparatus

In measuring properties of rocks or ores, it is important to keep the samples in the same condition as have been buried and to maintain reproducibility of measured values. The present measurements were made with the Nikko Sample IP Measuring Apparatus devised in consideration of the above-mentioned points. The outline of the apparatus is described in the following :

#### (1)      Thermostat and sample-holders

The iron-made thermostat, 30 x 30 x 50 cm , is equipped with a vacuum pump, a vaporizing water-bath with heater and a thermometer. We have two different types of sample-holders; one is 2.5 cm in diameter and the other 3.0 cm. The thermostat holds four sample-holders.

#### (2)      Transmitter

Burr-Brown Model 801 Transmitter, composed of a constant-current pulse generator and a pre-amplifier, is used in time-domain and frequency-domain IP measurements of rock samples.



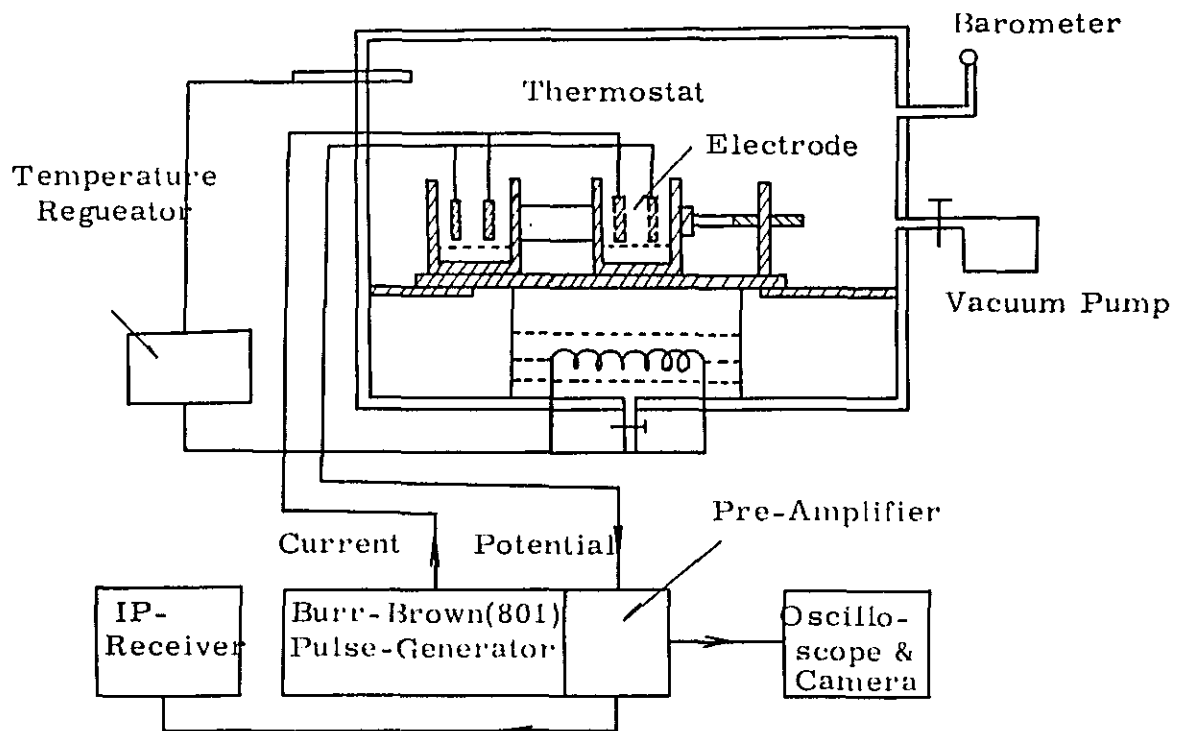


Fig. 3-5 Outline of Apparatus

4-1-2 Remarks on measurements

The frequency effect and resistivity were measured for seven standard rock samples representing geology in the survey area. Results of the measurements give us fundamental data for geophysical researches. The obtained results are shown in Table 3.

Table 3. Results of Measurements on Rock Samples

Sample number	Depth	Name of rock	FE(%)	$\rho$ (ohm-m)
1	Surface	Biotite granite	4.6	7350
2	Surface	Garnet-biotite Gneiss	1.0	1810
3	Surface	Graphite bearing Garnet-biotite gneiss	1.9	2050
4	Surface	Graphite bearing garnet-biotite gneiss	20.9	870
5	Surface	Graphite bearing garnet-biotite gneiss (silicified)	0.0	5750
6	Surface	Hornblende-biotite schist	3.2	3080
7	Surface	Diorite	3.6	2330

It is noticed from the results given in Table 3, that FE is much higher in Sample No. 4 than the other samples. We observed that Sample No. 4 is much sulphide-mineralized compared with the other samples and also microscopically includes chalcopyrite, pyrrhotite and graphite. The high FE value of this sample may be caused by these facts. In case of the other samples, we do not recognize any minerals related to IP phenomena, so that FE is about 3 % as seen in Table 3.

Resistivity is generally high in the survey area, fluctuating from 800 to 7,000 ohm-m. Such fluctuation may be caused by the resistivity difference characteristic of rock-type, water content and thickness of surface layer.

In order to analyze the IP anomalies, we applied "the methods of two-dimensional profile analyses of resistivity, FE and MCF" which were published by Geoscience Co., Ltd. The typical examples of the profile analyses practically obtained here are shown in Fig. 3-6.

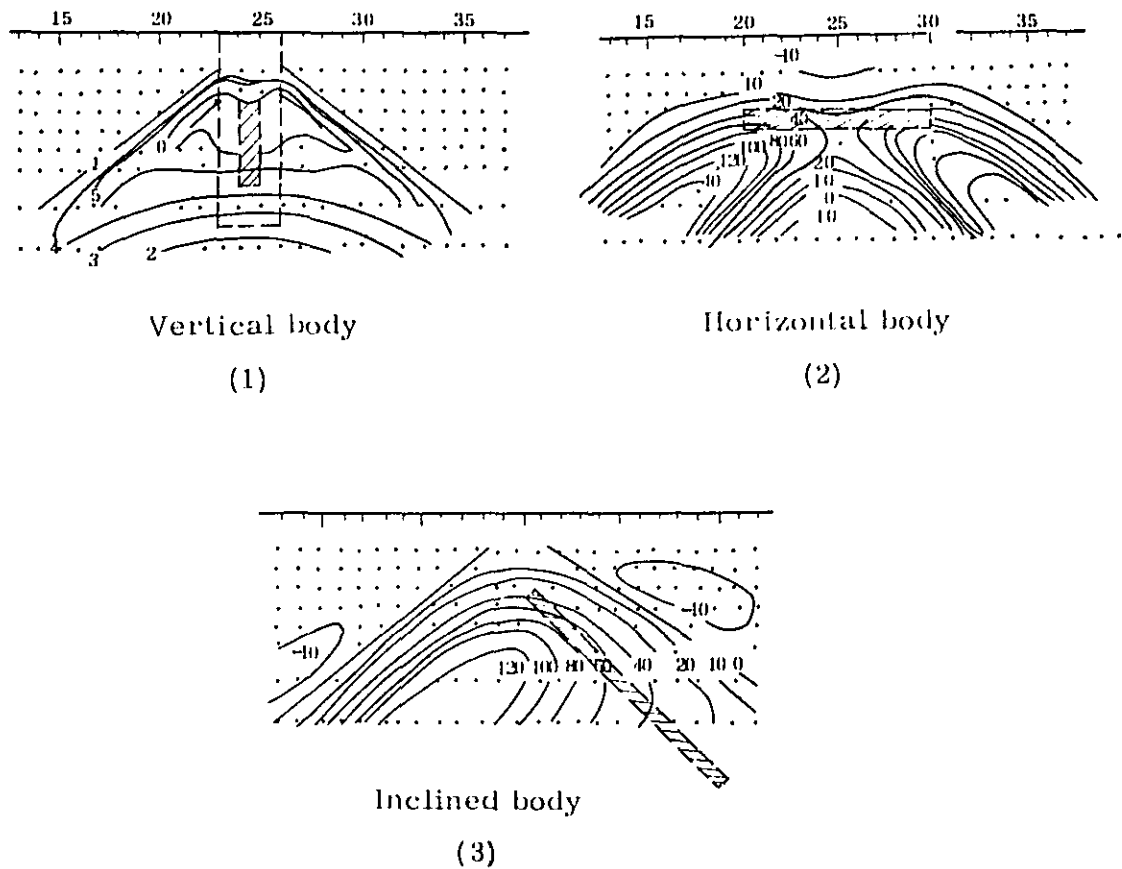


Fig. 3-6 Examples of FE pattern

## 4-2 Remarks on Electromagnetic Survey

### 4-2-1 Vertical loop method

In the present survey results twelve anomalies are regarded as significant patterns. As the observed data consist of many small-scale anomalies which are presumably due to effects of rough topography, the analyses were rather difficult.

We presume that these anomalies represent low resistive zones such as sulphide mineralized ones.

Anomalies A, B, C, D and L are the most promising ones as seen in plan map PL. 3-2-1. The detailed explanations about them are presented in the following.

Anomalies A and B have extensive patterns, the negative zones being dominant. As S. Webose mineralized zone have been determined by the surface geological surveys in some parts of this area, we assume that the vertical loop patterns are induced by the sulphide mineralized zone. Anomaly C is expressed by a complex pattern of positive and negative zones. This may be caused by differences of the concentration rates of sulphide minerals in the mineralized zone. Anomaly D has an extensive form, but we can not catch the whole extension beyond the end of the traverse line. The local anomalies E - L may be caused by low resistive bodies such as weakly mineralized zones.

Very few anomalies were detected on Line 32 established along the great valley. This fact may be one of the masking phenomena which appear over the thick gravel bed.

4-2-2 Horizontal loop method

For the analyses of the survey results, we stressed the out-of-phase components, which are relatively free from topographic effects, while the in-phase components readily affected with terrain condition. (Refer to Note 2.)

However, the anomalous in-phase component takes more exaggerated value than that of the anomalous out-of-phase component.

In determining out-of-phase anomalies we referred to in-phase data obtained over the flat terrain. By using Argand maps, we estimated the inclinations, depths and conductivity-thickness products of the low resistive bodies expected from the outstanding profile anomalies. The detailed explanations about the anomalies are presented in the following :

(1) PL. 3-2-10 (Line D)

Relatively significant anomalous in-phase component and corresponding anomalous dip angle located at Station No. 10 may reflect an low resistive body lying near the surface. This region is one of the promising areas.

(2) PL. 3-2-11 (Line E)

Small-scale anomalous in-phase and out-of-phase components are noticed around Station No. 10. Both the component patterns are similar to each other. The corresponding anomalous dip angle are also found there. We analyzed these anomalies by means of Argand maps on the assumption that the anomalies are caused by a laminal conductive body. We obtained  $d/r = 0.4$  and  $w = 25$  from observed in-phase component

of 5 % on the basis of Argand maps (Fig. 3-7). The coil separation  $r$  being 200 feet putting it into the equation  $d/r = 0.4$ , then we obtain the depth of burrial  $d$  to be 80 feet. The dip angle of the conductive body was also calculated to be  $70^\circ$  from the ratio of two maxima of the in-phase components, in this case 0.5, making use of the curves illustrated in Fig. 3-8. The conductivity-thickness product,  $\sigma t$ , is given by

$$\sigma t = \frac{fW}{\pi \mu_0 r}$$

$$W = \frac{tS}{\delta^2} \quad \delta^2 = \frac{2}{\sigma \mu_0 \omega}, \quad \omega = \frac{2\pi f}{f}$$

where  $\sigma$  is conductivity,  $\mu_0$  permeability,  $f$  frequency,  $t$  thickness and  $r$  coil separation. In our case, we obtained  $\sigma t = 64$  ( $t$  in feet). Thus we obtained the depth of burrial, the dip angle and the conductivity - thickness product of the conductive body to be 80 feet,  $70^\circ$  and 64, respectively.

(3) PL. 3-2-11 (Line G)

An anomalous in-phase component of about 80 % is seen around Stations No. 25 - 40. The possible cause may be a deep-seated low resistive body such as mineralized zone.

(4) PL. 3-2-12 (Line Y)

We see a complex-shaped anomaly at Station No. 30. This is corresponding to the previously mentioned Anomaly F of dip angle and Anomaly A<sub>2</sub> of in-phase component (Station No. 10, Line D). And we highly estimated these anomalies.

(5) PL. 3-2-12 (Line Z)

A number of anomalous in-phase components shown in this figure may be caused by the rough topography. It is therefore difficult to estimate the conductor from these anomalous in-phase components. Based on the relation between the in-phase and out-of-phase components, we regard anomalies at Stations No. 2 and 13 as indicating the local conductor distribution.

The anomalous in-phase and out-of-phase components obtained in the survey are described in the following.

(1) In-phase component plan map (PL. 3-2-13)

Anomaly A<sub>1</sub> shows a typical positive-negative pattern. We presume that the conductive zone such as disseminated zone is widely distributed below the Anomaly A<sub>1</sub>.

Distinct negative anomaly A<sub>2</sub> corresponding well to the anomalous dip angle is promising, while Anomalies A<sub>3</sub> and A<sub>4</sub> are of no significance.

(2) Out-of-phase plan map (PL. 3-2-14)

Out-of-phase component is relatively free from topographic effects, so that out-of-phase anomalies A<sub>1</sub> to A<sub>4</sub> are much more reliable than the in-phase components.

However, the anomalies above mentioned can not be highly estimated in the mineral exploration because of no distinct relation between the anomalous in-phase component and anomalous dip angle.

Note 1        It can be pointed out that possible observation errors of the horizontal loop method are mainly caused by errors in coil separation and orientation.

- (1)        If a ratiometer is adjusted to read 100 % at a coil separation (r) and through some surveying error of the actual coil separation is  $r_a$ , the observation error of this method becomes  $\left| 1 - (r/r_a)^3 \right| \times 100$  %. Thus, for example, an error of 2 % in the coil separation will cause an error of about 6 % in the measurement.
- (2)        If one of the coils is misoriented from its proper position through an angle  $\delta$ , the error in measurements will be  $(1 - \cos \delta) \times 100$  %. For example, if the angle  $\delta$  is  $8^\circ$ , the error in measurement will be only about 1 %.
- (3)        If the terrain makes an angle  $\alpha^\circ$  with the horizontal, the error in measurement is  $(1 - 3 \sin^2 \alpha) \times 100$  %. For a slope of  $8^\circ$ , the error is 5.8 %. Hence, we must be careful in an interpretation of the results of the horizontal loop method when the measurements were made in the rugged mountainous area.

In the actual survey, the coil separation is apt to be shorter than the original separation because we use a wire-cable connecting the coils. The underestimated coil separation increases the in-phase component, meanwhile the misorientation of coils decreases. It is practically impossible to avoid the errors in the in-phase component in case of rugged terrain. It is therefore desirable for the horizontal loop method to be conducted in a flat area if possible.



Note 2 In the interpretation of the results from horizontal loop method, the concept of the conductivity-thickness product, which represents the product of the conductivity and thickness of an ore body, is brought out. If either conductivity (or resistivity) or thickness is known by some means, the other can be determined on the assumption that the conductivity-thickness product is given.

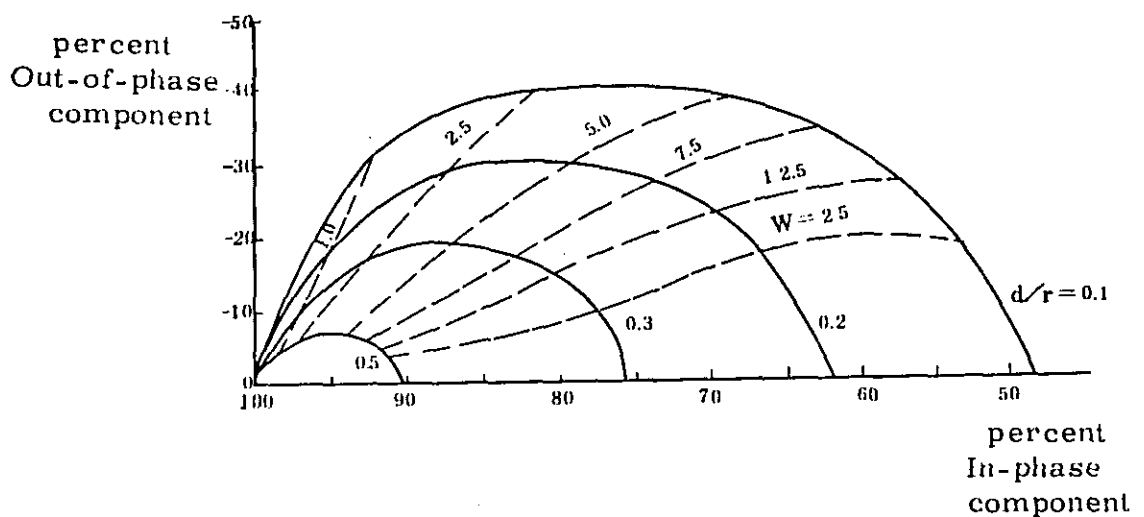


Fig. 3-7 Argand Diagram

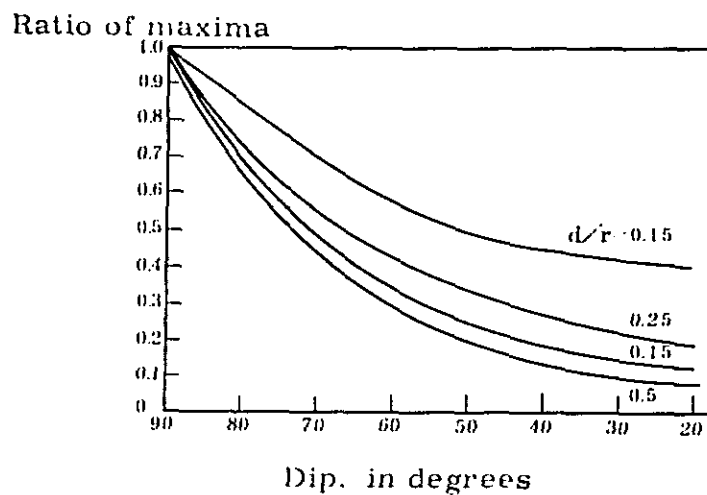


Fig. 3-8 Ratio of Maxima Observed on a Slingram Anomaly Curve over a Thin Sheet as a Function of Dip.

#### 4-3 Remarks on Induced Polarization Survey

There are no artificial noises affected on the IP measurements in the survey area, and moreover the electric current could be sufficiently supplied to the ground. Owing to such a good condition for IP measurements we obtained data satisfactory to the further analyses.

Three drillings were performed in the survey area. Two of them were originally undertaken to disclose the cause of FE anomalies. As a result, all the drillings succeeded to capture sulfide-disseminated zones despite of some differences in degree between them. As sulfide generally shows frequency effect, it may be sure that the FE anomalies originate from disseminated sulfide in the present survey area.

As seen from PLs. 3-3-14 to 3-3-16, the most promising is an oblong anomalous zone (1.5 km x 1.2 km) which extends over Lines D, E, F and G. This zone coincides with S. Webose mineralized area newly discovered by the present geological survey.

It is also presumed on the basis of pattern analyses of computer models shown in Fig. 3-9 that the anomaly centering around Stations No. 3 - 4, Line D, is caused by a small-scale mineralized area extending downwards but not horizontally. On the other hand, the other FE anomaly observed in the eastern parts of Lines H, I and J has a tendency of stretching in the EW direction as seen in PL. 3-3-15, and seems likely to continue to the shallow part of S. Webose mineralized area. However, as shown in PL. 3-3-16, this anomaly is thought to represent a shallow and small-scale polarized body, so that it can not be identified with S. Webose mineralized area.

Resistivity, ranging from 50 to 700 ohm-m, is the most favorable condition for an IP measurement. A high resistivity zone,

more than 300 ohm-m, corresponds approximately to that of FE anomaly extending to the NW direction in the survey area. On the other hand, a low resistivity zone of 100 ohm-m or less also corresponds, but the correlation between resistivity and FE is not always obvious. Such a tendency is often found in field measurements, especially in case of porphyry copper deposits.

A low resistivity zone of 100 ohm-m or less is observed around Stations No. 3 - 9, Line B, No. 8 - 14, Line C, and No. 7 - 9, Line D. The resistivity feature may be caused not only by topographic effect but also by resistivity change due to the argillization judging from the feature of the FE distribution explicitly changing around these Stations No. 3.

MCF anomalies are not always correspond to FE but resistivity anomalies in the survey area. MCF anomaly, in general, is observed in an area of low resistivity and high FE. However, in the present survey, we can not see any strong correlation between resistivity and FE, and furthermore the MCF anomalies tend to correspond to the high resistivity zones. As a matter of fact, we cannot consider MCF anomalies to indicate mineralization.

Some remarks on each of the FE anomalies are described in the following :

(1) Stations No. 3 - 4, Line D

Assuming that this FE anomaly is similar to a computer model pattern shown in Fig. 3-9, the mineralized zone estimated from the model pattern centers around Stations No. 3 and 4 and extends downwards. Drilling No. 3 (DH-3) pinpointed at the polarized body corresponding to the FE anomaly and brought to light the weak sulphide dissemination at depths from 15 to 130 m below the surface. Thus it may

be possible that the anomaly is caused by the disseminated sulphide.

(2) Stations No. 15 - 18, Line D

This FE anomaly seems to be caused by a complex structure because no computer model pattern fits it. Anyway, we can approximately assume a plane model of polarized body horizontally distributed in the shallow. However, we can expect neither northward nor downward extension of the body.

(3) Stations No. 6 - 9, Line E

A comprehensive distribution of the induced-polarized body of 5 to 6 % FE in the shallow and 2 to 4 % FE in the deep can be assumed for the explanation of this FE anomaly. Such an anomaly can also be explained by the combination of high FE models with low FE in a laboratory IP experiment. Accordingly, supposing the FE anomaly to be promising, we assume a polarized body centering within a depth of 100 m below the surface. Aiming at the body, Drilling No.2(DH-2) was conducted at the location nearby Station No. 7, Line E. As a result, the sulphide disseminated zone was disclosed at a depth of 100 m below the surface. Judging from the above example, we have to bear in mind that an anomalous FE of 5 % or more possibly represents a pyrite-bearing mineralized zone.

(4) Stations No. 10 - 16, Line E

One of the highest values of FE is found around here. This corresponds to the polarized body obviously extending from shallow to deep. However, it is impossible to exactly estimate the depth of the body for lack of the spatial concentricity of

the anomalous values. The FE values are decreased in the northern part of the anomalous area, so that no mineralization can be expected there.

(5) North of Station No. 6, Line F

Although we can not capture the whole feature of the anomaly, because it extends beyond the north end of the traverse line, we have to mark that the anomaly extends up to Line E.

(6) Stations No. 11 - 13, Line G

Corresponding to a V-shaped pattern, this anomaly can be estimated to be caused by a shallow mineralized body. The downward extension can not be expected.

(7) Stations No. 15 - 17, Line G

A negative anomaly is recognized around here. The anomaly can be approximately explained by an inclined plane of mineralized body. However, the detailed structure of the body is obscure because the anomaly is small-scale and does not extend to the other traverse lines.

Negative FE is a singular phenomenon, and sometimes observed in an area adjacent to positive FE anomaly in case of a survey over argillitized or sheared zone. In some cases, negative FE is caused by an extremely high resistivity zone. The negative FE, observed on Line G, seems to belong to the former case.

(8) Southern Parts of Line H, I and J

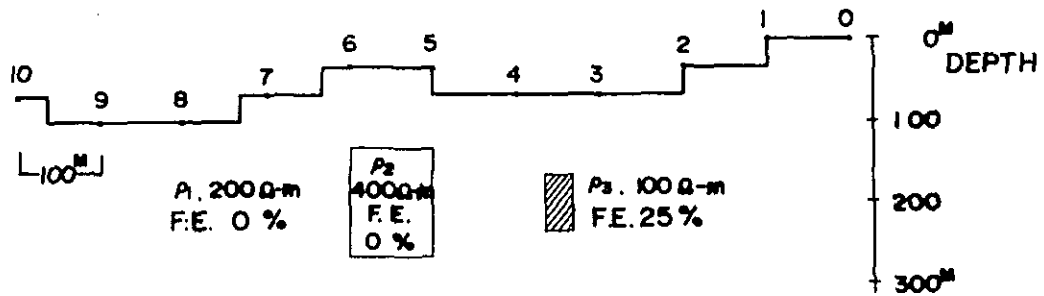
All of these anomalies in common have a tendency of decreasing their horizontal stretches with the depths. The anomaly observed on Line I has a feature similar to that of the anomaly around Stations No. 6 - 9, Line E. We suppose that the center

of the mineralized body associated with the anomaly exists within a depth of 100 m below the surface. It may be sure that the center is not located beyond the depth.

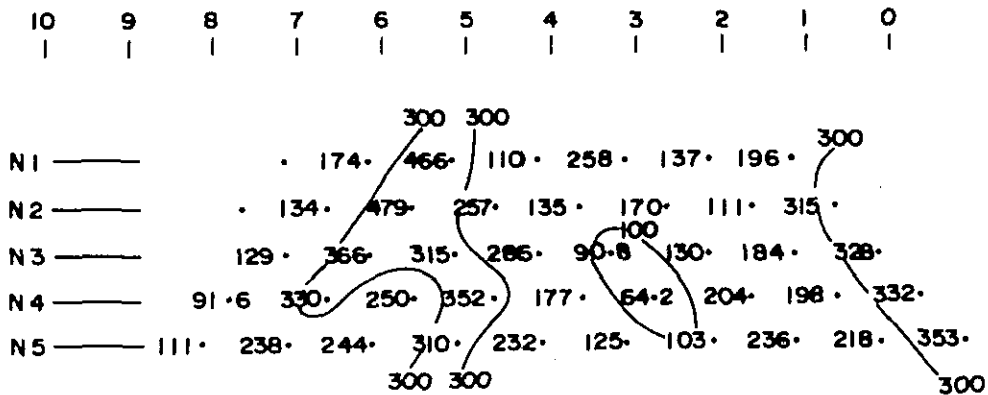
(9) Lines A, B and C

No FE anomalies are observed on these lines. This implies that no sulphide minerals such as disseminated pyrite are distributed around here.

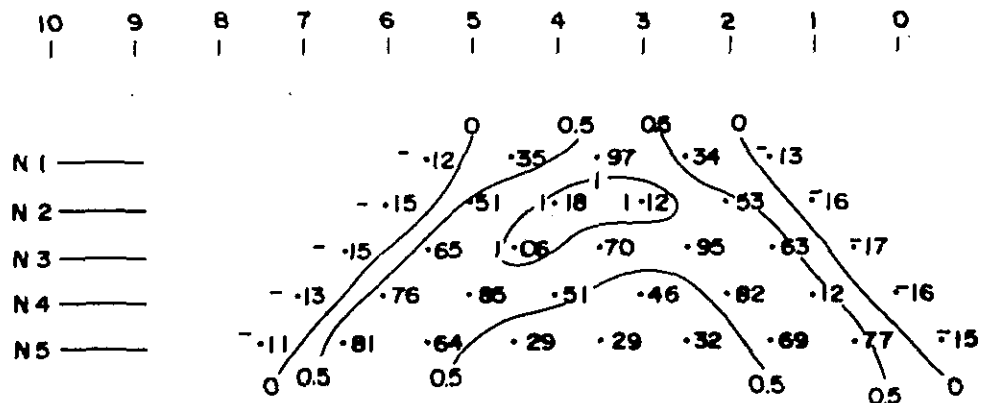
TWO-DIMENSIONAL MODEL CALCULATION  
FOR RESISTIVITY AND FREQUENCY EFFECT



DIPOLE-DIPOLE RESISTIVITY;  $\rho$  ( $\Omega$ -m)



DIPOLE-DIPOLE FREQUENCY EFFECT; F.E. (%)



## **PART IV**

# **CONCLUSIONS**



## Chapter 1 Outline of Drilling

Drilling was carried out in the S. Webose mineralized area which was delineated as being promising for mineral deposits from the results of the geological, geochemical, and geophysical surveys carried out in the S. Bomba area.

The objective of the drilling was to obtain information concerning the subsurface mineralization.

The depth of the drilling was 130 m for each hole and three holes with the total depth of 390 m were drilled.

The period of drilling was mentioned in the part of INTRODUCTION.

## Chapter 2. Drilling Method and Equipment

The method employed in this operation was rotary drilling with coring method. The bit used was diamond bit (Boltz) which is capable of high core recovery even with small diameters.

Mud fluid was used during drilling.

The specifications of the machine used were as follows.

This machine was capable of drilling deeper than the 300 m listed.

The accessory equipment is not listed.

Table 4-1. Drilling Equipments

Model "TF-2"	Specifications	(Tone Boring Co., Ltd.)	1 set
Capacity (m)	:	Ex rods	400 m
Size of Machine	:	Height	1,380 mm
		Length	2,200 mm
		Width	1,000 mm
Weight	:	without Engine	1,180 kg
Spindle Speed	:	Type "A"	
		300. 750	1,500 r. p. m.
		Type "B"	
		200. 500.	1,000 r. p. m.
Hoist	:	Type : Planetary Gear	
		Drum Diameter	220 mm
		Drum Length	153 mm
Pump	:	Type : Variable Delivery Oil Pump	
		Capacity :	variable vol 0 - 40 ℓ/min
		Pressure :	max. 50 kg/cm <sup>2</sup>

Motor : Yanmer Diesel Engine  
 Model "2TR 22L"  
 Horsepower/r. p. m.  
 18 PS/1,800 - 2,000 r. p. m.

Drilling Pump Model NB<sub>3</sub> - 60 Specifications (Tone Boring Co., Ltd.)  
 2 sets

Type : Single Cylinder,  
 Double Acting  
 Capacity : Discharge Volume 0 - 50 ℓ/min.  
 Max. Pressure 40 kg/cm<sup>2</sup>  
 Weight : without Engine 160 kg  
 Piston Diameter : 65 m/m  
 Stroke : 60 m/m  
 Motor : Yanmer Diesel Engine  
 Model "NS - 65C"  
 Horsepower/r. p. m.  
 5.5 PS/1,800 - 2,000 r. p. m.

Mud Mixer Model "MCE - 100 A" Specifications 1 set

Volume of Tank : 130 ℓ  
 Mixing Volume : 100 ℓ  
 Propeller Speed : 800 - 1,000 r. p. m.  
 Motor : Yanmer Diesel Engine  
 Model "NS - 65 C"  
 Horsepower/r. p. m.  
 5.5 PS/1,800 - 2,000 r. p. m.

Derrick Specifications

1 set

Type : 3 - Legs Steel Tubules  
Crossed Derrick  
Height : 6 m  
Maximum Load Capacity : 4 ton

Generator Y. S. - 15 Specifications

1 set

Capacity : 1.5 KW, 1.5 KVA  
Voltage : 100 V  
Electric Current : 15 A  
Motor : Yanmer Diesel Engine  
Model "NS - 40 C"  
Horsepower/r. p. m.  
4 PS /2,000 r. p. m.

Drilling Tools

Drill	Rods	D. C. D. M. A. AW - 3m	70 pec.
Casing	Pipe	D. C. D. M. A. NX - 3m	7 pec.
Casing	Pipe	D. C. D. M. A. BX - 3m	20 pec.
Casing	Pipe	D. C. D. M. A. AX - 3m	47 pec.

### Chapter 3 Selection of Drilling Sites

The drilling sites were selected on the basis of the results of the geological, geochemical, and geophysical (EM and IP methods) surveys.

In actual operation, however, topographical conditions limited the sites and it was not necessarily possible to drill at the most geologically suitable location. Efforts were made to drill as close to the optimum sites as possible.

The depth of the drilling was determined from the results of the survey of the previous year (1971); vertical 130 m for all three holes.

The basis for the determination of the drilling sites were as follows.

Drill hole No. 1 (DH-1) ( $1^{\circ}18'11''\text{S.}$ ,  $120^{\circ}11'32''\text{E.}$ ) was selected on the basis of detailed geological survey at the outcrop of the iron sulphide dissemination at the western margin of the S. Webose mineralized area.

Drill hole No. 2 (DH-2) ( $1^{\circ}18'0''\text{S.}$ ,  $120^{\circ}11'18''$ ) was selected mainly on the basis of geophysical results, EM and IP methods and with topography in consideration, Point 7 of the IP traverse was used. This was located in geologically interesting area between the silicified zones of DH-1 and at 1.2 km northwest of DH-1.

DH-1 and -2 were drilled at the marginal parts of the S. Webose mineralized area, but DH-3 was planned at Point 3 of IP traverse which is in an anomalous zone independent from the S. Webose mineralized area.

The topography near the anomaly, however, was steep and the drilling was carried out 150 m north of the projected site at  $1^{\circ}18'121''\text{S}$  ,  $120^{\circ}10'58''\text{E}$ .

## Chapter 4 Results of Drilling

### 4-1 Operation

For drilling, cutting oil, mud fluids were used in order to drill in both hard and soft rocks. Also as the drilling was rather shallow, core drilling was used in order to increase the recovery of the cores. The work was done in two shifts with one Japanese engineer and one staff member of the Geological Survey of Indonesia in each shift to facilitate cooperative operation.

Generally, there were large amount of altered soft rock from the higher horizon, and loss of circulating fluid and underground water often slowed the process. Thus the operation was more difficult than anticipated, but every effort was made to complete the work within the planned time.

As the drilling sites were in the valleys, the equipment was flooded during the rainy season, but preventive measures were taken, communication with the base camp was maintained and we managed without any accidents.

The drilling of the three holes was as follows.

DH-1 The operation was started with NX metal bit, and after reaching the rock bed under 9.7 m of soil, BX casing pipe was inserted and continued drilling with BX diamond bit. The lithology was poor for drilling and caved a few times, bentonite circulating fluid was used.

DH-2 The operation was started with NX metal bit and changed BX diamond bit after reaching the rock bed under 10.5 m of top soil.

The hole collapsed often from about 25 m and AX casing pipe was inserted at 37.4 m.

AX diamond bit was used, but the lithology deteriorated from 56 m and efforts were made for core recovery by adjusting the rotation, drilling speed, and the amount of circulating fluid but the results were dissapointing and the geology below 56 m was inferred from the slime.

DH-3 The operation was started with NX metal bit and changed to BX diamond bit after reaching the rock-bed under 6.5 m of soil.

The lifting of the rod became difficult due to the collapse from about 28 m and AX casing pipe was inserted. Drilling was done by AX diamond bit after this depth. A water layer (150ℓ/min.) was met at 64 m and from about 101 m the lithology became alternation of hard and soft rocks, and thus almost impossible to recover core. The geology was inferred from the slime from this depth on.

4-2 Geologic Columns (Appendix 4)

DH-1 In this drill hole, under about 10 m of soil, sand and gravel layer, leucocratic gneiss, epidiorite, biotite granite, and leucocratic gneiss occur downward in this order. Gneissose structure with 20° - 30° dip is clearly seen in the leucocratic gneiss.



Table 4 - 2 Drilling Condition (DH-1)

Depth : 130.00 m  
Core Length: 67.00 m

Depth M	Geological Column	Remarks		Depth M	Geological Column	Remarks		Depth M	Geological Column	Remarks															
		Lithology	Drilling Condition			Lithology	Drilling Condition			Lithology	Drilling Condition														
10	~ ~	Soil	Drilled by NX metal bit from 0m to 9.7m	-50	+ + + + + + + + + + + + + + + + + + + +				-100	~ ~															
		Gravel	Soil 9.7m																						
		Blotite gneiss	BX casing (9.7m)																						
	20	x x x x x x x x x x x x x x x x x x x x	Garnet-biotite gneiss	Drilled by BX diamond bit from 9.7m	-60	+ + + + + + + + + + + + + + + + + + + +	Blotite gneiss		Drilled by BX diamond bit Used mud water	-110	~ ~	Garnet-biotite gneiss (argillaceous)	Drilled by EX diamond bit. Used mud water												
				Garnet-biotite gneiss										Used mud water											
			30	x x x x x x x x x x x x x x x x	Epidiorite	35m-38m Cu < 0.01% S 0.16%	-70	+ + + + + + + + + + + + + + + + + + + +	Blotite granite			-120	~ ~	Garnet Gneiss (silicified)											
																40	+ + + + + + + + + + + + + + + +	Blotite Granite	-80				-130		
																+ + + + + + + + + + + + + + + +	Epidiorite	-90							
																									+ + + + + + + + + + + + + + + +
+ + + + + + + + + + + + + + + +																	91m-99m Cu < 0.01% S 0.14%	-90							
																									+ + + + + + + + + + + + + + + +



Table 4-4 Drilling Condition (DH-3)

Depth : 130.00 m  
Core Length : 18.80 m

Depth M	Geological Column	Remarks		Depth M	Geological Column	Remarks		Depth M	Geological Column	Remarks	
		Lithology	Drilling Condition			Lithology	Drilling Condition			Lithology	Drilling Condition
-10	o o o	Soil	Soil 6.5 m	+ + + + + + + + + + + + + + + + + + + +	~ ~			-100	~ ~		
	o o o	Gravel			~ ~				~ ~		
	~ ~	Biotite gneiss	~ ~				~ ~				
	~ ~	Biotite granite	~ ~				~ ~				
	~ ~		~ ~				~ ~				
	~ ~	Biotite gneiss	~ ~				~ ~				
	~ ~	Biotite granite	~ ~				~ ~				
	~ ~		~ ~				~ ~				
	~ ~	Biotite gneiss	~ ~				~ ~				
	~ ~	Biotite granite	~ ~				~ ~				
-20	~ ~	Biotite gneiss	BX casing (15.5 m) Drilled by BX diamond bit from 15.5 m	-60	~ ~			-110	~ ~		Difficult to drill because of hard rock and soft rock alteration around 101 m
	~ ~	Biotite gneiss		~ ~			~ ~				
	~ ~			~ ~			~ ~				
	~ ~			~ ~			~ ~				
	~ ~			~ ~			~ ~				
	~ ~			~ ~			~ ~				
	~ ~			~ ~			~ ~				
	~ ~			~ ~			~ ~				
	~ ~			~ ~			~ ~				
	~ ~			~ ~			~ ~				
-30	~ ~		BX casing (28.5 m) Drilled by BX diamond bit from 28.5 m	-70	~ ~			-120	~ ~		114~115m Cu < 0.01% S 0.09%
	~ ~			~ ~			~ ~				
	~ ~			~ ~			~ ~				
	~ ~			~ ~			~ ~				
	~ ~			~ ~			~ ~				
	~ ~			~ ~			~ ~				
	~ ~			~ ~			~ ~				
	~ ~			~ ~			~ ~				
	~ ~			~ ~			~ ~				
	~ ~			~ ~			~ ~				
-40	~ ~			-80	~ ~			-130	~ ~		
	~ ~			~ ~			~ ~				
	~ ~			~ ~			~ ~				
	~ ~			~ ~			~ ~				
	~ ~			~ ~			~ ~				
	~ ~			~ ~			~ ~				
	~ ~			~ ~			~ ~				
	~ ~			~ ~			~ ~				
	~ ~			~ ~			~ ~				
	~ ~			~ ~			~ ~				

Biotite granite has intruded into leucocratic gneiss and epidiorite in many parts.

Diorite is greenish dark gray, and the major rock-forming minerals are plagioclase, augite, biotite, garnet and quartz and the accessory minerals are amphibole, allanite, chlorite, and laumontite.

Biotite granite is medium-grained granular, and most of the plagioclase is montmorillonized and biotite chloritized.

Most of the leucocratic gneiss contains garnet, and quartz, plagioclase, biotite, and augite are observed.

Intensely silicified zone exists below 107.5 m. The zone consists sericite-chlorite zone, and chlorite - (montmorillonite) zone from the bottom of the hole upward. Weak silicification is observed near the mouth of the hole. Sulphide dissemination is observed mainly in these zones, especially in the sericite-chlorite zone, but the grade is low with less than 0.01 per cent Cu, 0.16 per cent S (35.0 - 38.0 m) and less than 0.01 per cent Cu, 0.14 per cent S (91.0 - 98.0 m).

Fractured zones with widths of 0.2 - 1.5 m are found at 41 m, 106 m, and 112 m, and montmorillonite, chlorite, and zeolite occurs in these zones.

DH-2 In this drill hole, soil, sand and gravel layer is 10 m thick and is underlain by melanocratic gneiss which continues to the bottom. Intrusion of biotite granite into the melanocratic gneiss is observed at 10.5 - 11.0 m and 31.8 - 34.5 m. The gneiss has a dip of 60 - 70° at 11.0 - 31.8 m and 40 - 45° below 35 m.

Melanocratic gneiss is dark gray with quartz, plagioclase, biotite as major components and garnet, sillimanite, clinopyroxene, and muscovite as accessory components, but gneiss without garnet is more common. The biotite granite is medium-grained, granular and contains weak dissemination of sulfide.

Strong silicified zone is observed at 101 - 107 m, and sericite-chlorite zone and chlorite - (montmorillonite) zone are seen upward. It was difficult to obtain cores under the silicified zone, but the results of the X-ray diffraction studies using sludge show the mineral assemblage to be chlorite - (laumontite). Weak sulphide dissemination is observed mainly in the silicified zone and at sericite-chlorite zone. The grade of the mineralization, however, is low at 0.02 per cent Cu, 1.30 per cent S, (67.0 - 71.0 m) and less than 0.01 per cent Cu, 0.19 per cent S (125.0 - 130.0 m).

There are fractured zones at 80.1 - 82.5 m and 86.9 - 91.1 m and graphite, montmorillonite, chlorite, and laumontite are found.

DH-3 In this drill hole, soil, sand and gravel layer is 6.5 m thick and is underlain by melanocratic gneiss, biotite granite, melanocratic gneiss, and biotite-hornblende quartz porphyry respectively. Melanocratic gneiss is often intruded by biotite granite, and the dip of the gneissose structure is 35° in the upper parts and 50°-60° in the lower parts.

The major portion of the melanocratic gneiss consists of dark gray biotite gneiss. The biotite granite is medium-grained and granular with the major constituent minerals of quartz, potash feldspar, plagioclase, biotite, and hornblende.

The fringe of some of the plagioclase has altered to potash feldspar and some of the biotite grains have altered to chlorite. The biotite-hornblende quartz porphyry is pale greenish gray and the phenocrysts are corroded quartz, plagioclase, chloritized biotite, epidotized hornblende and the matrix consists of quartz and plagioclase and has graphic to granophyric texture.

The biotite-hornblende quartz porphyry in the lower part of this drill hole shows chlorite-epidote zone (propylitic zone) and chlorite facies in the upper parts.

Weak sulphide dissemination is observed throughout the total core, but the grade is less than 0.01 per cent Cu, 0.33 per cent S (69.0 m - 75.0 m) and less than 0.01 per cent Cu, 0.09 per cent S (114.0 - 115.0 m).

#### 4-3 Discussion

Geological cross sections (Fig. 4-1) through the drilled sites were prepared from the geological column of the drill holes (Appendix 4) and the geological map. (PL. 1-1). It is seen from this section that in DH-1, epidiorite and biotite granite which are exposed near the drill hole are intruded into the leucocratic gneiss. At DH-2, a small dyke of biotite granite has intruded into melanocratic gneiss. A fault inferred to exist between DH-1 and -2 from geological survey, also seems to exist from the results of the drilling. At the upper part of DH-3, xenoliths of melanocratic gneiss in the granite are seen, this is considered to be the extension of the xenolith seen at the surface near the drill hole. Biotite-hornblende quartz porphyry which exists below 100 m is not observed on the surface and it is considered to have intruded after the formation

of the granite.

The relation between the altered zone found in the drill holes and the altered and mineralized area on the surface is expressed as cross section of the S. Webose mineralized area in Fig. 4-2. The zones of sulphide mineralization are in good agreement with the distribution of the sericite-chlorite zone and small silicified zones occur in several places in this altered zone. The sericite-chlorite zone is surrounded by chlorite-(montmorillonite) zone and the boundary between these zones is believed to be generally steeply dipping. The propylitization found at the lower part of DH-3 is considered to be due to hydrothermal activities related to biotite-hornblende quartz porphyry, but here it will be treated as a propylitized zone at the outermost side of the argillitized zone.

Thus the following zonal arrangement of hydrothermal alteration related to S. Webose mineralization is observed from the center outward.

- |     |  |   |                     |
|-----|--|---|---------------------|
| (1) | Quartz-sericite-potash feldspar zone   | ) | Potassium-rich zone |
| (2) | Sericite-chlorite zone                 | ) |                     |
| (3) | Chlorite-(montmorillonite) zone        | ) |                     |
| (4) | Chlorite-epidote zone (propylite zone) | ) |                     |

The mineralized zone coincides fairly well with the potassium-rich zone and the boundary to the outer chlorite-(montmorillonite) zone dips steeply. This feature is in good agreement with the results of geophysical surveys. That is the IP anomaly of the S. Webose mineralized area has more or less constant shape and intensity from the surface down to 200 m, and this fact indicates a steep boundary.

From the results of the geological survey, drilling, and geophysical survey, the shape of the S. Webose mineralized zone does not change from the surface downward, in other words

the boundary is very steep. The maximum grade of the cores of DH-1 and -2 are only 0.02 per cent Cu, 1.30 per cent S, and the normal values are in the order of 0.01 per cent Cu and 0.2 per cent S. Also the weak mineralization found in the core of DH-3 is considered to be a local phenomenon caused by hydrothermal activity of the quartz porphyry intrusion. In these drill holes, the grade does not increase downward and secondary enrichment is not observed.



Fig. 4-1 Geological Cross Section along DH-1,  
DH-2 and DH-3 (V; 1: 5,000)  
(H; 1:10,000)

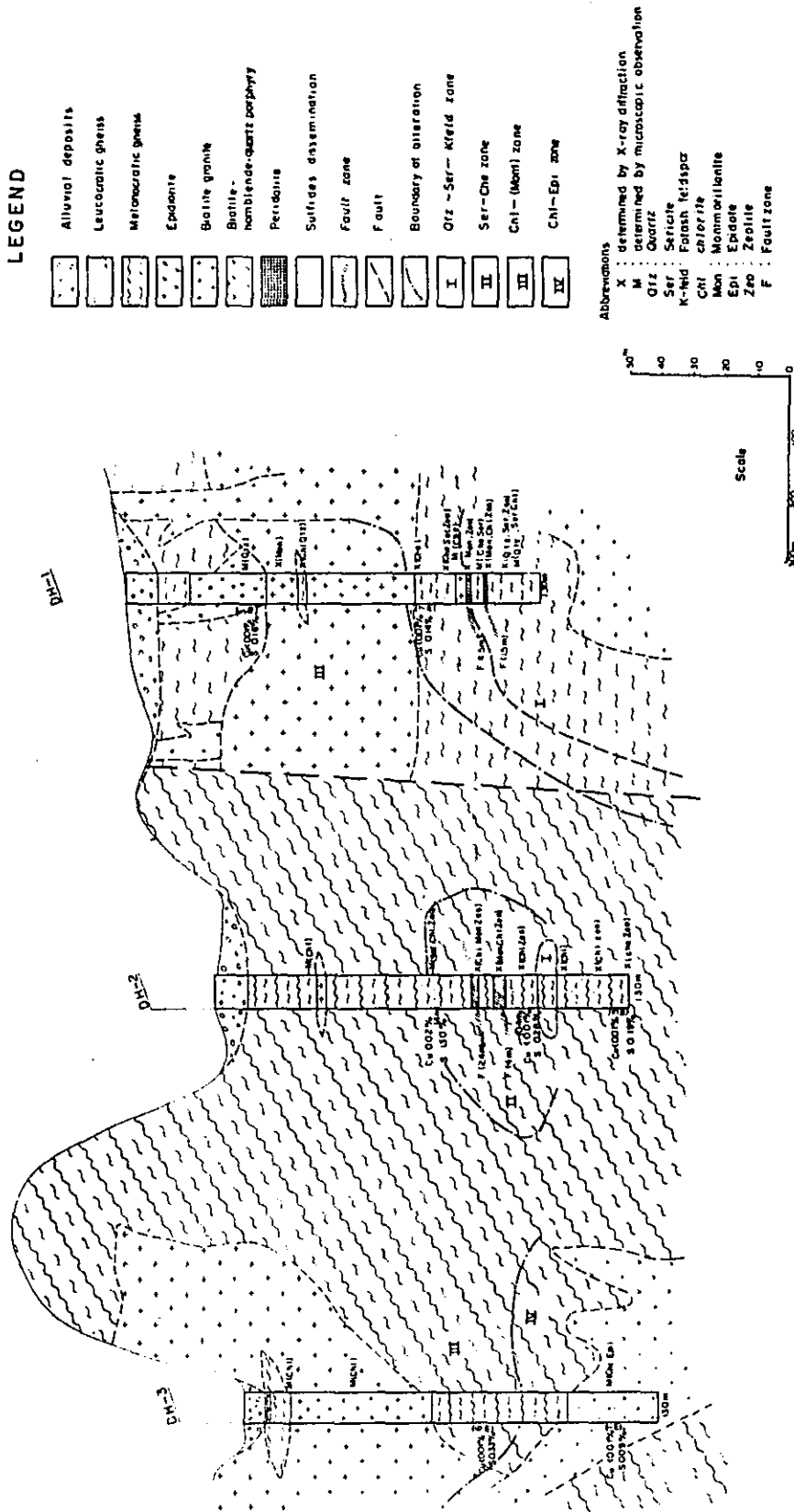
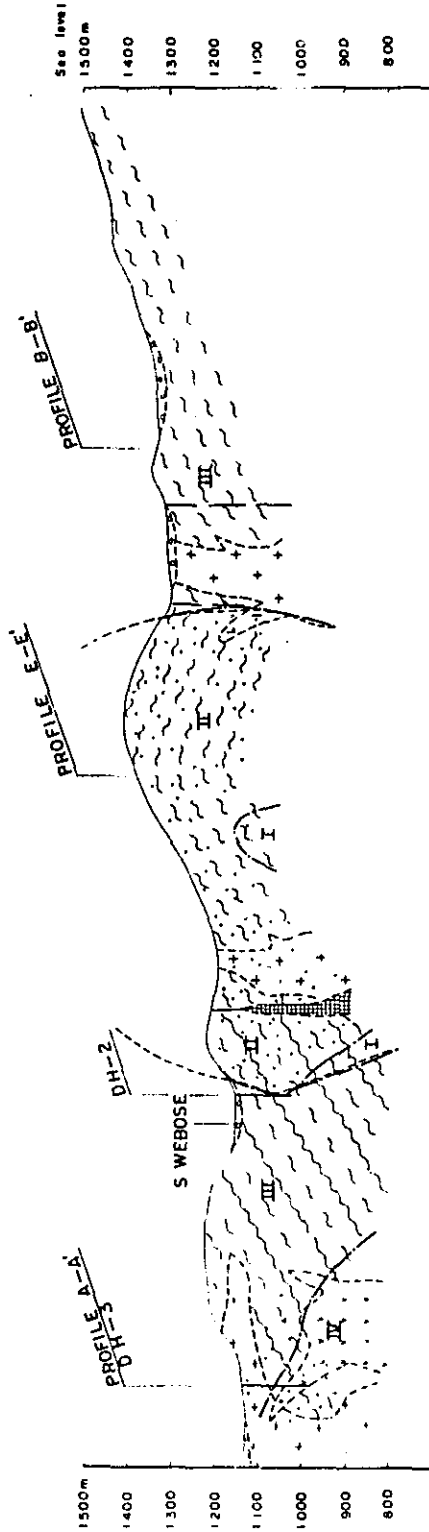


Fig. 4-2  
 Cross Section of S. Webose  
 Mineralized Area (1 : 10,000)

D - D' SECTION



LEGEND

	Alluvial deposits		Biotite-hornblende quartz porphyry		Zone I: Quartz-sericite-k-feldspar zone
	Leucocratic gneiss		Pendolite		Zone II: Sericite-Chlorite zone
	Melanocratic gneiss		Sulfide dissemination		Zone III: Chlorite-(Montmorillonite) zone
	Biotite granite (earlier stage)		Assumed boundary of disseminated area		Zone IV: Chlorite-Epidote zone
	Biotite granite (later stage)		Fault		Boundary of alteration zone

## **PART V**

### **CONCLUDING REMARKS**

The survey project of this area, S. Bomba mineralized area, consisted of geological survey, geochemical survey, geophysical surveys (EM and IP methods), and drilling exploration. As the result of these works, the geological conditions of this area have been clarified.

### Geological Survey

The results of the above work are summarized as follows.

- (1) The geology of this area consists of the following formations from the lower horizon upward. Metamorphic rocks such as gneiss (G. Nokila laki gneiss), schist (S. Rompo schist), sedimentary formations such as sandstone and conglomerates (S. Tinauka formation) and intrusive rocks represented by biotite granite.
- (2) The metamorphic rocks constitute the host rocks of the mineralized zones. Therefore, it was necessary to distinguish the minerals formed by regional metamorphism and those formed by hydrothermal alteration in order to clarify the nature of the alteration related to the mineralizing process. From these studies, the nature of the metamorphic facies and the alteration process associated with mineralization are now known in fair detail.

The metamorphic grade seems to belong as a whole to the intermediate stage between amphibolite and granulite facies. Sericite, chlorite, epidote, laumontite, and potash feldspar (adularia) are considered to be the product of hydrothermal alteration after the regional metamorphism.

(3) There were two stages of biotite granite activity and the earlier type formed the batholith and the later type formed the stocks which branched out from the former.

(4) The project area is situated between the Tawaëlia graben (the central tectonic line) and the Fossa Sarasina (Palu fault).

The metamorphic rocks are cut into several blocks by the faults and are intruded by many intrusive bodies.

It has been shown by the survey of 1971, that the principal direction of geologic structure of the block No. 4 has a trend of N-S. In the present area, however, the strike of the planar structures (gneissosity and schistosity) are mainly in E-W direction and does not agree with those of the neighboring areas (N-S).

It is likely that there were two stages of faulting. The earlier stage formed the NEE - SWW faults in the metamorphic rocks in the southern part of the area and also the NNW - SSE series which intersect the former series. The later movement developed the NWW - SEE and NNE - SSW faults in the metamorphic and biotite granite bodies in the north.

(5) The largest mineralization of this area is found along the estuary of the Webose river. It consists of pyrrhotite dissemination in gneiss extending for 3 km with a maximum width of 1 km.

The copper content of the S. Webose mineralized area is maximum 0.14 per cent, and average 0.049 per cent, the sulphur content is maximum 6.8 and the average 2.4 per cent.

(6) Hydrothermal alteration is observed in this area in the vicinity of the S. Webose mineralized area and the alteration zone is arranged in the order of the following 1 - 2 - 3 zones.

- 1) Quartz-sericite-potash feldspar zone (silicified zone).
- 2) Sericite-chlorite zone.
- 3) Chlorite-(montmorillonite) zone.

The mineralized area coincides fairly well with the (i) sericite-chlorite zone.

From the consideration of the factors of igneous rocks related to the genesis of the mineralization, forms of the ore deposits, distribution of ore minerals and the alteration, the S. Webose mineralized area is inferred to be a process similar to the formation of porphyry copper deposits.

It is a fact, however, that there are geologic features which are uncommon in normal porphyry copper deposits such as the lack of molybdenite which occurs in almost all porphyry copper deposits, the abundant occurrence of pyrrhotite.

#### Geochemical Survey

The results of the above survey are as follows.

- (1) In the S. Webose mineralized area, the copper content in soils is in the range of 8 - 48 ppm, and associated geochemical anomalies could not be found.
- (2) The twelve anomalies found in this area are in the range of 30 - 60 ppm Cu and they are all with small dispersion and none could be considered to be the results of mineralization.

- (3) Therefore, it is not possible to select areas for further prospecting from the geochemical data alone.

### Geophysical Survey

The results of the geophysical surveys (electromagnetic survey and induced polarization survey) are as follows.

#### Electromagnetic survey

- (1) A comprehensive anomalies of electromagnetic field were detected widely by means of the vertical loop method. These anomalies which extend in the NW direction coincide well with S. Webose mineralized area.
- (2) Small- scaled anomaly was detected around Station No. 10, D Line, at the southern part of S. Webose mineralized area by the horizontal loop method.
- (3) Some detected anomalies have such rather complex patterns that the distinct anomalies are not found. These may be possibly caused by the wide distribution of sulphide minerals as well as the topographic effect.

#### Induced polarization survey

- (1) Four IP anomalies were detected around S. Webose mineralized area. We noticed EW extensions of these anomalies, about 1.5 km long, passing through

the central area of S. Webose mineralized area.

- (2) An extent of the anomalous area is almost equal to that of S. Webose mineralized area, which was determined by precise geological surveys. The discovery of the anomaly proves that the IP survey is effective to the area concerned. The anomalous area disappears in the northern part of the survey area, so that we can not expect the northern extension.
- (3) According to drilling exploration carried out around S. Webose mineralized area, we detected disseminated areas of sulphide minerals (pyrrhotite, pyrite), although the dissemination varies from place to place. Therefore, it is sure that the IP anomaly over this area is caused by the disseminated sulphide minerals.

### Drilling Exploration

The drilling exploration were performed in the S. Webose mineralized area which were delineated as the most promising area from the geological, geochemical, and geophysical surveys. The results are as follows.

- (1) The alteration zones found from the drill cores are similar to those found on the surface and they are as follows.

- 1) Quartz-sericite-potash feldspar )  
(adularia)zone ) potassium-rich zone
- 2) Sericite-chlorite zone )



- 3) Chlorite-(montmorillonite) zone
  - 4) Chlorite-epidote zone (propylitic zone)
- (2) The shape of the mineralized area coincides with that of the potassium rich zone, and it is in contact with the outer chlorite-(montmorillonite) zone with a steep dip. This fact also agrees well with the results of the IP survey. The shape and the intensity of the IP anomalies are more or less constant from the surface down to 200 m which suggests that the boundary of the mineralized area is very steep.
- (3) The grade from the drill cores show a maximum of Cu 0.02 per cent and S 1.30 per cent, other analyses are less than 0.01 per cent Cu and about 0.2 per cent S.
- (4) It was shown that the dimensions of the mineralized area were constant downward, but also the increase of grade was not observed and secondary enrichment was also not found.

#### Recommendation

As the result of the surveys, the geologic feature of the area and the S. Webose mineralized area have been clarified. It is recommended that the above mentioned area is not workable at present judging from the feature of mineralization.

## REFERENCES

(General & Geological Survey)

1. Holland, H. D. (1959) : Some applications of thermochemical data to problems of ore deposits. I. Stability relations among the oxides, sulfides, sulfates and carbonates of ore and gangue metals, *Econ. Geol.*, vol. 54, (2), 184 - 233.
2. Holland, H. D. (1965) : Some applications of thermochemical data to problems of ore deposits. II. Mineral assemblages and the composition of ore-forming fluids. *Econ. Geol.*, vol. 60, 1101 - 1166.
3. Krauskopf, K. B. (1964) : The possible role of volatile metal compounds in ore genesis. *Econ. Geol.*, vol. 59, (1), 22 - 45.
4. Miyashiro, A. (1964a) : Oxidation and reduction in the earth's crust with special reference to the role of graphite. *Geochim. Cosmochim. Acta*, vol. 28, 717 - 729.
5. Miyashiro, A. (1964b) : Notes on rock-forming minerals (32). Geochemistry of oxygen and the origin of native iron and native nickel-iron. *Jour. Geol. Soc. Japan*, vol. 70, no. 828, 493 - 499.
6. Miyashiro, A. (1965) : Metamorphic rocks and metamorphic belt. (in Japanese) Iwanami Book Shop.
7. Overseas Technical Cooperation Agency (1971) : Report on Geological Survey of Central Sulawesi, Indonesia. vol. 1, General.

8. Overseas Technical Cooperation Agency (1971) : Report on Geological Survey of Central Sulawesi, Indonesia. vol. 2, part 2, Photogeology.
9. Overseas Technical Cooperation Agency (1972) : Report on Geological Survey of Central Sulawesi, Indonesia. vol. 4.
10. Skinner, B. J. (1956) : Physical properties of end-members of the garnet group. Amer. Minerl. , vol. 38, 428 - 436.
11. Van Bemmelen. (1949) : The Geology of Indonesia.
12. Yui, S. (1966) : Stability relations among iron oxide, sulphide, and carbonate minerals during magmatic ore deposition with special reference to the role of graphite. Journ. Society of Mining Geologist of Japan. vol. 16, (1), 16 - 27.

(Geophysical Survey)

1. Keller, G. V. and Frischknecht, F. C. (1966) : Electrical Methods in Geophysical Prospecting. Pergamn Press.
2. Madden, T. R. (1958) : Two-dimensional resistivity and induced polarization. Geoscience Co. , U. S. A.
3. Metallic Minerals Exploration Agency of Japan (1969) : Report on electrical survey of Andes Copperbelt, The Republic of Chile (in Japanese).
4. Metallic Minerals Exploration Agency of Japan (1970) : Report on electrical survey of Mokambo area, Republique Democratique du Congo (in Japanese)

5. Society of Exploration Geophysicist (1966) : Mining Geophysics  
vol. II. The SEG. Mining Geophysics Volume  
Editorial Committee
6. Sumita, H. (1966) : Computation on IP models. Journal of  
the Nippon Mining Technical Research Center  
(in Japanese) unpublished.

## APPENDIXES

Appendix 1-1 Observation of Handspecimens

Abbreviations :	*	:	Distinct sulfidation	Gn	:	Gneissosity
	Loc.	:	Locality	w.	:	weak
	C. I.	:	Color Index	m.	:	medium
	gar.	:	garnet	str.	:	strong
	silic.	:	silicification	v.	:	very
	chl.	:	chlorite	thin.	:	thin layered gneissosity
	sulf.	:	sulfides	Equigrn.	:	Equigranular
	T	:	Thin section	+++	:	abundant
	P	:	Polished section	++	:	common
	X	:	X-ray diffraction	+	:	little
	A	:	Analyses			

Notes : Color index is measured by unaided eye, the index mainly shows the amount of biotite flakes.

The rock which is more than 25 of color index is represented as melanocratic rock, and also less than 25 of color index as leucocratic.

Sample No.	Loc.	Rock Name	Color & C.I.	gar.	silic.	white clay	chl.	sulf.	Structure	Remarks	T	P	X	A
102301	B-2	Garnet-biotite gneiss	15	++		+		+	Gn : w.					
102302	B-2	Garnet-biotite gneiss	20	+++	+				Gn : w.					
102303	B-2	Biotite granite	7			++	+	+	Equigrn.		O	O		
102304	B-2	Garnet-biotite gneiss	15	+	++				Gn : w.	Weathered, fine grained				
102305	B-2	Biotite gneiss	10					+	Gn : thin, m					
102401	B-2	Diorite	25				+			Composed of glomerophyric hornblende, biotite, plagioclase and quartz				
102402	B-2	Garnet-biotite gneiss	15	++	+			+	Gn : m.					
102403	B-2	Garnet-biotite gneiss	*20-30	++	+++			++	Gn : w.	Fine grained, sulfides dissemination, silicification				O
102404	B-2	Biotite gneiss	50						Gn : m.	Biotite shows band-structure				
102601	A-2	Garnet gneiss	7-10	+	+++		+	+	Gn : w.	Strong silicification, graphite bearing	O			O
102602	A-2	Garnet-biotite gneiss	10	++	++				Gn : thin, str.	Fine grained, graphite bearing				
102603	A-2	Garnet gneiss	10-15		++					Silicified, graphite bearing				
102604	A-2	Biotite-garnet gneiss	* 50	+++				++	Gn : w.	Sulfides as veinlet, heavy				
102701	B-3	Biotite granite	15				+		Equigrn.	Fine to medium grained				
102702A	B-3	Hornblende-biotite schist	*60-70		+++			++	Schistose	Fine grained, apite (quartz - plagioclase) vein				
102702B	B-3	Garnet-biotite gneiss	30	++		+		+	Gn : m.					
102703	B-3	Biotite-quartz schist	*10-20					++	Fine gneissose or schistose	Sulfide dissemination along schistosity	O			
102704	B-3	Garnet-biotite gneiss	40	+					Gn : str.	Minor folding				
102705	B-3	Biotite granite	15						Equigrn.	Medium grained, plagioclase shows milky feature				
102706	B-3	Biotite granite	15						Equigrn.	Medium grained, fresh				



Sample No.	Loc.	Rock Name	Color & C. I	gar.	silic.	white clay	chl.	sulf.	Structure	Remarks	T	P	X	A
102707	B-3	Garnet-biotite gneiss	40-50	++					Gn : m.					
102708	B-3	Quartz schist	pale gray 5					+	Cherty	Biotite band, one chalcopyrite grain	O			
102709	B-3	Biotite granite	10			+			Equigrn.	Plagioclase shows milky feature				
102710	B-3	Biotite granite	10-15						Equigrn.					
102711	B-3	Garnet-biotite gneiss	15-20	+		+	+		Gn : w.	Sheared rock				
102712	B-3	Biotite gneiss	10-15			++			Gn : thin, str.	Fine grained	O			
102713	B-3	Clay	pale green			+++	++			Fault zone				O
102714	B-3	Biotite gneiss	1		+++				Gn : thin.	Siliceous, graphite bearing	O			
103101	B-2	Garnet-biotite gneiss	white 10-15	++	+++				Gn : m.	Strong silicification				
103102	A-2	Garnet-biotite gneiss	15-20	++				+	Gn : w.					
103103	A-2	Garnet-biotite gneiss	40	++	+			++	Gn : w.	Graphite bearing, sulfides veinlet and dissemination	O	O	O	O
103104	A-2	Garnet-biotite gneiss	30	++				+	Gn : m.	Graphite bearing	O			O
103105	A-2	Altered rock	pale green		+	+++	++	+	Brecciated	Clay, fault zone				O
103106	A-3	Biotite gneiss	10						Gn : thin.	Weathered				
110401	A-2	Biotite gneiss	7		++		+	++	Gn : thin, m.	Siliceous				
110402	A-2	Garnet gneiss	5	+++	++			+	Gn : w.	Siliceous, graphite bearing				
110403	A-2	Garnet-biotite gneiss	15	+	+			+	Gn : m.	Graphite bearing				
110404	A-2	Biotite gneiss	15		+			+	Gn : thin, m.		O	O		
110405	A-2	Hornblende-biotite schist	60					+	Schistose					
110406	A-2	Biotite granite	7							Medium grained, some large (1 cm long) plagioclase crystals are observed				
110407	A-2	Biotite gneiss	5					+	Gn : w.	Siliceous, graphite bearing				

Sample No.	Loc.	Rock Name	Color & C.I.	gar.	silic.	white clay	chl.	sulf.	Structure	Remarks	T	P	X	A
110408	A-2	Garnet gneiss	* 1	+	++		+	++	Massive	Silicification caused by leaching out, sulfides veinlet	O			
111301	A-1		brown						Porphyritic	Plagioclase (0.5 - 1 cm long) in brown matrix				
111302	A-1	Garnet-biotite gneiss	10	+++			+	+	Gn : m.					
111303	A-1	Garnet-biotite gneiss	15-20	+	++		+	+	Gn : w.					
111304A	A-2	Garnet-biotite gneiss	* 20	++				++	Gn : w.	Graphite bearing				
111304B	A-2	Garnet-biotite gneiss	25	++				+	Gn : w.					
111305	A-2	Garnet-biotite gneiss*	25	+				++	Gn : w.	Graphite bearing				O
111306	A-1	Peridotite	black						Massive	Garnet bearing	O			
111501	A-2	Garnet-biotite gneiss	25	+		+	++		Gn : w.	Argillized			O	
111502	A-2	Biotite granite	7			++				Some large (0.5 cm long) plagioclase crystals are observed				
111503	A-2	Peridotite	black						Banded	Calcite vein				
111504A	A-2	Garnet-biotite gneiss	10	+	+				Gn : v.w.					
111504B	A-2	Garnet-biotite gneiss	15	++				+	Gn : w-m.	Graphite bearing				
111505	A-2	Argillized rock	greenish gray	+		++	++			Graphite bearing, fault zone			O	
111506	A-1	Garnet gneiss	5	+	++			+	Gn : w.	Siliceous				
111701	B-1	Biotite gneiss	30-40						Gn : w.					
111702	B-2	Biotite granite	15						Equigrn.	Medium grained				
111703	B-2	Biotite gneiss	50						Gn : thin, str.	Similar to schistose structure				
111704	B-2	Biotite granite	10-15			+			Equigrn.	Large crystals (0.5 cm in size) of plagioclase are dotted				
111705	B-2	Biotite schist	60						Schistose					
111706	B-2	Biotite schist	50						Schistose					

Sample No.	Loc.	Rock Name	Color & C.I.	gar.	silic.	white clay	chl.	sulf.	Structure	Remarks	T	P	X	A
111707	B-2	Biotite granite	10						Equigrn.	Large plagioclase (0.5 to 1.0 cm in size) is observed				
111708	B-2	Biotite schist	50						Schistose		O			
111709	B-2	Biotite granite	10-15						Equigrn.	Medium grained				
111710	C-2	Garnet-biotite gneiss	40	+					Gn : str.					
111711	C-2	Biotite schist	50						Schistose					
111712	B-2	Biotite gneiss	50						Gn : w.					
111801	B-2	Biotite granite	15						Equigrn.	Medium grained				
111802	B-2	Biotite schist	* 60					++	Schistose		O			O
111803	B-3	Biotite schist	50						Schistose		O			
111804	B-2	Biotite gneiss	15						Partly foliated					
111805	B-2	Biotite gneiss	50						Gn : str.					
111806	B-3	Garnet-biotite gneiss	20	+	+			+	Gn : str.					
111807	B-3	Biotite gneiss	30						Gn : str.	Graphite bearing				
111808	B-3	Biotite granite	10						Equigrn.	Fresh				
112001	C-3	Garnet-biotite gneiss	* 15	++				++	Gn : m.	Sulfides in cracks				O
112002	C-3	Biotite granite	15			+			Equigrn.	Large plagioclase crystals (1 cm in length) are observed				
112003	C-3	Garnet-biotite gneiss	40	++				+	Gn : str.	Sulfides in cracks				
112004	B-2	Biotite schist	30-40					+	Schistose	Sulfides in cracks				O
112005	B-2	Garnet-biotite schist	40	+		+	+							
112006	B-2	Clay	grayish green			+++	++			Clay in granite				O
112101	A-2	Garnet-biotite gneiss	* 20	++				++		Graphite bearing	O	O	O	O

Sample No.	Loc.	Rock Name	Color & C.I.	gar.	silic.	white clay	chl.	sulf.	Structure	Remarks	T	P	X	A
112201	B-3	Garnet-biotite schist	30	+					Schistose	Graphite bearing				
112202	B-3	Biotite gneiss	30						Gn : w.					
112203	B-3	Garnet-biotite gneiss	30	++				+	Gn : w.					
112301	B-3	Peridotite	black											
112302	B-3	Altered peridotite	*green					++						
112501	B-3	Biotite gneiss	30		+				Gn : thin, str.					
112502	B-3	Biotite granite	15					+	Equigrn.	Weakly oriented			O	
112503	C-4	Biotite gneiss	15						Gn : str.					
112801	B-3	Biotite gneiss	30						Gn : m.					
112802	B-3	Garnet-biotite gneiss	30-40	+	+			+	Gn : str.	Sulfides in cracks				
112803	B-3	Garnet-biotite gneiss	50	+					Gn : m. - w.					
112804	B-3	Biotite granite	10						Equigrn.	Medium grained				
112901	B-1	Biotite gneiss	40						Gn : str.-m.	Ferruginous stain				
112902	B-2	Garnet-biotite gneiss	40	+					Gn : str.-m.				O	
120201	D-2	Hornblende-biotite gneiss	40-50						Gn : w.					
120202	D-2	Garnet-hornblende-biotite gneiss	50	+					Gn : v. w.					
120203	D-2	Garnet-biotite gneiss	10	++					Gn : m.	Fine grained				
120204	D-2	Biotite gneiss	* 10				+	++	Gn : str.	Sulfides impregnated				O
120205	D-2	Hornblende-biotite gneiss	40-50						Gn : v. w.					
120206	D-3	Biotite granite	10						Equigrn.	Large plagioclase crystals (0.5 cm in size) are observed				
120207	D-3	Garnet-biotite gneiss	5-7	++	++				Gn : w.	Siliceous				
120208	D-3	Hornblende-biotite gneiss	50					+	Gn : w.					

Sample No.	Loc.	Rock Name	Color & C.I.	gar.	silic.	white clay	chl.	sulf.	Structure	Remarks	T	P	X	A
120401	D-3	Biotite-garnet gneiss	7	++					Gn : m-str.	Fine grained				
120402	D-3	Garnet-biotite gneiss	* 30	++	++			++	Gn : w.	Sulfides impregnation, quartz veinlet		O		O
120403	D-3	Hornblende-biotite gneiss	50					+	Gn : w.					
120404	D-3	Biotite gneiss	50						Gn : str.					
122001	D-2	Garnet-biotite gneiss	<5	+	++			+	Gn : v. w.	Siliceous				
122002	D-2	Garnet-biotite gneiss	* 25	++				++	Banded structure					
122003	D-2	Gabbro	100											
122004	D-2	Biotite gabbro	100											
122005	D-2	Garnet-biotite gneiss	* 10	++				++	Gn : str.	Sulfides in cracks		O		O
122101	D-2	Garnet-biotite gneiss	15	++					Gn : str.	Biotites show layer structure		O		
122102	D-2	Garnet-biotite gneiss	40	++					Gn : m.	Graphite bearing				
122103	D-2	Biotite gneiss	20						Gn : w.					
122201	D-3	Garnet-biotite gneiss	30	++	+				Gn : w.					
122203	D-3	Garnet-biotite gneiss	* 10-15	++				++	Gn : w.	Graphite bearing				O
122204	D-3	Garnet-biotite gneiss	30	++				+	Gn : str.					
122205	D-3	Garnet-biotite gneiss	40	+					Gn : w.					
122301	D-3	Biotite gneiss	2						Gn : v. w.	Leucocratic				
122302	D-3	Garnet-biotite gneiss	40	++				+	Gn : w.					
122303	D-4	Biotite granite	15						Equigrn.	Medium grained				
122601	C-3	Biotite granite	15						Equigrn.	Medium grained				
122602	C-3	Garnet-biotite gneiss	30	++					Gn : m.					
122603	C-3	Biotite gneiss	10						Equigrn.					

Sample No.	Loc.	Rock Name	Color & C.I.	gar.	silic.	white clay	chl.	sulf.	Structure	Remarks	T	P	X	A
122604	C-3	Biotite gneiss	40	+				+	Gn : str.	Pyrite in cracks				O
122605	C-3	Hornblende-biotite granite	10						Equigrn.	Large plagioclases (0.5 cm in size) are observed				
122606	C-3	Garnet-biotite gneiss	40	+				+	Gn : m.					
122607	C-3	Biotite gneiss	30						Gn : thin, str.					
122701	D-3	Biotite-garnet gneiss	10	++				+	Gn : str.	Sulfides in cracks				
122702	D-3	Garnet-biotite gneiss	15	++				++	Gn : m.	Sulfides in cracks, graphite bearing				O
122703	D-3	Garnet-biotite gneiss	50	+			+		Gn : w.					
122704	D-3	Biotite-garnet gneiss	15	+++				+++	Gn : w.	Sulfides dissemination		O		O
122705	D-3	Garnet-biotite gneiss	50	+				+	Gn : str.					
122706	D-3	Biotite granite	15						Equigrn.					
122707	D-3	Garnet-biotite gneiss	40	++	+		+	+	Gn : m.	Sulfides in cracks				
122708	D-3	Garnet-biotite gneiss	25	+				+	Gn : w.	Sulfides dissemination				
122801	D-2	Biotite-garnet gneiss	10	++				+	Gn : m.					
122802	D-2	Garnet-biotite gneiss	30	+				+	Gn : str.	Graphite bearing				
122803	D-2	Garnet-biotite gneiss	30	+++	++			+	Gn : m.					
122804	C-2	Garnet-biotite gneiss	40	+	++			+	Gn : m.					
122805	C-2	Biotite granite	10						Equigrn.	Large plagioclase crystals (0.5 cm in length)				
122806	C-3	Hornblende-biotite gneiss	5						Gn : w.					
122807	C-2	Biotite granite	10						Equigrn.					
122808	C-2	Biotite gneiss	30					+	Gn : str.					
122809	C-2	Garnet-biotite gneiss	30	++				++	Gn : thin, str.	Sulfides in cracks and disseminated along layer	O			O

Sample No.	Loc.	Rock Name	Color & C.I.	gar.	silic.	white clay	chl.	sulf.	Structure	Remarks	T	P	X	A
122810	C-2	Biotite granite	10							Large plagioclase crystals (0.5 - 1.0 cm in size) are dotted.				
123001	E-2	Biotite gneiss	30						Gn : m.					
123002	E-2	Biotite gabbro	100					+						
123003	E-2	Hornblende-biotite gabbro	dark green					+						
123004	E-2	Biotite gneiss	15						Gn : str.	Minor folding				
123005	E-2	Biotite granite	10						Equigrn.	Weathered				
123006	E-2	Garnet-biotite gneiss	15	+					Gn : w.	Fine grained				
123007	E-2	Biotite-garnet gneiss	5	++					Gn : w.	Siliceous				
123008	E-2	Biotite gneiss	40					+	Gn : v. w.					
123009A	E-3	Metamorphosed diorite	dark green											
123009B	E-3	Hornblende-biotite granite	15						Equigrn.	With aplite vein, medium grained				
123010	D-3	Biotite gabbro	50									O		
123011	D-3	Garnet-biotite gneiss	* 30	++	++			++	Gn : m.	Sulfides dissemination				O
123012	D-3	Biotite granite	15						Equigrn.	Medium grained				
123013	D-3	Garnet-biotite gneiss	* 30	+				++	Gn : str.	Sulfides dissemination and veinlets				O
123014	D-3	Garnet-biotite gneiss	10	+					Gn : thin, str.					
123015	D-3	Biotite granite	15						Equigrn.	Large plagioclase crystals (0.5 cm in size) are dotted				
010101	C-1	Biotite gneiss	30-40						Gn : str.			O		
010102	C-1	Biotite gneiss	>50					+	Gn : str.					
010103	C-1	Garnet-biotite gneiss	* 40	++				++	Gn : thin, str.	Sulfides dissemination and veinlets				O

Sample No.	Loc.	Rock Name	Color & C.I.	gar.	silic.	white clay	chl.	sulf.	Structure	Remarks	T	P	X	A
010104	C-2	Garnet-biotite gneiss	7	+					Gn : w.					
010105	C-2	Garnet-biotite gneiss	30	+				++	Gn : str.	Sulfides dissemination, graphite bearing		O		O
010106	C-2	Garnet-biotite gneiss	15	+					Gn : w.	Large plagioclase (0.5 cm in size) are observed				
010107	C-2	Biotite gabbro	50								O			
010108	C-2	Biotite granite	10						Equigrn.					
010701	C-1	Biotite granite	15						Equigrn.	Medium grained but partially fine grained				
010702	C-1	Biotite granite	10						Equigrn.	Xenolith of schist is enclosed				
010703	C-2	Biotite gneiss	40						Gn : str.					
010704	C-1	Biotite gneiss	40-50						Gn : w.					
010705	C-1	Biotite granite	10						Equigrn.					
DH-1, 18.6 <sup>m</sup>		Garnet-biotite gneiss	20-30	+++					Gn : str.					
29.0 <sup>m</sup>		Metamorphosed diorite	50		++				Gn : w.	Quartz veinlet				
38.0 <sup>m</sup>		Metamorphosed diorite	40	+++	++			++			O			O
48.5 <sup>m</sup>		Argillized granite	10			+++								O
55.4 <sup>m</sup>		Altered rock	pale Green		++		++							O
65.0 <sup>m</sup>		Biotite granite	10							Xenolith of biotite gneiss is included				
91.5 <sup>m</sup>		Garnet-biotite gneiss	20	+		+		+	Gn : m.		O			O
100.2 <sup>m</sup>		Altered brecciated gneiss	pale Green			++	++			Graphite layer	O			O
105.0 <sup>m</sup>		Biotite granite	10			++								



Sample No.	Loc.	Rock Name	Color & C. I.	gar.	silic.	white clay	chl.	sulf.	Structure	Remarks	T	P	X	A
DH-1, 107.0 m		Clay	dark gray			+++								O
111.6 m		Brecciated gneiss	black							Graphite rich,	O			O
113.6 m		Silicified rock	white		+++									
116.0 m		Garnet bearing melanocratic gneiss	40			++			Gn : v. w.	Zeolite veinlet, brecciated				
118.5 m		Silicified garnet gneiss	white		+++						O			O
DH-2, 10.9 m		Biotite granite	10						Equigrn.					
14.4 m		Biotite gneiss	40						Gn : str.					
30.5 m		Biotite gneiss	40-50						Gn : str.		O			
33.0 m		Biotite granite	10						Equigrn.					
36.5 m		Biotite gneiss	40						Gn : str.	Minor folding				
46.6 m		Biotite gneiss	30-40						Gn : str.					
53.8 m		Biotite gneiss	40						Gn : w.					
60.0 m		Biotite gneiss	50					+	Gn : m.	Sulfides veinlets				
68.4 m		Garnet-biotite gneiss	40	++				+	Gn : str.	Graphite bearing, sulfides veinlets	O			O
77.0 m		Sludge												
82.0 m		Clay	greenish gray			+++	++							O
84.0 m		Sludge												
87.0 m		Clay	dark gray			++	++			Graphite bearing				O
94.0 m		Biotite gneiss	40						Gn : m.					
95.7 m		Garnet gneiss	40	+++		+		+	Gn : str.	Graphite rich, biotite is not observed				O
103.5 m		Silicified rock	white	+										

Sample No.	Loc.	Rock Name	Color & C.I.	gar.	silic.	white clay	chl.	sulf.	Structure	Remarks	T	P	X	A
DH-2, 109.0 <sup>m</sup>		Sludge												
120.0 <sup>m</sup>		Sludge												O
130.0 <sup>m</sup>		Sludge												O
DH-3, 7.1 <sup>m</sup>		Biotite granite	15						Equigrn.					
7.8 <sup>m</sup>		Garnet-biotite gneiss	40	+					Gn : str.					
14.3 <sup>m</sup>		Biotite gneiss	40-50						Gn : str, thin.	Minor folding				O
14.7 <sup>m</sup>		Biotite granite	10		+			+	Equigrn.	Medium grained				
28.5 <sup>m</sup>		Biotite granite	15						Equigrn.					
34.8 <sup>m</sup>		Biotite granite	10											
47.5 <sup>m</sup>		Biotite granite	15							Large plagioclase crystals (1 cm long) are dotted				
54.5 <sup>m</sup>		Biotite granite	10					+		Large plagioclase crystals (1 cm long) are dotted				
56.4 <sup>m</sup>		Sludge												
69.5 <sup>m</sup>		Biotite gneiss	40-50		+			+	Gn : w.	Quartz vein				O
77.0 <sup>m</sup>		Sludge												
84.6 <sup>m</sup>		Garnet-biotite gneiss	40	+	++			+	Gn : str.	Quartz vein				
99.5 <sup>m</sup>		Biotite gneiss	40	+	+			+	Gn : m.	Sulfides veinlets, zeolite veinlet				
102.0 <sup>m</sup>		Hornblende quartz porphyry	#pale green 10				+	++		Fine grained				O
104.0 <sup>m</sup>		Sludge												
114.3 <sup>m</sup>		Hornblende quartz porphyry					+	+						O
117.5 <sup>m</sup>		Hornblende quartz porphyry					+	+						

Sample No.	Loc.	Rock Name	Color & C.I.	gar.	silic.	white clay	chl.	sulf.	Structure	Remarks	T	P	X	A
DH-3, 128.5 <sup>m</sup>		Sludge												
129.1 <sup>m</sup>		Hornblende quartz porphyry					+	+						

Appendix 1-2

Microscopic Observation in Thin Sections

(1) Sillimanite-biotite gneiss

1.	Sample No.	Locality	Color/Color index	Rock name
	DH-3, (14.3 <sup>m</sup> )	DH-3	40 - 50	Biotite gneiss
	DH-2, (30.5 <sup>m</sup> )	DH-2	40 - 50	Sillimanite-biotite gneiss
	112902	B-2	50	Sillimanite-muscovite-biotite gneiss

2. Observation of handspecimen

This rock is melanocratic, and gneissose texture is remarkable. Micro-foldings can be observed in the sample of DH-3.

3. Constituent minerals

Persistent minerals : quartz, plagioclase, biotite  
Other minerals : sillimanite, potash feldspar, muscovite  
Accessory minerals : chlorite, sphene, apatite, opaque mineral, sericite

4. Microscopic observation

Major constituents are quartz, plagioclase and biotite, and they are holocrystalline and show schistose texture under the microscope. Quartz is granular or leuticular and shows mosaic texture in the thin section of DH-3. Plagioclase is anhedral or subhedral, and shows albite twinning and occurs with quartz and biotite and so on. The pleochroism of most biotite changes from pale brown

to brown, but from brown to reddish brown in the thin section of 112902.

Sillimanite occurs aciculary among crystals of quartz, plagioclase and potassium feldspars.

In the thin section of 112902, a small amount of potassium feldspar can be observed and quartz, biotite and sillimanite are included in potassium feldspar, and a small amount of rectangular or acicular crystals of muscovite occurs radially.

(2) Biotite-augite - (hornblende) gneiss

1.	Sample No.	Locality	Color/ Color index	Rock name
	102712	B-3	10 - 15	Augite-hornblende -biotite gneiss
	102714	B-3	1	Diallage-augite gneiss (silicified)
	110404	A-2	15	Biotite-augite gneiss
	010101	C-1	30 - 40	Sillimanite-augite -muscovite-biotite gneiss

2. Observation of handspecimen

This rock changes from leucocratic to melanocratic in color. The sample of 102714 is very siliceous. Gneissose texture is observed remarkably in all samples.

3. Constituent minerals

Persistent minerals : quartz, plagioclase, augite

Other minerals : biotite, muscovite, hornblende,  
sillimanite, potash feldspar,  
diallage

Accessory minerals : apatite, sphene, tourmaline,  
graphite, epidote, zoisite,  
cristobalite, chlorite, sericite,  
zeolite

Melanocratic feature is caused by abundant biotite.

#### 4. Microscopic observation

Major constituents are quartz, plagioclase, biotite amphibole, augite and so on, and they are holocrystalline. Quartz is anhedral or subhedral and granular or lenticular.

In the thin section of 102714, a large amount of quartz is observed and most of them show wavy extinction. Plagioclase is anhedral or subhedral and usually shows albite twinning. And plagioclase often occurs with quartz.

A small amount of potash feldspar is observed in the thin sections of 102714 and 110404.

The pleochroism of biotite changes from yellowish brown to reddish brown. Biotite shows foliation, and often coexists with or includes opaque minerals. Amphibole can be identified as hornblende because its pleochroism changes from yellowish green to green, and it is subhedral and has the extinction angle ( $C \wedge Z$ ) of  $17^\circ$ . Augite is subhedral and has the extinction angle ( $C \wedge Z$ ) of  $40^\circ$  to  $45^\circ$ , and cleavages develops very well. In the thin section of 102714, diallages showing remarkable parting are comparatively abundant.

Besides, apatite, sphene, tourmaline, opaque minerals and zeolite can be observed in the thin section of 102712, and zeolite occurs in veinlets or druses.

Zoisite, epidote, cristobalite, and zeolite, all of which occur in veinlets, and sphene and carbonates are observed in the thin section of 102714, and bent, foliated graphite, sphene, apatite, epidote, and chlorite which is pale green and altered from biotite and shows weak interference color and is accompanied with small grains of sphene in 110404.

And in the thin section of 010101, aggregates of acicular sillimanite are observed mainly in quartz, and a small amount of radial or feathery muscovite and sericite-like minerals which occur at the marginal part of pyroxenes.

(3) Biotite-garnet gneiss

1.	Sample No.	Locality	Color/Color index	Rock name
	103103A	A-2	40	Biotite-garnet gneiss
	110408	A-2	white	Silicified muscovite-biotite-garnet gneiss
	122101	D-2	15	Spinel-garnet-sillimanite-biotite gneiss
	DH-1, (100.2 <sup>m</sup> )	DH-1	pale green	Brecciated biotite-garnet gneiss
	DH-1, (118.5 <sup>m</sup> )	DH-1	white	Silicified biotite-garnet gneiss
	DH-2, ( 68.4 <sup>m</sup> )	DH-2	40	Spinel-sillimanite-biotite-garnet gneiss



2. Observation of handspecimen

This rock changes from leucocratic to melanocratic in color and generally shows gneissose texture.

In the sample of 103103A, pyrrhotite and chalcopyrite are observed as disseminated minerals or veinlets.

Samples of 110408 and DH-1, (118.5m) are white, siliceous and show obscure gneissose texture.

Sample of DH-1, (100.2<sup>m</sup>) is pale green, rich in clay minerals and shows cataclastic texture.

3. Constituent minerals

Persistent minerals : quartz, plagioclase, garnet, biotite

Other minerals : sillimanite, spinel, potash feldspar, muscovite

Accessory minerals : graphite, sphene, rutile, opaque mineral, chlorite, sericite, adularia

Melanocratic feature is caused by abundant biotite flakes and/or opaque minerals.

4. Microscopic observation

Major constituents are quartz, plagioclase, garnet, biotite, etc., but in the thin section of 103103A, quartz can hardly be observed. Quartz has irregular form and vein-like or lenticular quartz is abundant in the thin sections of 110408 and DH-1, (118.5m). Plagioclase is subhedral or anhedral and usually shows albite twinning. Garnet is subhedral or anhedral and colorless and optical anomaly can not be

found. And in some cases, the crystals of garnet are broken in pieces.

The pleochroism of biotite changes from pale brown to reddish brown and biotite shows foliation and sometimes bending. In the thin sections of 122101 and DH-2, spinel being green and granular and sillimanite being acicular or rectangular are found.

As minor constituents, in 103103A, opaque minerals are comparatively abundant and a small amount of graphite, sphene and rutile is found, and opaque minerals are often accompanied with biotite which altered into chlorite.

Pale green chlorite is found abundantly, and it replaces biotite and it is found in the crystals of garnet in veinlets. A small amount of feathery or radial sericite is observed in the crystals of plagioclase. In 110408, sphene, opaque mineral, and ziosite, potash feldspar (adularia) both as vein minerals, a small amount of feathery sericite as altered mineral of plagioclase, and chlorite altered from biotite can be observed. In 122101, biotite alters into chlorite partially and is accompanied with opaque minerals, and a small amount of sericite is found at the marginal part of plagioclase and garnet.

In DH-1,(100.2m),opaque mineral, sphene, chlorite altered from biotite, feathery sericite in plagioclase, and carbonates as cementing mineral or vein mineral can be observed, and in DH-1,(118.5m), feathery sericite altered from a part of plagioclase, chlorite which replaces biotite, a lot of sphene, and potash feldspar (adularia) showing perthite, and in DH-2, aggregate of micro crystals of sericite which are maybe altered from feldspars, and veinlets of chlorite.

(4) Garnet-biotite-augite gneiss

1.	Sample No.	Locality	Color/Color index	Rock name
	102601	A-2	7 - 10	Augite- biotite- garnet gneiss (silicified)
	103104	A-2	30	Biotite- diopside- sillimanite- garnet gneiss
	112101	A-2	20	Biotite- muscovite- augite- sillimanite- garnet gneiss
	122005	D-2	10	Spinel- sillimanite- garnet-biotite- augite gneiss
	DH-1, (91.5 <sup>m</sup> )	DH-1	20	Augite- garnet- biotite gneiss
	DH-1, (111.6 <sup>m</sup> )	DH-1	black	Garnet- biotite- augite gneiss

2. Observation of handspecimen

This rock changes from leucocratic to melanocratic in color and shows gneissose texture.

Silicification is observed at the sample of 102601. Sample of DH-1, (111.6<sup>m</sup>) is black in color and crushed.

3. Constituent minerals

Persistent minerals : quartz, plagioclase, biotite, augite, garnet

Other minerals : muscovite, spinel, sillimanite, potash feldspar, diopside

Accessory minerals : sphene, graphite, apatite,  
chlorite, sericite, actinolite,  
diopside, opaque mineral

Melanocratic feature in 103104 is mainly caused by graphite.

#### 4. Microscopic observation

Major constituents are quartz, plagioclase, garnet, biotite, augite, and so on, and they are holocrystalline, showing remarkable gneissose texture. Quartz has irregular form and most of quartz grains are granular or lenticular.

Plagioclase is anhedral or subhedral and generally shows albite twinning. Garnet is colorless or pale pink and has granular or irregular form. The pleochroism of biotite changes from brown to reddish brown. Pyroxene is considered to be clinopyroxene which is pale green and has the extinction angle ( $C \wedge Z$ ) of  $40^\circ$ . In the thin section of 122005, aggregates of green granular spinels are observed.

As altered minerals, in 103104, feathery sericite can be found as the partial replacement of plagioclase or in veinlets, and in all of 102601, 112101, 22005 and DH-1, ( $111.6^m$ ), chlorite which is altered from biotite, garnet, pyroxene, in veinlets, and in DH-1, ( $111.6^m$ ), diopside-like minerals in veinlet.

#### (5) Biotite-hornblende schist

1.	Sample No.	Locality	Color/Color index	Rock name
	111708	B-2	50	Biotite-hornblende schist



(6) Diopside-hornblende-biotite schist

1.	Sample No.	Locality	Color/Color index	Rock name
	102703	B-3	10 - 20	Diopside-hornblende-biotite schist

2. Observation of handspecimen

This rock is leucocratic and schistosity is remarkable.

3. Constituent minerals

quartz, plagioclase, biotite, hornblende, diopside, opaque mineral, sphene, apatite

4. Microscopic observation

This rock is holocrystalline and schistose texture can be observed.

Quartz both granular and lenticular is abundant, and crystals of quartz are clear. Plagioclase is anhedral, small, cementing material and generally shows albite twinning. Crystals of biotite showing the pleochroism from pale yellowish brown to yellowish brown are arranged in parallel to schistosity. Amphibole showing the pleochroism from pale green to pale yellowish brown is subhedral, and cleavages develop very well. And it is identified to be hornblende which has the extinction angle ( $C \wedge Z$ ) of about  $26^\circ$ . Diopside is colorless, subhedral and long rectangular and has the extinction angle ( $C \wedge Z$ ) of about  $45^\circ$ . Opaque minerals are accompanied with mafic minerals. A small amount of sphene and apatite is found sporadically.

(7) Biotite-diopside-quartz schist

1.	Sample No.	Locality	Color/Color index	Rock name
	102708	B-3		Biotite- diopside- quartz schist

2. Observation of handspecimen

This rock is gray in color and siliceous.

Banded structure due to fine-grained mafic minerals can be observed.

3. Constituent minerals

quartz, plagioclase, diopside, biotite, sphene, opaque mineral

4. Microscopic observation

A large amount of quartz and clinopyroxene and a small amount of plagioclase and biotite are constituents, and they are holocrystalline under the microscope. There are two types of quartz grains : one, fine-grained and granular, and the other, coarse-grained and lenticular, and they are arranged in parallel with each other.

Plagioclase shows remarkable albite twinning and coexists with quartz. Clinopyroxene is granular or long rectangular and is identified to be diopside which has the extinction angle ( $C \wedge Z$ ) smaller than  $40^\circ$ . A small amount of biotite showing pleochroism from pale yellowish brown to reddish brown is found. A small amount of sphene accompanied with biotite and clinopyroxene is observed.

Opaque minerals are found sporadically.

(8) Epidiorite

1.	Sample No.	Locality	Color/Color index	Rock name
----	------------	----------	-------------------	-----------

	DH-1,(38.0 <sup>m</sup> )	DH-1	40	Epidiorite
--	---------------------------	------	----	------------

2. Observation of handspecimen

This rock is melanocratic, massive and compact.  
Veinlets of quartz can be observed.

3. Constituent minerals

plagioclase, quartz, augite, biotite, garnet

Accessory and alteration minerals :

quartz, chlorite, allanite, zeolite,  
apatite, opaque mineral, amphibole

4. Microscopic observation

Major constituents are plagioclase, quartz, clinopyroxene, biotite, garnet etc.

Holocrystalline under the microscope and show graphic texture. Plagioclase is anhedral or subhedral and shows remarkable albite twinning.

There are two kinds of quartz grains : one, it shows graphic texture with plagioclase and pyroxene etc., the other, lenticular or vein-like quartz grains. Pyroxene is augite, which is small, pale green, granular, waterdrop-like and rectangular. And a part of pyroxene is altered into green amphibole. Biotite is a foliated crystal showing



the pleochroism from brown to reddish brown. Garnet is pink and has inclusions of plagioclase, pyroxene etc. , in some cases. Besides, the following minerals are sporadically found : chlorite altered from pyroxene, allanite showing the pleochroism from pinky red to pale pink, apatite, opaque minerals which are replacements mainly of mafic minerals and zeolite as vein minerals.

(9) Biotite granite

1.	Sample No.	Locality	Color/Color index	Rock name
	102303	B-2	7	Biotite granite
	112502.	B-3	15	Biotite granite
	DH-3, (34.8 <sup>m</sup> )	DH-3	10	Hornblende-biotite granite

2. Observation of handspecimen

This rock is leucocratic, medium-grained, equigranular and holocrystalline.

3. Constituent minerals

Major constituents : quartz, potash feldspar, plagioclase, biotite, (hornblende)

Accessory and alteration minerals :

sphene, apatite, opaque mineral, chlorite, carbonate mineral, allanite

4. Microscopic observation

Quartz is anhedral and clear. Potassium feldspar is anhedral or subhedral, mostly large and generally shows carlsbad twin and perthite texture, and includes biotite, plagioclase and so on in cases.

Plagioclase is usually subhedral and small, and shows albite twinning. In the thin section of DH-3, zonal structure can be observed, and thin mantle of potassium feldspar is often found. Biotite shows the pleochroism from pale yellowish brown to brown, and in many cases alters into chlorite. In DH-3, a small amount of green hornblende can be observed.

Sphene, apatite and opaque minerals occur commonly, and in 102303, a comparatively large amount of opaque minerals occurs sporadically. In 102303 and DH-3, biotite or amphibole alters partially into chlorite in many cases. Veinlets of carbonates occur in 102303 and 112502, and long rectangular allanite in DH-3.

(10) Biotite-hornblende quartz porphyry

1.	Sample No.	Locality	Color/Color index	Rock name
	DH-3, (114 3 <sup>m</sup> )	DH-3	pale green 10	Biotite-hornblende quartz porphyry

2. Observation of handspecimen

This rock is pale green in color, compact and hard, and shows porphyritic texture.

3. Constituent minerals

quartz, plagioclase, hornblende, biotite, chlorite, epidote, opaque mineral

4. Microscopic observation

Porphyritic textures can be observed under the microscope. Phenocrysts are quartz, plagioclase, amphibole, biotite.

Groundmass is composed of quartz and plagioclase and shows micrographic or myrmekitic texture. Most of quartz grains are corroded magmatically, and halo showing the micrographic intergrowth of quartz and feldspar can be observed at the marginal part of quartz crystals. Plagioclase, in general, shows albite twinning. Amphibole mostly alters into chlorite and epidote and also biotite mostly alters into chlorite.

Pyrite is found sporadically as opaque mineral.

(11) Peridotite

1.	Sample No.	Locality	Color/Color index	Rock name
	111306	A-1	dark gray	Garnet bearing augite peridotite (Garnet bearing wehrite)

2. Observation of handspecimen

This rock is dark gray in color, massive and compact.

3. Constituent minerals

augite, garnet, olivine, diopside, serpentine, diallage, opaque mineral

4. Microscopic observation

Though this rock is holocrystalline, large crystal (about 0.5 mm) of clinopyroxene and garnet, and small crystals (about 0.1 mm) of abundant olivine, few pyroxene, opaque minerals, are observed, and porphyritic texture can be seen.

Large crystals : subhedral, colorless augite and brown garnet are main constituents, and pyroxene is partially altered into diallage.

Small crystals : olivine is colorless and has irregular form and is serpentinized along cracks and the remained olivine is granular. Most of pyroxene are colorless but a very small amount of pyroxene is pale pink. All these pyroxenes are diopside. A small amount of brown garnet and opaque mineral is found sporadically.

Vein mineral : Serpentine which forms along cracks in the crystal of olivine occurs in net work.

(12) Gabbro

1.	Sample No.	Locality	Color/Color index	Rock name
	123010	D-3	50	Hypersthene-augite-hornblende-biotite- quartz gabbro
	010107	C-2	50	Hornblende- augite-biotite- quartz gabbro

2. Observation of handspecimen

This rock is dark gray in color, coarse-grained and holocrystalline.

3. Constituent minerals

Persistent minerals : plagioclase, quartz, biotite, augite, hornblende

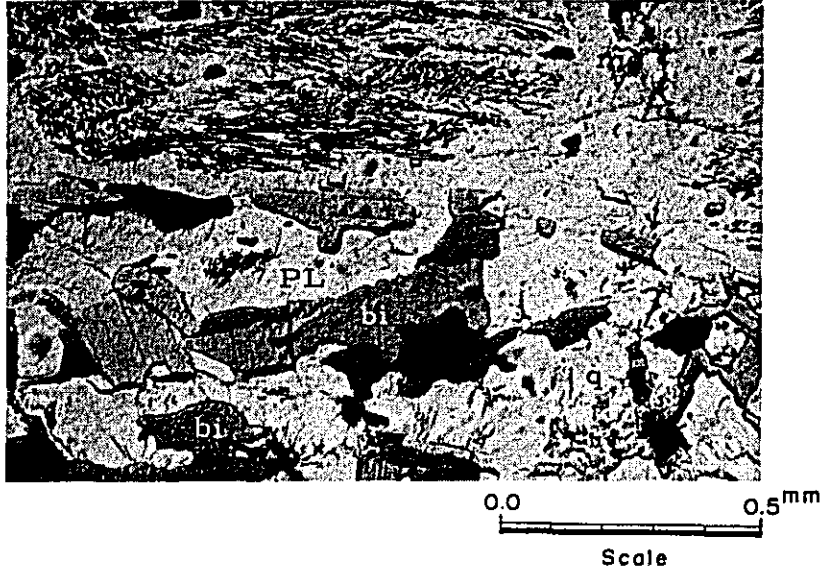
Other minerals : hypersthene, apatite, opaque mineral

4. Microscopic observation

Main constituents are plagioclase, quartz, biotite, augite, amphibole and so on, and graphic texture can be observed. Plagioclase is abundant and many crystals of it shows albite twinning. A small amount of quartz is found as cementing material, and in 010107, waterdrop-like or wedge-like quartz, is included in the crystal of plagioclase.

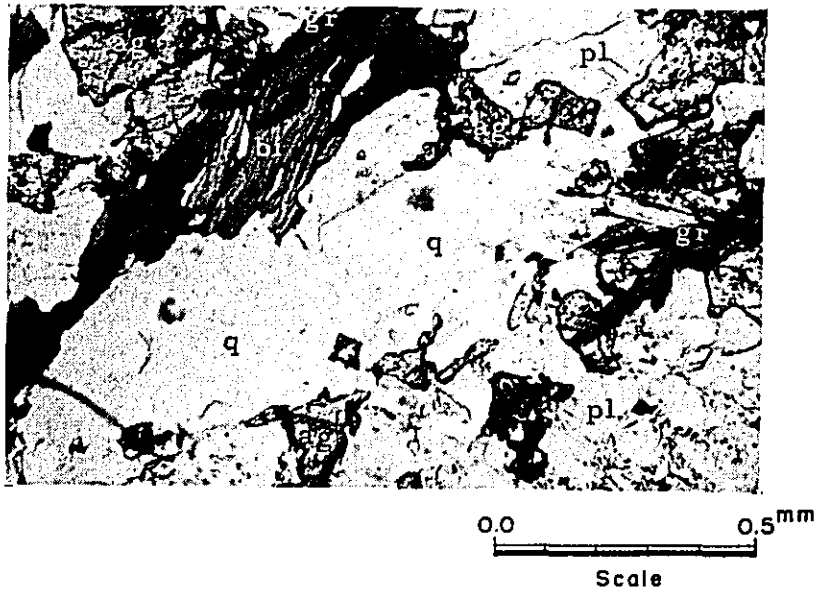
Biotite, showing the pleochroism from yellowish brown to reddish brown, coexists with plagioclase and clinopyroxene. Clinopyroxene is anhedral or subhedral, and is augite which has the extinction angle ( $C \wedge Z$ ) of about  $40^\circ$ . And in 010107, waterdrop-like augite is included in the crystal of plagioclase in many cases. Amphibole, showing the pleochroism from pale green to green, is hornblende which has the extinction angle ( $C \wedge Z$ ) of about  $15^\circ$ .

In 123010, a small amount of subhedral diopside showing the pleochroism from pale green to pale pinky red, and apatite can be observed. A small amount of opaque minerals is found and they, in many cases, are accompanied with mafic minerals.



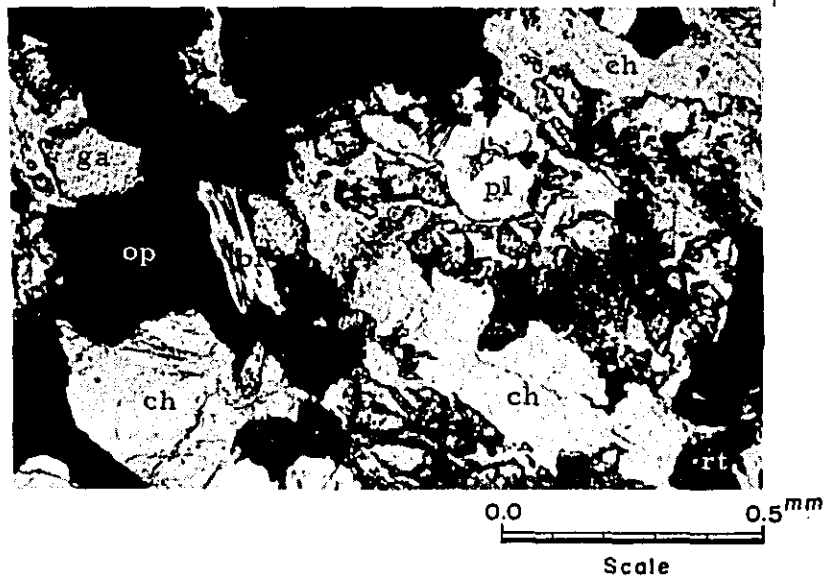
PL-1 Sillimanite-muscovite-biotite gneiss (Sample No. 112902)

si : sillimanite, mc : muscovite, bi : biotite,  
pl : plagioclase, q : quartz



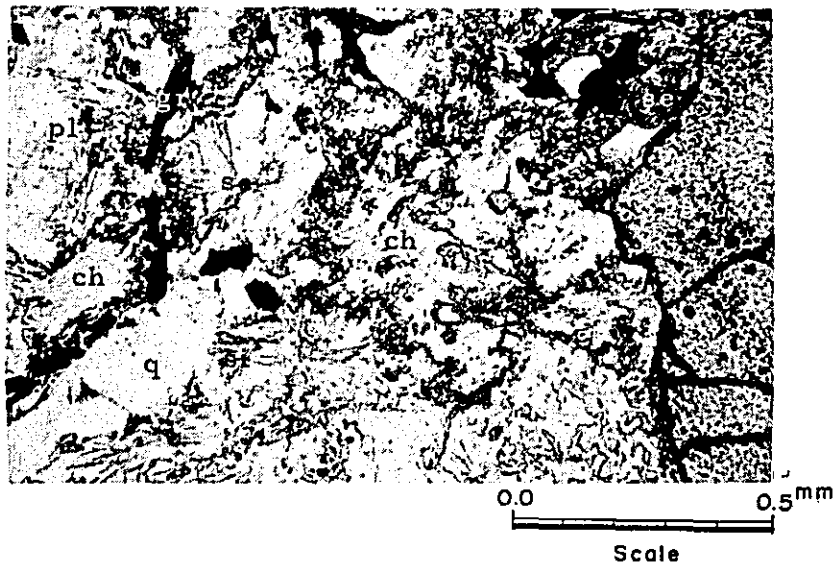
PL-2 Biotite-augite gneiss (Sample No. 110404)

bi : biotite, ag : augite, pl : plagioclase,  
q : quartz, gr : graphite



PL-3 Biotite-garnet gneiss (Sample No. 103103A)

ch : chlorite, op : opaque mineral,  
pl : plagioclase, rt : rutile, ga : garnet



PL-4 Spinel-sillimanite-biotite-garnet gneiss (Sample No. DH-2, 68.4<sup>m</sup>)

ga : garnet, se : sericite, ch : chlorite,  
gr : graphite, si : sillimanite, q : quartz,  
pl : plagioclase



0.0 0.5<sup>mm</sup>  
Scale

PL-5 Augite-garnet-biotite gneiss (Sample No. DH-1, 91.5<sup>m</sup>)  
ag : augite, ga : garnet, bi : biotite,  
op : opaque mineral, pl : plagioclase, q : quartz

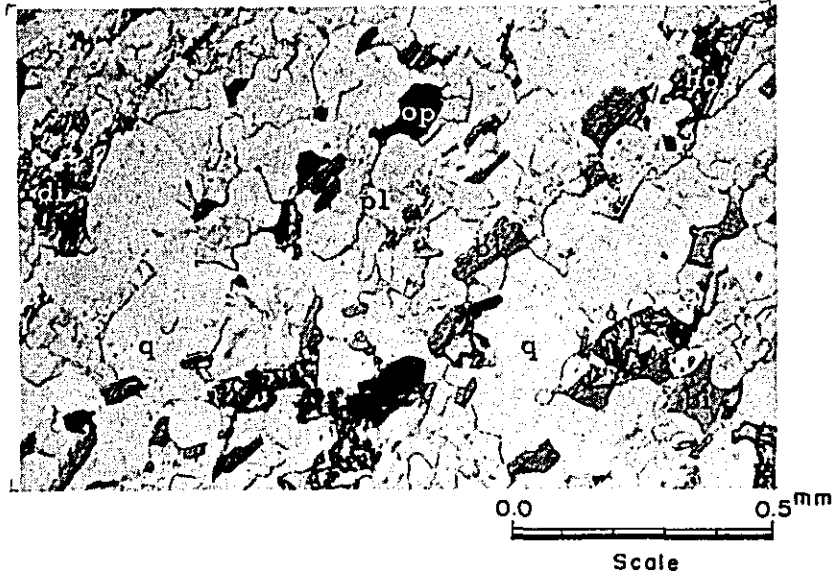


0.0 0.5<sup>mm</sup>  
Scale

PL-6 Garnet-hornblende-biotite schist (Sample No. 111803)

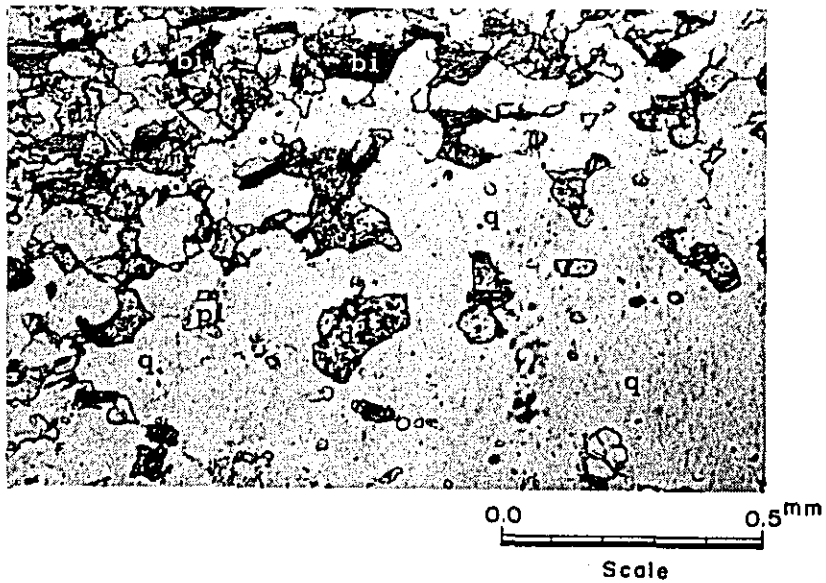
ga : garnet, ho : hornblende, bi : biotite,  
q : quartz, pl : plagioclase





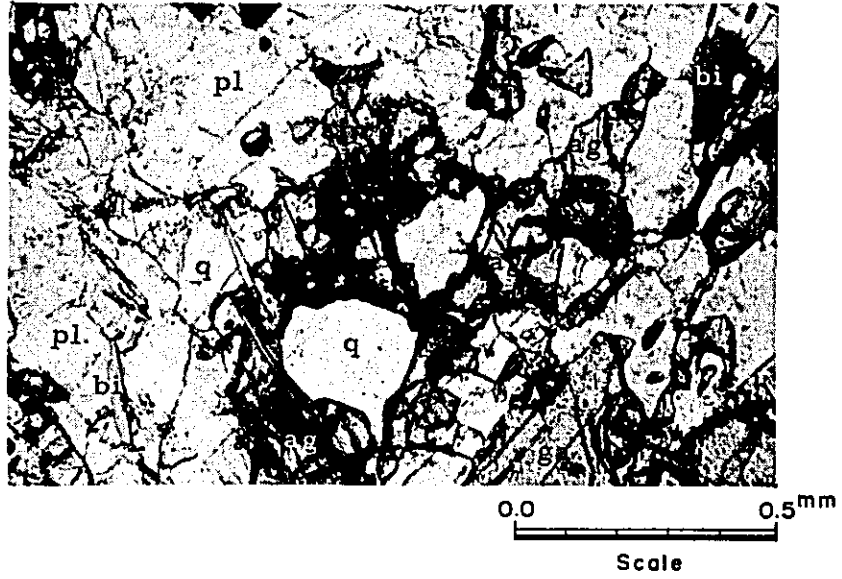
PL-7 Diopside-hornblende-biotite schist (Sample No. 102703)

di : diopside, ho : hornblende, bi : biotite,  
 op : opaque mineral, pl : plagioclase, q : quartz

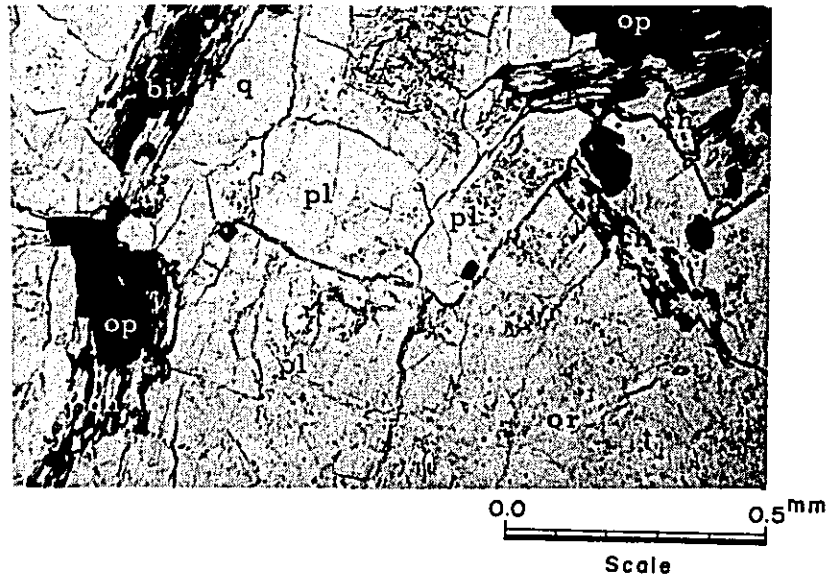


PL-8 Biotite-diopside-quartz schist (Sample No. 102708)

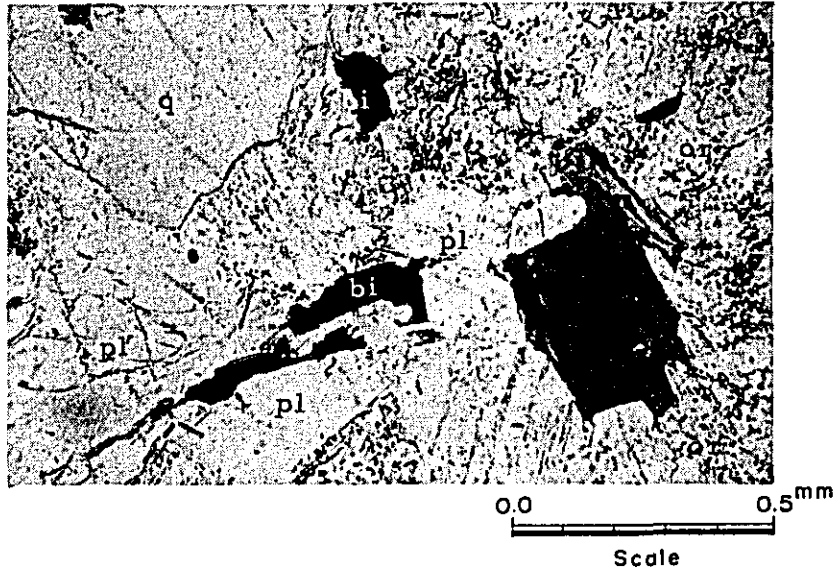
bi : biotite, di : diopside, q : quartz,  
 pl : plagioclase



PL-9 Epidiorite (Sample No. DH-1, 38.0<sup>m</sup>)  
 ag : augite, ho : hornblende, bi : biotite,  
 ga : garnet, q : quartz, pl : plagioclase

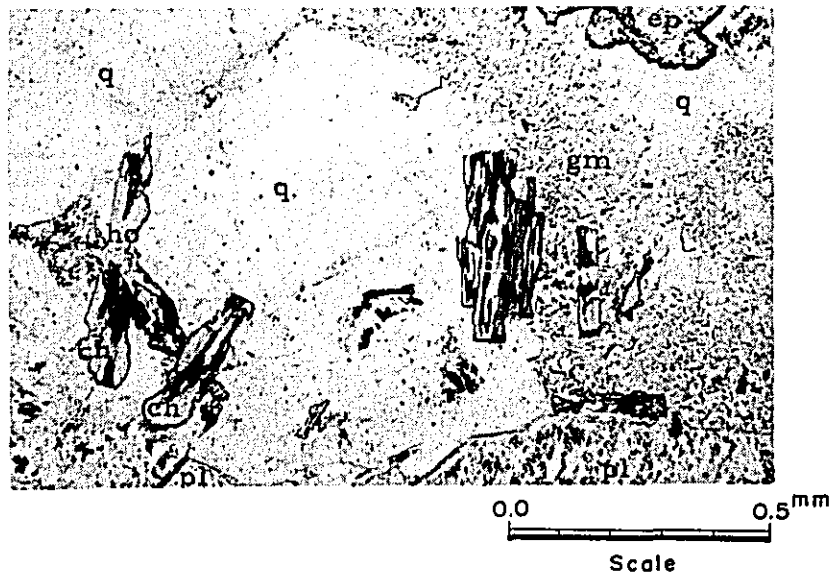


PL-10 Biotite granite (Sample No. 102303)  
 bi : biotite, ch : chlorite, op : opaque mineral,  
 pl : plagioclase, q : quartz, or : orthoclase



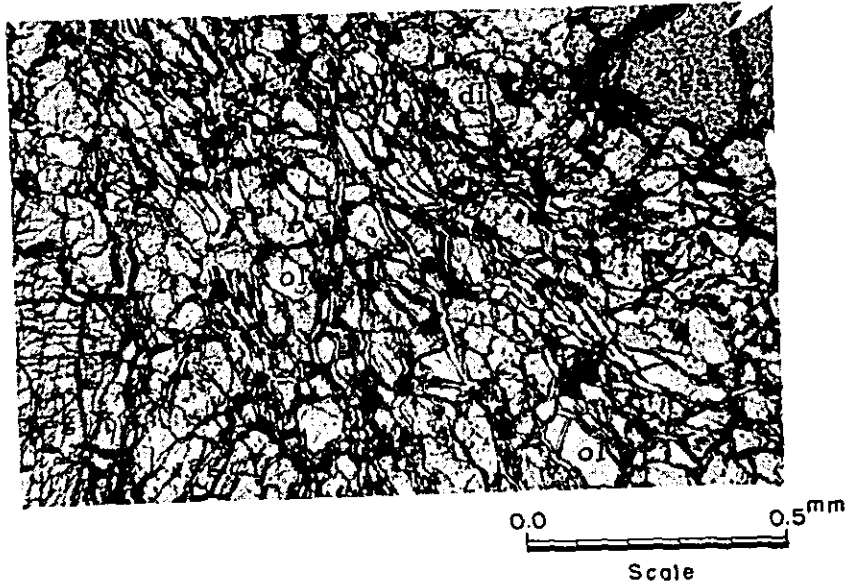
PL-11 Biotite granite (Sample No. 112502)

bi : biotite, q : quartz, or : orthoclase,  
 pl : plagioclase



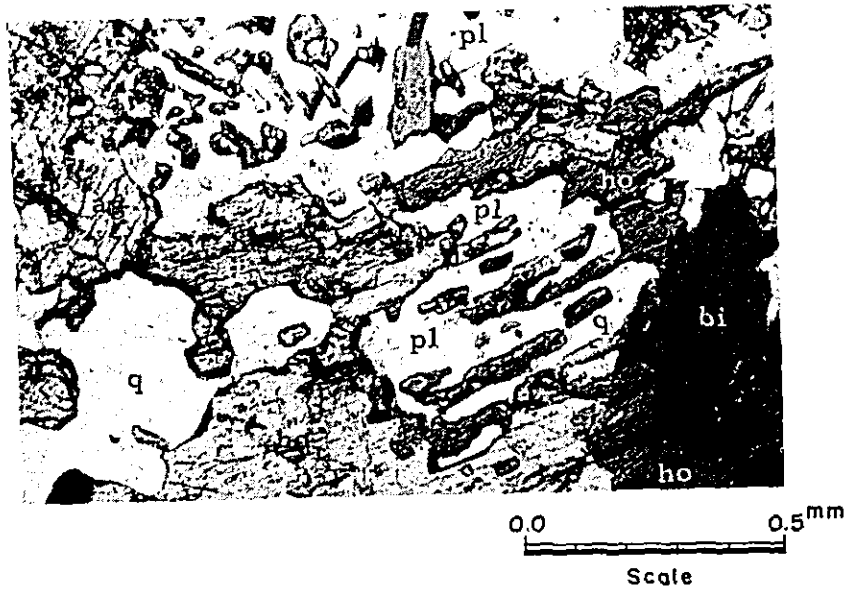
PL-12 Biotite-hornblende quartz porphyry (Sample No. DH-3, 114.3<sup>m</sup>)

bi : biotite, ho : hornblende, ch : chlorite,  
 pl : plagioclase, q : quartz, ep : epidote,  
 gm : groundmass



PL-13 Garnet bearing augite peridotite (Sample No. 111306)

sp : serpentine, ag : augite, ga : garnet,  
di : diopside, ol : olivine



PL-14 Hornblende-augite-biotite-quartz gabbro (Sample No. 010107)

ho : hornblende, ag : augite, bi : biotite,  
q : quartz, pl : plagioclase

Appendix 1-3. Mineral Assemblages of Metamorphic Rocks in Thin Sections

Sample Number	Rock Name	Quartz	Plagioclase	K-feldspar	Biotite	Muscovite	Garnet	Augite	Diallage	Diopside	Hypersthene	Hornblende	Actinolite	Spinel	Sillimanite	Sphene	Rutile	Tourmaline	Apatite	Graphite	Epidote	Zoisite	Allanite	Adularia	Sericite	Chlorite	Zeolite	Opaque mineral	Carbonates	Cristobalite								
DH-3, 14.3m	Biotite gneiss	+	+	+	+											+			+							+												
DH-2, 30.5m	Sillimanite-biotite gneiss	+	+	+	+										+										+													
112902	Sillimanite-muscovite-biotite gneiss	+	+	+	+	+									+										+													
111708	Biotite-hornblende schist	+	+	+	+							+																										
102708	Biotite-diopside-quartz schist	+	+	+	+			+		+																												
102703	Diopside-hornblende-biotite schist	+	+	+	+			+				+																										
102712	Augite-hornblende-biotite gneiss	+	+	+	+			+				+														+												
010101	Sillimanite-augite muscovite-biotite gneiss	+	+	+	+			+																	+													
102714	Diallage-augite gneiss	+	+	+	+			+																														
110404	Biotite-augite gneiss	+	+	+	+			+																														
111803	Garnet-hornblende-biotite schist	+	+	+	+																																	
110408	Silicified muscovite-biotite-garnet gneiss	+	+	+	+																																	
DH-1, 118.5m	Silicified biotite-garnet gneiss	+	+	+	+																																	
103103A	Biotite-garnet gneiss	+	+	+	+																																	
DH-1, 100.2m	Brecciated biotite-garnet gneiss	+	+	+	+																																	

Appendix 1-3. Mineral Assemblages of Metamorphic Rocks in Thin Sections (Cont'd)

Sample Number	Rock Name	Quartz	Plagioclase	K-feldspar	Biotite	Muscovite	Garnet	Augite	Diallage	Dioptside	Hyperssthene	Hornblende	Actinolite	Spinel	Sillimanite	Sphene	Rutile	Tourmaline	Apatite	Graphite	Epidote	Zoisite	Allanite	Adularia	Sericite	Chlorite	Zeolite	Opaque mineral	Carbonates	Cristobalite								
122101	Spinel-garnet-sillimanite-biotite gneiss	+	+	+	+	+	+	+						+	+										+	+	+	+	+	+								
DH-2, 68.4 <sup>m</sup>	Spinel-sillimanite-biotite-garnet gneiss	+	+	+	+	+	+	+						+	+										+	+	+	+	+	+	+							
DH-1, 38.0 <sup>m</sup>	Garnet-biotite-augite diorite	+	+	+	+	+	+	+				+								+																		
103104	Biotite-dioptside-sillimanite-garnet gneiss	+	+	+	+	+	+	+	+	+					+										+	+	+	+	+	+	+	+						
122005	Spinel-sillimanite-garnet-biotite-augite gneiss	+	+	+	+	+	+	+	+	+				+	+										+	+	+	+	+	+	+	+	+					
DH-1, 111.6 m	Garnet-biotite-augite gneiss	+	+	+	+	+	+	+	+	+										+																		
DH-1, 91.5m	Augite-garnet-biotite gneiss	+	+	+	+	+	+	+	+	+																												
102601	Augite-biotite-garnet gneiss	+	+	+	+	+	+	+	+	+										+																		
112101	Biotite-muscovite-augite-sillimanite-garnet gneiss	+	+	+	+	+	+	+	+	+										+																		

Appendix 1-4. Mineral Assemblages Determined by X-ray Diffraction

Sample No.	Quartz	Feldspar	Amphibole	Biotite or Muscovite	Sericite	Chlorite	Montmorillonite	Zeolite (Laumontite)	Calcite	Others
102713	+++	++	+	-	-	+++	(+)	++	-	
103105	++	++	-	-	-	+	-	++	-	3.06 Å mineral
111501	++	++	-	-	+++	++	-	-	-	
111505	++	++	-	+	-	+++	(+)	(+)	-	
112006	+++	++	-	-	-	++	+++	-	-	
DH-1, 48.5m	+++	+++	+	+	-	-	+	-	-	
55.4m	++	+++	-	-	-	++	-	-	-	
91.5m	++	++	-	-	-	+++	-	-	-	
100.2m	+++	+	-	-	(+)	+++	-	+	-	
107.0m	+	-	+	-	-	-	+++	+	+	3.08 Å mineral
111.6m	++	-	-	-	-	++	++	+++	-	
118.5m	+++	+	-	-	+	-	-	+++	-	
DH-2, 82.0m	++	++	-	++	-	+++	(+)	(+)	-	
87.0m	+	-	++	+	-	+	+++	(+)	-	2.99 Å mineral 3.14 Å mineral
95.7m	+	+	-	+	-	+++	-	+	-	
109.0m	++	+++	+++	(+)	-	+++	-	-	-	
120.0m	++	+++	+	++	-	+++	-	+	-	
130.0m	++	++	+++	++	-	+++	-	+	-	

Notes :      +++ Abundant      ++ Common      + Little      (+) Minor

Appendix 1-5

Microscopic Observation of Polished Sections



(1) 102303 (Biotite granite)

Mineral Assemblage : pyrite, magnetite, chalcopyrite

Pyrite : Euhedral small crystals (0.1 - 0.2 mm in diameter) are impregnated.

Thin veinlets of pyrite are rarely observed. In some places, magnetite is replaced by pyrite.

Magnetite : A bit of magnetite is remained in pyrite crystals. Most crystals are fine grained, irregular shaped and are enclosed in pyrite.

Chalcopyrite : Minor amount of granular crystals of 0.05 mm size is observed.

In some places, chalcopyrite coexists with pyrite.

(2) 103103-A (Garnet-biotite gneiss)

Mineral Assemblage : marcasite, rutile, pyrrhotite, chalcopyrite, graphite

Marcasite : Large amount of marcasite shows irregular shaped form of 0.1 to 0.5 mm (maximum 1.5 mm) in size.

Colloform texture is distinctly developed in marcasite crystals. In some places, a bit of pyrrhotite is included in marcasite grains.

Chalcopyrite : Small amount of chalcopyrite is observed.

It shows irregular shape of less than 0.1 mm in size.

Coexistence of chalcopyrite with pyrrhotite which is altered to marcasite is common.

Rutile : Large amount of rutile of lod-like shape of 0.1 to 0.5 mm size is found.

Graphite : Relatively large amount of graphite exists.  
It has lamellae texture of 0.1 to 0.5 mm in length.

(3) 103103-B (Garnet biotite gneiss)

Mineral Assemblage : pyrrhotite, rutile, ilmenite, marcasite,  
chalcopyrite, graphite

Pyrrhotite : Large amount of elongated-shaped pyrrhotite crystals  
of 0.1 to 1.0 mm in length is observed. Rim of the crystals is  
altered to marcasite.

Chalcopyrite : Chalcopyrite assumes granular shape of 0.05 mm  
in diameter.

Coexistence with pyrrhotite is common.

Rutile, Ilmenite : They are 0.05 to 0.1 mm in size, and commonly  
coexist with each other. Exsolution texture of rutile from  
ilmenite is observed.

Graphite : abundant.

Weak preferred orientation of mineral grains is observed.

(4) 110404 (Biotite gneiss)

Mineral Assemblage : pyrrhotite, rutile, chalcopyrite, graphite

Pyrrhotite : Small amount of irregular shaped pyrrhotite crystals  
of 0.1 mm size is disseminated.

Rutile : Small amount of rutile crystals of 0.05 x 0.1 - 0.2 mm  
size is dispersed.

Chalcopyrite : Minor amount of chalcopyrite grains of 0.01 -  
0.05 mm size coexists with pyrrhotite.

Graphite : Large amount of lamellae graphite is observed.

(5) 111802 (Biotite schist)

Mineral Assemblage : ilmenite, pyrite, marcasite, chalcopyrite

Ilmenite : Large amount of ilmenite grains of 0.05 mm size is observed.

They are orientated in sub-parallel with schistosity.

Pyrite : Pyrite crystals show euhedral form of 0.05 - 0.2 mm size and are roughly orientated in sub-parallel with schistosity.

Marcasite : Marcasite looks like to be altered partially from pyrite.

Chalcopyrite : Minor amount of chalcopyrite (0.05 mm in size) is coexisted with pyrite.

(6) 112101 (Garnet-biotite gneiss)

Mineral Assemblage : pyrrhotite, rutile, ilmenite, chalcopyrite, graphite

Pyrrhotite : Irregular shaped pyrrhotite crystals of 0.05 - 0.2 mm in size are abundant, some of them being coexisted with rutile.

Rutile, Ilmenite : Abundant. Ilmenite is partially exsolved to rutile.

Chalcopyrite : Small amount of fine grained (0.01 - 0.02 mm in size) granular crystals of chalcopyrite is observed.

(7) 120402 (Garnet-biotite gneiss)

Mineral Assemblage : ilmenite, rutile, pyrrhotite, pyrite, chalcopyrite

Pyrrhotite, Pyrite : Granular crystals of 0.05 - 0.1 mm in size are disseminated.

Chalcopyrite : Chalcopyrite grain of 0.05 x 0.1 mm in size is rarely found.

Ilmenite : Grains of about 0.05 x 0.2 mm size are dispersed.

Rutile : Small amount of rutile crystals less than 0.05 mm in size is observed.

Graphite : Not present.

(8) 122704 (Biotite-garnet gneiss)

Mineral Assemblage : pyrrhotite, pyrite, ilmenite, rutile, chalcopyrite

Pyrrhotite, Pyrite : The crystals of 0.05 - 0.1 mm in size are disseminated.

Chalcopyrite : Very fine grained chalcopyrite is coexisted with pyrrhotite.

Graphite : Not present.

(9) 122809 (Garnet-biotite gneiss)

Mineral Assemblage : pyrrhotite, ilmenite, marcasite  
Small amount of pyrrhotite of less than 0.05 mm in size is disseminated.

A part of pyrrhotite crystals is altered to marcasite.

Ilmenite crystals of 0.05 - 0.1 mm in size are disseminated.

Weak preferred orientation of mineral in sub-parallel to gneissosity is observed.

(10) 010105

Mineral Assemblage : marcasite, pyrrhotite, rutile, ilmenite

Small amount of pyrrhotite grains of 0.1 x 0.2 mm in size exists. They are oriented and mostly altered to marcasite. Rutile of less than 0.05 mm in size and minor amount of ilmenite are dispersed.

(11) DH-3(102.0<sup>m</sup>)(Biotite-hornblende quartz porphyry)

Mineral Assemblage : pyrite

A bit of pyrite of 0.5 mm in size is observed.

Appendix 1-6

Chemical Analyses of Sulfides-disseminated Rock Samples

Sample No.		Cu %	S %	Sample No.		Cu %	S %
1	102403	0.02	1.42	16	122604	<0.01	0.47
2	102601	<0.01	0.25	17	122702	<0.01	0.22
3	103103A	0.07	5.47	18	122704	<0.01	0.19
4	103103B	0.03	2.78	19	122809	<0.01	0.40
5	103104	0.01	0.70	20	123011	0.01	1.80
6	111304A	<0.01	1.08	21	123013	<0.01	0.36
7	111305	0.02	1.49	22	010103	0.02	0.85
8	111802	0.02	1.94	23	010105	0.01	1.30
9	112001	<0.01	0.13	24	DH-1, 38.0 <sup>m</sup>	<0.01	0.16
10	112004	0.01	0.25	25	DH-1, 91.5 <sup>m</sup>	<0.01	0.14
11	112101	0.02	1.60	26	DH-2, 68.4 <sup>m</sup>	0.02	1.30
12	120204	0.01	0.36	27	DH-2, 95.7 <sup>m</sup>	<0.01	0.28
13	120402	<0.01	0.32	28	DH-2, 130.0 <sup>m</sup>	<0.01	0.19
14	122005	<0.01	0.32	29	DH-3, 69.5 <sup>m</sup>	<0.01	0.33
15	122203	<0.01	0.13	30	DH-3, 114.3 <sup>m</sup>	<0.01	0.09

Appendix 2

Copper Contents of Geochemical Soil Samples

Abbreviations :

SL : Soil  
 SN : Sandy  
 B : Brown  
 Y : Yellow  
 G : Grey

No.	Sample No.	Nature of Sample	Color	Cu (p. p. m.)	No.	Sample No.	Nature of Sample	Color	Cu (p. p. m.)
1	1 - 1	SL	B	10	46	37	SN	B	30
2	3	SL	B	13	47	39	SN	B	5
3	5	SL	B	10	48	41	SN	B	8
4	7	SL	B	18	49	4 - 1	SL	B	40
5	9	SL	G	33	50	3	SL	B	20
6	11	SL	B	18	51	4 - 5	SL	B	60
7	13	SL	B	10	52	7	SL	G	75
8	15	SL	G	13	53	5 - 3	SL	B	25
9	17	SL	B	23	54	5	SL	B	18
10	19	SL	G	28	55	7	SL	B	55
11	21	SL	B	57	56	9	SL	G	3
12	23	SL	B	38	57	11	SL	B	12
13	25	SL	B	60	58	13	SL	B	10
14	27	SL	Y	40	59	15	SL	G	50
15	29	SL	G	73	60	17	SL	B	50
16	31	SL	B	30	61	19	SL	B	40
17	33	SL	B	10	62	21	SL	B	25
18	35	SL	G	32	63	23	SN	B	20
19	37	SL	B	10	64	25	SL	B	3
20	39	SL	B	40	65	6 - 1	SN	Y	60
21	41	SL	G	40	66	3	SN	B	45
22	2 - 1	SN	B	20	67	5	SL	B	30
23	3	SL	B	5	68	7	SN	B	27
24	5	SN	G	10	69	9	SN	B	8
25	7	SN	G	3	70	11	SL	B	30
26	9	SL	Y	5	71	13	SN	B	48
27	11	SL	B	18	72	15	SL	B	63
28	3 - 1	SN	B	10	73	17	SN	B	30
29	3	SN	B	20	74	19	SN	B	30
30	5	SL	B	10	75	21	SN	G	65
31	7	SL	B	10	76	23	SN	Y	25
32	9	SL	B	35	77	25	SN	G	35
33	11	SL	B	40	78	27	SN	G	40
34	13	SL	B	60	79	29	SL	B	25
35	15	SL	B	40	80	31	SL	B	40
36	17	SL	Y	30	81	33	SL	B	25
37	19	SL	B	60	82	35	SL	B	45
38	21	SL	B	50	83	37	SN	B	33
39	23	SL	B	3	84	7 - 2	SL	B	40
40	25	SN	B	35	85	4	SL	B	48
41	27	SN	B	45	86	6	SL	Y	45
42	29	SN	B	55	87	8	SN	B	8
43	31	SN	B	30	88	T - 1	SN	B	45
44	33	SN	B	10	89	3	SN	B	35
45	35	SN	B	20	90	5	SN	Y	70

No.	Sample No.	Nature OF SAMPLE	Color	Cu (p. p. m.)	No.	Sample No.	Nature of Sample	Color t	Cu (p. p. m.)		
91		2'	SN	B	48	151	19	SL	B	20	
92	8 -	3	SN	B	30	152	21	SL	G	15	
93		5	SL	B	50	153	23	SL	G	43	
94		7	SL	Y	40	154	25	SL	B	75	
95		9	SL	Y	40	155	12 -	1	SL	B	30
96		11	SL	Y	75	156		3	SL	G	45
97		13	SL	B	13	157		5	SL	G	20
98		15	SN	Y	10	158		7	SN	Y	20
99		17	SN	Y	40	159		9	SL	B	63
100		19	SN	G	55	160		11	SL	G	45
101	8 -	21	SL	B	60	161	12 -	13	SL	G	33
102	9 -	3	SL	G	23	162	13 -	1	SL	G	20
103		5	SL	B	25	163		3	SL	G	175
104		7	SL	G	35	164		5	SL	G	15
105		9	SL	B	30	165		7	SL	B	20
106		11	SL	G	30	166		9	SL	G	13
107		13	SL	B	13	167		11	SL	Y	10
108		15	SL	G	10	168		13	SL	G	35
109		17	SL	B	13	169		15	SL	B	13
110		19	SL	G	3	170		17	SL	B	7
111		21	SL	B	3	171		19	SL	B	10
112		23	SL	G	13	172		21	SL	B	10
113		25	SL	B	5	173		23	SL	Y	13
114		27	SL	B	13	174		25	SL	G	8
115		29	SL	B	5	175		27	SL	B	40
116	10 -	1	SL	B	30	176		29	SL	Y	10
117		3	SL	Y	30	177	14 -	1	SL	Y	25
118		5	SL	B	25	178		3	SL	Y	15
119		7	SL	Y	25	179		5	SL	B	22
120		9	SL	B	40	180		7	SN	B	23
121		11	SL	G	40	181		9	SL	B	20
122		13	SL	B	50	182		11	SL	B	35
123		15	SL	Y	23	183		13	SN	B	23
124		17	SL	B	25	184		15	SL	Y	15
125		19	SN	B	20	185		17	SL	B	5
126		21	SN	G	33	186		19	SN	B	10
127		23	SN	B	10	187		21	SL	B	15
128		25	SL	G	55	188		23	SL	Y	35
129		27	SL	B	35	189		25	SN	B	20
130		29	SL	B	100	190		27	SN	B	50
131		31	SL	B	60	191		29	SL	B	60
132		33	SL	B	45	192		31	SL	B	13
133		35	SL	G	23	193		33	SN	Y	28
134		37	SL	G	3	194	15 -	1	SN	B	22
135		39	SL	B	40	195		3	SL	B	40
136		41	SL	B	35	196		5	SL	B	23
137		43	SL	B	50	197		7	SL	Y	13
138		45	SL	Y	150	198		9	SL	B	20
139		47	SL	Y	60	199	16 -	0	SL	B	23
140		49	SL	B	40	200		2	SL	B	23
141		51	SL	Y	35	201		4	SL	B	30
142	11 -	1	SL	B	15	202		6	SL	B	23
143		3	SL	G	15	203		8	SL	B	30
144		5	SL	G	15	204		10	SL	B	30
145		7	SL	Y	20	205		12	SL	G	23
146		9	SL	B	15	206		14	SL	B	23
147		11	SL	B	33	207		16	SL	B	33
148		13	SL	B	15	208		18	SL	B	23
149		15	SL	G	13	209		20	SL	B	23
150		17	SL	B	33	210		22	SL	B	20



No.	Sample No.	Nature of Sample	Color	Cu (p. p. m.)	No.	Sample No.	Nature of Sample	Color	Cu (p. p. m.)
211	24	SL	B	30	271	35	SL	B	40
212	26	SL	B	23	272	37	SL	B	63
213	28	SL	B	20	273	39	SL	B	20
214	30	SL	B	60	274	41	SL	B	35
215	32	SL	G	18	275	43	SL	B	33
216	34	SL	B	13	276	45	SL	B	23
217	36	SL	B	40	277	47	SL	G	43
218	38	SL	B	50	278	49	SL	B	28
219	40	SL	B	10	279	51	SL	G	43
220	17 - 0	SL	B	53	280	53	SL	G	45
221	17 - 1	SL	B	50	281	20 - 55	SL	B	35
222	3	SL	B	50	282	57	SL	G	50
223	5	SL	B	43	283	59	SL	G	53
224	7	SL	B	20	284	61	SL	G	40
225	9	SL	B	28	285	63	SL	B	60
226	11	SL	Y	20	286	65	SN	G	58
227	13	SL	B	33	287	67	SL	B	23
228	15	SL	B	30	288	69	SL	B	40
229	17	SL	B	63	289	71	SN	G	45
230	19 - 2	SL	Y	20	290	73	SL	G	70
231	4	SL	B	20	291	75	SL	B	10
232	6	SL	Y	28	292	77	SN	G	55
233	8	SL	B	40	293	79	SN	G	40
234	10	SL	B	13	294	81	SN	G	53
235	12	SL	B	10	295	83	SL	Y	80
236	14	SL	B	40	296	85	SN	G	60
237	16	SL	G	30	297	87	SL	Y	70
238	18	SL	B	50	298	89	SN	G	40
239	20	SL	B	40	299	21 - 0	SL	B	38
240	22	SL	G	30	300	2	SL	Y	30
241	24	SL	G	20	301	4	SL	B	30
242	26	SL	B	28	302	6	SL	B	33
243	28	SL	B	28	303	8	SL	Y	73
244	30	SL	B	8	304	10	SL	B	50
245	32	SL	B	30	305	12	SL	B	35
246	34	SL	B	20	306	14	SL	Y	50
247	36	SL	B	8	307	16	SL	Y	55
248	38	SL	B	8	308	18	SL	B	40
249	40	SL	B	15	309	20	SL	G	45
250	42	SL	B	10	310	22	SL	G	50
251	44	SL	B	13	311	24	SL	B	30
252	46	SL	G	3	312	26	SL	B	30
253	48	SL	B	18	313	28	SL	B	30
254	20 - 1	SL	B	20	314	22 - 1	SL	B	33
255	3	SL	G	40	315	3	SL	G	23
256	5	SL	G	40	316	5	SL	B	60
257	7	SL	Y	20	317	7	SL	B	43
258	9	SL	B	30	318	9	SL	B	48
259	11	SL	B	20	319	23 - 1	SL	B	3
260	13	SL	B	40	320	3	SL	G	20
261	15	SL	G	43	321	5	SL	G	30
262	17	SL	G	23	322	7	SL	Y	30
263	19	SL	Y	30	323	9	SL	G	23
264	21	SL	B	40	324	11	SL	B	73
265	23	SL	G	33	325	13	SL	Y	40
266	25	SL	B	30	326	15	SL	Y	60
267	27	SL	B	43	327	17	SL	G	10
268	29	SL	B	50	328	19	SL	B	18
269	31	SL	B	125	329	21	SL	B	20
270	33	SL	B	40	330	24 - 2	SL	G	40

A-52

No.	Sample No.	Nature of Sample	Color	Cu (p. p. m.)	No.	Sample No.	Nature of Sample	Color	Cu (p. p. m.)
331	4	SL	Y	43	391	37	SL	G	18
332	6	SL	G	37	392	39	SL	B	33
333	8	SL	G	35	393	41	SL	B	18
334	10	SL	G	10	394	43	SL	B	20
335	12	SL	G	15	395	45	SN	G	13
336	14	SL	G	40	396	47	SN	G	13
337	25 - 2	SL	G	38	397	49	SN	B	18
338	4	SL	B	50	398	51	SN	G	10
339	6	SL	Y	43	399	53	SN	G	13
340	8	SL	G	40	400	54	SN	G	20
341	25 - 10	SL	Y	50	401	29 - 56	SN	B	13
342	12	SL	G	33	402	57	SN	G	10
343	14	SL	G	23	403	61	SL	B	23
344	16	SL	G	8	404	63	SN	G	13
345	18	SL	B	50	405	65	SL	B	23
346	20	SL	G	45	406	67	SN	G	10
347	22	SL	G	40	407	69	SN	B	13
348	24	SL	B	60	408	73	SN	B	18
349	26	SL	B	33	409	75	SN	G	20
350	28	SL	B	40	410	77	SL	B	20
351	30	SL	Y	40	411	79	SN	G	18
352	32	SL	G	50	412	81	SN	B	43
353	34	SL	B	80	413	83	SN	B	18
354	36	SL	Y	63	414	85	SL	B	20
355	38	SL	B	90	415	87	SN	B	13
356	40	SL	Y	28	416	89	SL	B	40
357	26 - 1	SN	G	38	417	91	SL	B	3
358	3	SL	G	23	418	93	SL	B	3
359	5	SL	B	20	419	95	SN	B	20
360	7	SL	B	23	420	30 - 1	SL	B	13
361	9	SL	B	20	421	3	SN	G	23
362	11	SL	G	30	422	5	SN	B	20
363	13	SL	Y	30	423	7	SN	B	15
364	15	SL	B	23	424	9	SL	B	10
365	16	SL	G	30	425	11	SL	B	20
366	27 - 1	SL	B	30	426	13	SL	B	23
367	3	SL	G	13	427	15	SL	B	20
368	5	SL	B	33	428	17	SL	B	13
369	28 - 1	SL	B	13	429	19	SL	B	33
370	3	SL	B	20	430	21	SL	B	15
371	5	SL	B	10	431	23	SL	B	10
372	29 - 0	SL	B	10	432	25	SL	B	3
373	2	SN	G	18	433	27	SL	B	28
374	4	SN	G	13	434	29	SL	B	20
375	6	SN	B	20	435	31	SL	B	30
376	8	SL	B	20	436	33	SL	B	15
377	10	SL	Y	18	437	31 - 1	SL	B	20
378	11	SN	G	15	438	3	SL	B	18
379	13	SN	B	15	439	5	SL	B	20
380	15	SN	B	15	440	7	SL	B	20
381	17	SN	B	13	441	9	SL	B	13
382	19	SN	G	13	442	11	SL	B	20
383	21	SN	G	15	443	13	SL	B	3
384	23	SN	G	13	444	15	SL	B	3
385	25	SL	B	100	445	17	SL	B	3
386	27	SN	Y	10	446	19	SL	B	3
387	28	SN	B	20	447	21	SL	B	3
388	30	SN	G	13	448	23	SL	B	3
389	32	SL	B	33	449	25	SL	B	3
390	35	SN	G	13	450	27	SL	B	5

No.	Sample No.	Nature of Sample	Color	Cu (p. p. m.)	No.	Sample No.	Nature of Sample	Color	Cu (p. p. m.)
451	29	SL	B	20	511	47	SN	G	15
452	31	SL	Y	60	512	49	SL	B	50
453	33	SL	Y	30	513	51	SN	G	13
454	35	SL	B	28	514	53	SN	G	10
455	37	SL	B	40	515	55	SN	G	13
456	39	SL	B	3	516	57	SL	B	10
457	41	SL	G	8	517	59	SN	G	13
458	43	SL	G	13	518	61	SL	B	25
459	45	SL	B	50	519	63	SN	G	8
460	47	SL	B	63	520	65	SN	G	10
461	31 - 49	SL	Y	58	521	32 - 67	SL	G	23
462	51	SL	Y	30	522	69	SL	B	33
463	53	SL	G	3	523	71	SL	B	15
464	55	SL	B	33	524	73	SL	B	25
465	57	SL	Y	12	525	75	SL	B	23
466	59	SL	Y	10	526	77	SL	B	25
467	61	SL	B	18	527	79	SN	B	8
468	63	SL	G	3	528	81	SN	B	8
469	65	SL	B	20	529	83	SN	B	35
470	67	SL	G	25	530	85	SN	G	37
471	69	SL	Y	25	531	87	SN	B	30
472	71	SL	G	25	532	89	SL	B	35
473	73	SL	B	25	533	91	SN	B	30
474	75	SL	Y	10	534	93	SL	B	25
475	77	SL	B	18	535	95	SN	Y	25
476	79	SL	B	20	536	97	SL	G	15
477	81	SL	B	10	537	99	SN	B	30
478	83	SL	B	13	538	101	SN	G	30
479	85	SL	B	3	539	103	SN	B	23
480	87	SL	B	20	540	105	SL	Y	50
481	89	SL	Y	50	541	107	SN	B	20
482	91	SL	Y	20	542	109	SN	B	30
483	93	SL	Y	20	543	111	SN	Y	25
484	95	SL	Y	40	544	113	SL	B	25
485	97	SL	Y	30	545	115	SL	Y	10
486	99	SL	Y	23	546	117	SN	G	25
487	101	SL	B	10	547	119	SN	B	50
488	32 - 1	SL	Y	20	548	121	SL	B	3
489	3	SL	B	25	549	33 - 1	SL	G	30
490	5	SN	G	20	550	3	SL	G	30
491	7	SL	B	20	551	5	SN	G	30
492	9	SL	G	30	552	7	SN	G	30
493	11	SL	B	23	553	9	SN	Y	30
494	13	SL	G	20	554	10	SL	G	3
495	15	SL	B	23	555	12	SL	Y	20
496	17	SL	G	20	556	14	SL	G	40
497	19	SL	B	15	557	16	SL	G	38
498	21	SN	B	23	558	18	SL	Y	25
499	23	SN	G	30	559	20	SL	B	35
500	25	SN	B	25	560	22	SL	G	35
501	27	SN	G	10	561	24	SL	B	10
502	29	SN	G	20	562	26	SL	B	35
503	31	SN	G	15	563	28	SL	Y	8
504	33	SN	G	20	564	30	SL	B	18
505	35	SN	G	10	565	32	SL	Y	38
506	37	SL	B	15	566	34	SL	B	15
507	39	SL	Y	20	567	36	SL	B	30
508	41	SN	G	13	568	38	SL	G	28
509	43	SN	Y	10	569	40	SL	G	30
510	45	SL	Y	20	570	42	SL	B	20

No.	Sample No.	Nature of Sample	Color	Cu (p. p. m.)	No.	Sample No.	Nature of Sample	Color	Cu (p. p. m.)
571	44	SL	G	23	631	14	SL	B	28
572	46	SL	B	33	632	15	SL	Y	30
573	48	SL	B	30	633	16	SL	Y	10
574	50	SL	Y	53	634	17	SL	B	23
575	A - 0	SL	Y	30	635	18	SL	B	60
576	1	SL	Y	20	636	19	SL	G	28
577	2	SL	B	40	637	20	SL	G	23
578	3	SL	B	30	638	D - 1	SL	B	3
579	4	SN	G	30	639	2	SL	B	10
580	5	SL	G	13	640	3	SL	Y	20
581	A - 6	SN	B	22	641	4	SL	B	5
582	7	SL	G	10	642	5	SL	Y	3
583	8	SL	G	13	643	6	SL	Y	5
584	9	SL	B	13	644	7	SL	B	13
585	10	SL	B	10	645	9	SL	G	23
586	11	SL	Y	20	646	11	SL	G	30
587	12	SL	B	13	647	12	SL	B	45
588	13	SL	G	30	648	13	SL	B	28
589	14	SL	B	20	649	14	SL	B	20
590	15	SL	B	23	650	15	SL	G	40
591	16	SL	B	13	651	16	SL	G	20
592	17	SL	G	20	652	17	SL	Y	30
593	18	SL	B	20	653	18	SL	B	10
594	19	SL	B	30	654	19	SL	Y	13
595	20	SL	B	30	655	20	SL	Y	20
596	B - 0	SL	B	10	656	E - 0	SL	G	33
597	1	SL	G	8	657	1	SL	Y	25
598	2	SL	B	30	658	2	SL	G	10
599	3	SL	B	18	659	3	SL	B	20
600	4	SL	G	20	660	4	SL	G	25
601	5	SL	B	3	661	5	SL	G	35
602	6	SL	B	20	662	6	SL	G	13
603	7	SL	G	13	663	7	SL	B	20
604	8	SL	Y	20	664	8	SL	B	45
605	9	SL	Y	10	665	9	SL	B	10
606	10	SL	G	10	666	10	SL	B	30
607	11	SL	G	33	667	11	SL	B	30
608	12	SL	B	60	668	12	SL	B	15
609	13	SL	Y	23	669	13	SL	B	20
610	14	SL	B	8	670	14	SL	Y	20
611	15	SL	G	10	671	15	SL	Y	12
612	16	SL	B	3	672	16	SL	B	15
613	17	SL	Y	33	673	17	SL	Y	20
614	18	SL	Y	18	674	18	SL	Y	18
615	19	SL	Y	3	675	19	SL	Y	15
616	20	SL	B	33	676	F - 20	SL	G	10
617	C - 0	SL	G	25	677	1	SL	B	23
618	1	SL	G	20	678	2	SL	B	30
619	2	SL	G	30	679	3	SL	G	13
620	3	SL	B	20	680	4	SL	B	22
621	4	SL	G	22	681	5	SL	G	30
622	5	SL	B	20	682	6	SL	Y	30
623	6	SL	B	35	683	7	SL	G	12
624	7	SL	B	15	684	8	SL	B	25
625	8	SL	B	25	685	9	SL	Y	8
626	9	SL	B	15	686	10	SL	G	13
627	10	SL	Y	25	687	G - 1	SL	B	43
628	11	SL	B	33	688	2	SL	B	30
629	12	SL	B	30	689	3	SL	B	10
630	13	SL	B	23	690	4	SL	B	3

No.	Sample No.	Nature of Sample	Color	Cu (p. p. m.)	No.	Sample No.	Nature of Sample	Color	Cu (p. p. m.)
691	5	SL	Y	8	734	11	SL	B	23
692	6	SL	Y	8	735	J - 0	SL	G	30
693	7	SL	Y	100	736	1	SL	B	10
694	8	SL	Y	45	737	2	SL	G	10
695	9	SL	Y	5	738	3	SL	Y	40
696	10	SL	Y	8	739	4	SL	G	28
697	11	SL	G	3	740	5	SL	Y	43
698	12	SL	B	3	741	6	SL	B	20
699	13	SL	B	3	742	7	SL	Y	33
700	14	SL	B	5	743	8	SL	B	60
701	G - 15	SL	G	30	744	9	SL	B	125
702	16	SL	B	30	745	J' - 1	SL	B	13
703	17	SL	B	30	746	3	SL	G	100
704	18	SL	G	13	747	5	SL	B	40
705	19	SL	B	10	748	7	SL	B	30
706	20	SL	G	30	749	9	SL	G	50
707	H - 0	SL	G	10	750	X - 1	SL	B	13
708	1	SL	G	10	751	3	SL	B	13
709	2	SL	B	10	752	5	SL	G	3
710	3	SL	B	10	753	7	SL	Y	40
711	4	SN	G	10	754	9	SL	Y	20
712	5	SL	B	10	755	12	SL	Y	20
713	6	SL	B	10	756	14	SL	Y	23
714	7	SL	G	10	757	16	SL	G	23
715	8	SL	Y	8	758	18	SL	Y	65
716	9	SL	B	10	759	23	SL	Y	8
717	10	SL	Y	5	760	25	SL	B	50
718	I - 0	SL	B	10	761	27	SL	G	30
719	1	SL	G	3	762	29	SL	B	10
720	2	SL	Y	3	763	32	SL	B	30
721	3	SL	B	13	764	34	SL	B	33
722	4	SL	B	3	765	36	SL	G	12
723	5	SL	Y	8	766	38	SL	B	13
724	6	SL	B	20	767	41	SL	Y	33
725	7	SL	Y	3	768	43	SL	B	12
726	8	SL	Y	10	769	45	SL	B	40
727	9	SL	G	100	770	47	SL	Y	10
728	10	SL	G	30	771	49	SL	G	13
729	I' - 1	SL	G	28	772	52	SL	B	10
730	3	SL	B	13	773	54	SL	B	8
731	5	SL	Y	18	774	56	SL	G	30
732	7	SL	G	20	775	58	SL	B	20
733	9	SL	B	40					

Appendix 4

Drill Log







Depth (m)	Columnar Section	Color	Mineralization	Alteration		Rock Name	Description
				Distribution of Garnet	Zeolite (Laumontite) Montmorillonite Sericite Chlorite Secondary quartz		
						Alluvial deposit	Unconsolidated sand with pebble (3-10cm).
10.5 11.0		Pale gray				Biotite granite	
20		Dark gray				Biotite gneiss	Melanoclastic biotite gneiss (color index : 40) 11.0-17.0, thin iron sulfides film is observed along cracks. Strong gneissose structure shows 70 degree of dip.  Dip of gneissosity is about 60 degree. In thin section (DH-2, 30.5), mainly composed of quartz, plagioclase and biotite. Sillimanite is enclosed in quartz and plagioclase crystals. Montmorillonite-like minerals are observed in plagioclase crystals.
31.8 33.0 33.3 34.5		Pale gray				Biotite granite	Weak pyrite impregnation. 33.0-33.3, biotite gneiss.
40		Pale gray				Biotite gneiss	Color index : 40  Strong gneissosity with 45 degree of dip is observed. Color index : 30-40
50		Pale gray					
60							



Depth (m)	Columnar Section	Color	Mineralization	Alteration Distribution of Garnet	Zeolite (Laumontite) Montmorillonite Sericite Chlorite Secondary quartz	Rock Name	Description
6.5						Alluvial deposit	Unconsolidated sand with pebbles
6.6							6.50-6.60, biotite granite
7.0		Pale gray				Biotite gneiss	Strongly thin gneissose (like schistose) biotite gneiss. Intruded by quartz-feldspar-biotite aplite. Iron sulfide dissemination along foliation.
7.7		Dark brownish gray				Biotite granite	In some places, biotite granite intrusion is observed.
8.5		Pale gray				Biotite granite	Gneissosity is thin and strong. Minor folding of centimeter order is distinct. General trend of gneissosity shows 35 degree of dip.
8.8		Dark brownish gray				Biotite gneiss	
11.0							
11.5							
14.5							
20		Pale gray				Biotite granite	Medium grained equigranular biotite granite.  Core recovery is very low. Usually, fractured rock or only sludge. A bit of pyrite is disseminated in whole granite.
30							
40							In thin section (DH-3, 34.8), mainly formed by quartz, potash feldspar, plagioclase, biotite and hornblende. Some plagioclase has outer rim of potash feldspar. In some places, biotite is altered to chlorite.
50							
60							



